

Investigating Deiters' cell voltage-activated ionic conductances during a window of postnatal cochlear development

Nicole Levermore

Abstract

Only in recent years has the potential for understanding the auditory system through supporting cells been realised. Deiters' cells are a type of supporting cell that are known to play a role in cochlear homeostasis, outer hair cell development and postnatal cochlear development. However, there have been limited number of studies that have recorded from these cells during development. In this study, patch clamp techniques were used to investigate the electrical properties of Deiters' cells in rodents during a window of postnatal cochlear development. Specifically, the effects of extracellular calcium and electrical coupling between supporting cells were investigated. In some experiments, supporting cells were isolated using the gap junction blocker, 1-Heptanol. This study showed that Deiters' cells were not sensitive to changes in extracellular calcium. The findings from this study and subsequent related studies will potentially improve our knowledge of developmental hearing loss conditions.

Table of contents

Contents

Chapter 1.....	11
1.1 Hearing	12
1.2 Hearing loss	17
1.3 Cells of the auditory system.....	19
1.3.1 Hair cells: Mechanotransduction.....	19
1.4 The supporting cells	21
1.4.1 Fibrocytes.....	22
1.4.2 Hensen’s cells.....	22
1.4.3 Boettcher cells	22
1.4.4 Pillar cells	23
1.5 Deiters’ cells	23
1.5.1 Morphology	24
1.5.2 Variability in Deiters’ cell morphology	26
1.5.3 Deiters’ cells: OC location and function	27
1.6 Development of the auditory system	29
1.6.1 Mouse auditory system development.....	32
1.6.2 Auditory system development: spontaneous action potentials	37
1.6.3 Deiters’ cells and auditory system development	39
1.7 OC Physiology.....	39

1.7.1 Ion homeostasis in the cochlea	39
1.7.2 Ion channels of the cochlea	41
1.7.3 Voltage-gated sodium channels	45
Voltage-gated calcium channels	46
1.7.4 Voltage-gated potassium channels	48
1.7.5 Calcium-dependence of the Deiters' cell potassium current.....	51
1.8 Aims and Objectives	54
Chapter 2.....	56
2.1.1 Ethics statement	57
2.1.2 Tissue preparation	57
2.1.3 Electrophysiological recording	62
2.1.4 Whole-cell patch clamp recording.....	64
2.1.5 Data analysis	66
Chapter 3.....	68
3.1 Introduction:	69
3.2 Aims:.....	70
3.3 Results	70
3.4 Main findings	79
3.5 Discussion	79
Chapter 4.....	85

4.1	Introduction:	86
4.2	Aims:.....	88
4.3	Results	88
4.4	Main findings.....	96
4.5	Discussion	97
Chapter 5.....		99
5.1	Introduction:	100
5.2	Aims:.....	102
5.3	Results	102
5.4	Main findings.....	106
5.5	Discussion	106
Chapter 6.....		110
6.1	Limitations	113
6.2	Future directions	116
6.3	Concluding remarks.....	117
Chapter 7.....		118

Acknowledgements

I'd like to thank Professor Andrew Dilley and Doctor Andrew Penn for their fantastic supervision. Their attention to detail and knowledge has been extremely helpful, as well as their kindness and willingness to provide excellent supervision. Thank you both!

Abbreviations

Cav	Voltage-gated calcium channel
DC	Deiters' cell
IHC	Inner hair cell
I-V	Current-voltage
Kv	Outwardly rectifying voltage-gated potassium channel
Kir	Inwardly rectifying voltage-gated potassium channel
Nav	Voltage-gated sodium channel
OHC	Outer hair cell
Organ of Corti	OC
P	Postnatal day
TEA	Tetraethylammonium

List of figures

Figure 1: Diagram of the structures of the middle ear and inner ear.	13
Figure 2: Location and structure of the Organ of Corti.	16
Figure 3: The hair cell bundle and tip-link filaments.	20
Figure 4: Diagram of Deiters' cell morphology (shown in grey).	25
Figure 5: Schematic diagram of the organ of Corti.....	28
Figure 6: timelines of key developmental events.....	31
Figure 7: Locations of the otic placode and vesicle.....	33
Figure 8: The immature Organ of Corti and Kölliker's organ.....	35
Figure 9: The fluid filled compartments of the cochlea.	40
Figure 10: Channel conformational state transitions.	42
Figure 11: Voltage-gated potassium channel structure.....	49
Figure 12: Images of the cochlear tissue during dissection and at different magnifications.....	59
Figure 13: Flow diagram showing two experimental conditions	60
Figure 14: Photograph of the equipment set-up used for electrical recording.....	63
Figure 15: Schematic showing the steps involved in obtaining a whole-cell patch configuration.	65
Figure 16: Activation protocols utilised.	74
Figure 17: Graphs for ages postnatal day (P) 7 to P8 using peak of activation trace.	75
Figure 18: Graphs for ages postnatal day (P) 7 to P8 using the steady-state of the activation	

trace.

79

Figure 19: Schematic of the structure of voltage-gated potassium channel Kv1.5.

82

Figure 20: Absolute Deiters' cell current density at 40 mV and passive membrane properties for ages postnatal day (P) 7, P8 and P9 in high calcium (0 mM 1-Heptanol) and 3 mM 1-Heptanol

.....

94

Figure 21: Graphs for ages postnatal day (P) 7 and P8, comparing high calcium (0 mM 1-Heptanol) with 3 mM 1-heptanol

condition.....

96

Figure 22: Graphs for extent of inactivation during postnatal development

104

Figure 23: Graphs for recovery from inactivation during postnatal development

106

List of tables

Table 1: Common mechanisms of hearing loss.
18

Table 2: Composition of the perilymph and endolymph.
.....

41

Table 3: Summary of all known channels known to be present on Deiters' cells.

45

Table 4: Composition of extracellular solutions (in mM).

58

Table 5: Composition of 5 mM 1-Heptanol- containing extracellular solution (in mM).

61

Table 6: Composition of pipette-filling intracellular solution (in mM).
.....

64

Table 7: Input resistances ($M\Omega$) for P7 and P8 cells (n=6) in high calcium and 1-heptanol extracellular solution.
.....

96

Chapter 1

Introduction

1.1 Hearing

Hearing involves detecting the air compressions that vibrating objects produce, allowing for individuals to identify and recognise objects based on their sound and to communicate (Dobie and Van Hemel, 2004). The peripheral auditory system transduces the air compressions into neural-electrical signals, and this signal is analysed by the brain. For example, what made the sound, or where the sound came from (Dobie and Van Hemel, 2004).

The peripheral auditory system consists of the external, middle and inner ear. The external ear includes the pinna, which is the visible part of the outer ear and acts as a funnel to help capture sound, as well as the ear canal and the tympanic membrane (Dobie and Van Hemel, 2004; Kollmeier, 2008). The middle ear comprises the three ossicles, which are the malleus, incus and stapes, and the inner ear consists of the cochlea, which is both fluid- and tissue filled, and is where sound transduction occurs (Figure 1) (Dobie and Van Hemel, 2004; Kollmeier, 2008). Sound enters the ear via the pinna and moves into the ear canal, which channels the sound to the tympanic membrane (Dobie and Van Hemel, 2004). The tympanic membrane vibrates in response to sound, and this sound is conducted from the tympanic membrane to the three ossicles, the last of which (stapes) vibrates the perilymph in the cochlea via the oval window, which forms an opening to the vestibule of the cochlea (Alberti, 2001).

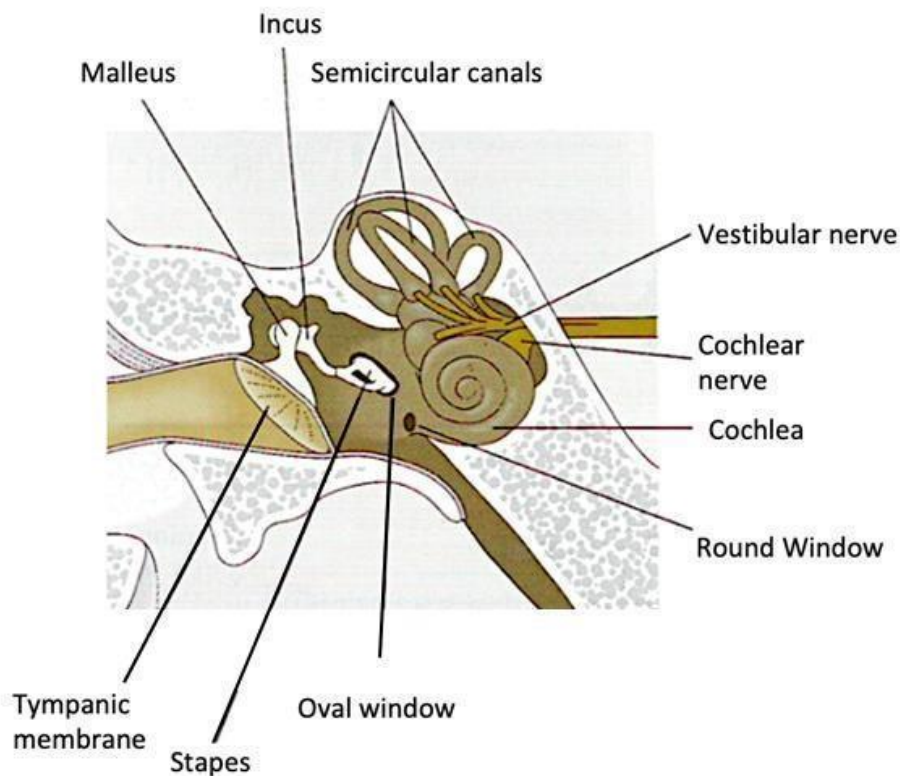


Figure 1: Diagram of the structures of the middle ear and inner ear.

Sound-induced vibrations are channelled to the tympanic membrane, which vibrates in response. These vibrations are transmitted along the three ossicles: the malleus, incus and the stapes. Figure adapted from (Blake and Sekuler, 2006).

The openings of the cochlea that form barriers between the middle ear and inner ear (cochlea) serve important roles in middle ear and cochlear mechanics (Sten Hellström et al., 1997). These openings are the round and oval window (Zhang and Gan, 2013). The round window vibrates with an opposite phase to acoustic vibrations entering the cochlea through the stapes at the oval window, allowing for vibrations to be transmitted along the cochlea (Alberti, 2001). The cochlea vibrates in response to sound, and the movement of the fluid

within the inner ear varies depending on the intensity, frequency, and temporal properties of the stimulus (Dobie and Van Hemel, 2004). Movement of the fluid in the space between the tectorial membrane and the reticular lamina indirectly deflects inner hair cell stereocilia, which stimulates them, and causes the opening of mechanically gated ion channels, leading to depolarisation. The shearing movement between the reticular lamina and the tectorial membrane that is caused by sound-induced vibrations directly deflects outer hair cell stereocilia (Geisler, 1998). Outer hair cells change their axial dimensions in response to this stimulation (i.e. display electromotility) (Geisler, 1998), which leads to amplification or dampening of the motion of the basilar membrane and therefore regulation of hearing sensitivity (Ashmore, 1987; Feher, 2012).

The hair cells are responsible for converting the mechanical stimuli into neural-electrical signals that are interpreted by the brain (Schwander et al., 2010). Important for regulating the function of hair cells, the cochlea contains two distinct types of fluid, endolymph and perilymph. Endolymph is essential for hearing and is unique when compared to other extracellular fluids in having a high potassium ion concentration and low sodium ion concentration. Perilymph exhibits a low potassium and high sodium concentration (Casale and Agarwal, 2023). The functions of these fluids and where they are in the cochlea will be expanded upon later in this introduction.

The Organ of Corti (OC) is the primary hearing organ and contains multiple sensory (hair cells) and non-sensory (supporting) cell types (White et al., 2023). There are two types of sensory hair cells within the inner ear, these being inner hair cells (IHCs) and outer hair cells

(OHCs). OHCs amplify the motion of the basilar membrane in response to sound, while IHCs act as the sensory receptors, with afferent input to the brain mostly stemming from IHCs (Dallos, 1992) (Figure 2). The sensory hair cells are arranged in rows, with there being a single row of IHCs and three rows of OHCs (White et al., 2023). These rows are separated by groupings of supporting cells that support cochlear functioning by, for example, playing a role in cochlear development and by maintaining cochlear homeostasis (Wan et al., 2013).

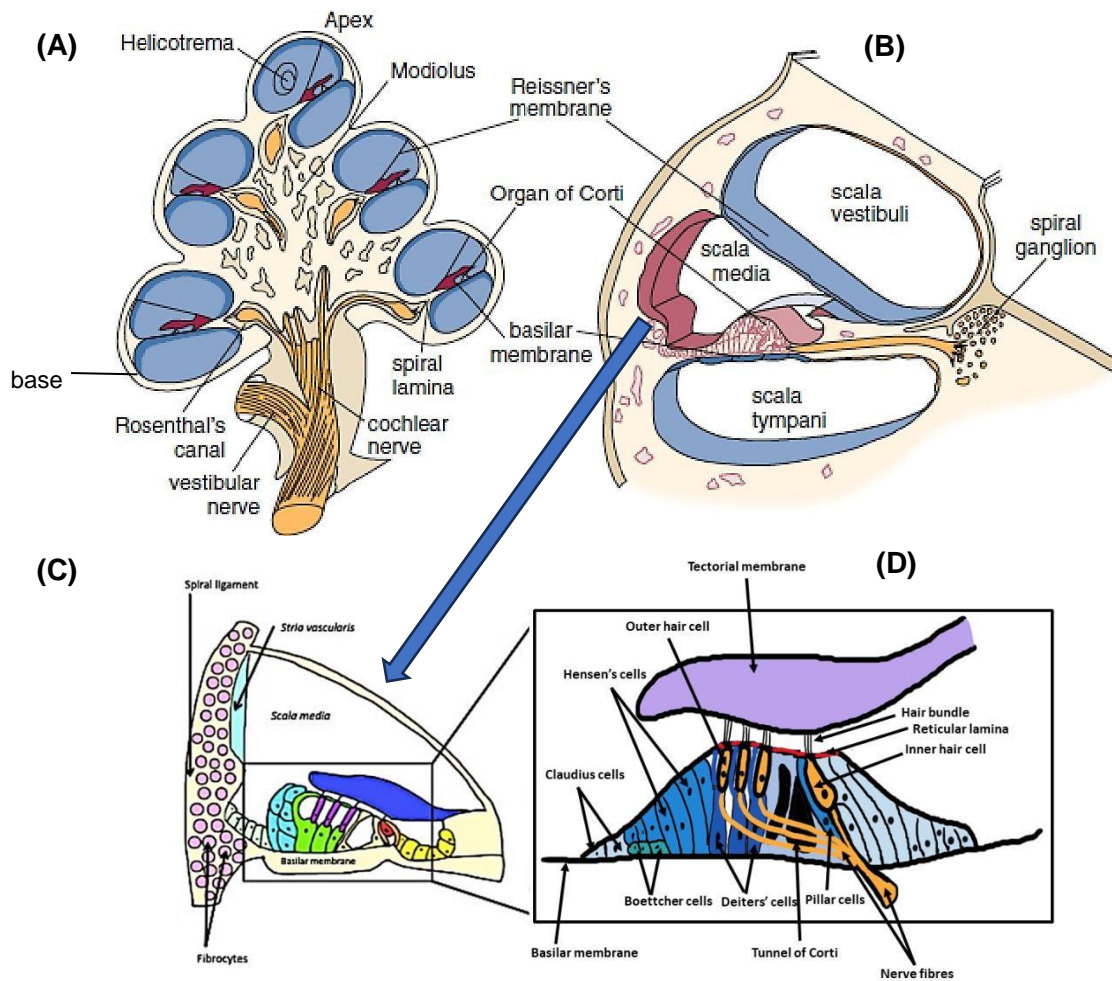


Figure 2: Location and structure of the Organ of Corti.

(A) Sagittal cross section of the cochlea, showing the structures from base to apex as well as the cochlear nerve. (B) Closer image of the structures surrounding the sensory structure known as the organ of Corti (OC). (C) Schematic of the cochlea in section, showing the fibrocytes located in the spiral ligament, the stria vascularis and basilar membrane- upon which rests the OC. The OC is located within a cochlear compartment known as scala media and rests on the basilar membrane. It is composed of two key sensory groups along its epithelium: mechanosensory hair cells-outer hair cells and inner hair cells, and supporting cells- the Claudius cells, Hensen's cells, pillar cells, Deiters' cells and Boettcher cells. (D) Magnified depiction of the OC cells. Figures adapted from (Furness, 2019) and (Runge-Samuelson and Friedland, 2016).

1.2 Hearing loss

According to the World Health Organisation, hearing loss is going to become an increasingly prevalent issue, with 2.5 billion people projected to have hearing loss in some form by 2050, and 700 million requiring treatment for hearing loss by the same year (World Health Organisation, 2022). Moreover, estimates suggest that by 2035 over 13 million people in England will be affected by hearing loss, which is equivalent to one in five of the population (Cunningham and Tucci, 2017). Currently more than 1.5 billion people have hearing loss, which accounts for almost 20% of the global population, with 80% of cases of disabling hearing loss happening in low- and middle-income countries. At the time of writing, the World Health Organisation reports that 430 million, or 5% of the world population, have disabling levels of hearing loss, with one billion young people currently at risk of developing hearing loss (World Health Organisation, 2022).

Some risk factors for developing hearing loss include persistent exposure to loud music or sound, nutritional deficiencies, and genetic predisposition (World Health Organisation, 2022). The prevalence of hearing loss increases with age, with one third of people over the age of 65 being affected by age-related hearing loss (Desai et al., 2001; World Health Organisation, 2022). Within the UK population, around 40% of people aged 50 years old and 71% of people aged 70 years and older have some degree of hearing loss. With hearing loss being the main cause of decreased life quality in those over 70, it is an issue that desperately needs solutions (Vos et al., 2015). A summary of common mechanisms of hearing loss is provided in (Table 1).

Type of hearing loss	Mechanism of hearing loss
Genetic congenital	<ul style="list-style-type: none"> • Abnormal/ disrupted inner ear homeostasis due to, for example: mutations of gap junction protein encoders, mutations in genes that code for maintenance of inner ear endolymph pH and ionic composition and mutations affecting the morphology of the stereociliary bundle of inner and outer hair cells • Acquired congenital hearing loss via infant infection (Korver et al., 2017)
Age-related hearing loss	<ul style="list-style-type: none"> • Inherited genetically • Caused by decline in number and quality of synaptic connections present between the hair cells and auditory neurons
Noise-induced	<p>Continuous exposure to damaging sound levels, resulting in pathologies such as:</p> <ul style="list-style-type: none"> • Decline in number and quality of synaptic connections present between the hair cells and auditory neurons (Viana et al., 2015; Liberman and Kujawa, 2017) • Changes in temporal and spatial resolution of hearing as well as frequency selectivity, hearing sensitivity and can result in a hearing defect known as tinnitus
Injury/ infection	<ul style="list-style-type: none"> • Blast injury causing hearing loss through effects like tympanic membrane perforation, rupturing of the connections between sensory hair cells and the supporting cells on the basilar membrane etc (Choi, 2012) • Ototoxic drugs such as antimalarials and certain antibiotics (Ganesan et al., 2018)

Table 1: Common mechanisms of hearing loss.

1.3 Cells of the auditory system

1.3.1 Hair cells: Mechanotransduction

Hearing critically depends on the sensory hair cells (OHCs and IHCs) of the cochlea, within the inner ear. The hearing process at the OC involves the shearing force generated by sound stimuli to deflect of the hair bundles connecting the sensory cells and their over-laying structure, the tectorial membrane, and subsequently the opening of mechanotransduction channels. The mechanosensory hair bundle is formed by stereocilia located at the apical domain of the hair cells (Figure 3) (Vélez-Ortega et al., 2017).

Each hair bundle consists of around 100 actin-filled stereocilia (Gillespie and Müller, 2009). Stereocilia bundles are arranged in a 'staircase' formation, in rows of graded heights- with ciliary height ranging from 1 to about 6 micrometres (μm) from the high-frequency cochlear base to the low-frequency apex (Vélez-Ortega et al., 2017).

Stereocilia are interconnected by filament structures known as tip-links (Figure 3) (Pickles et al., 1984). At resting state, there is tension on the tip-links, and this tension is modulated by sound-induced deflection of the hair bundle- of which deflections control the opening of mechanotransduction (MET) channels (Assad et al., 1991).

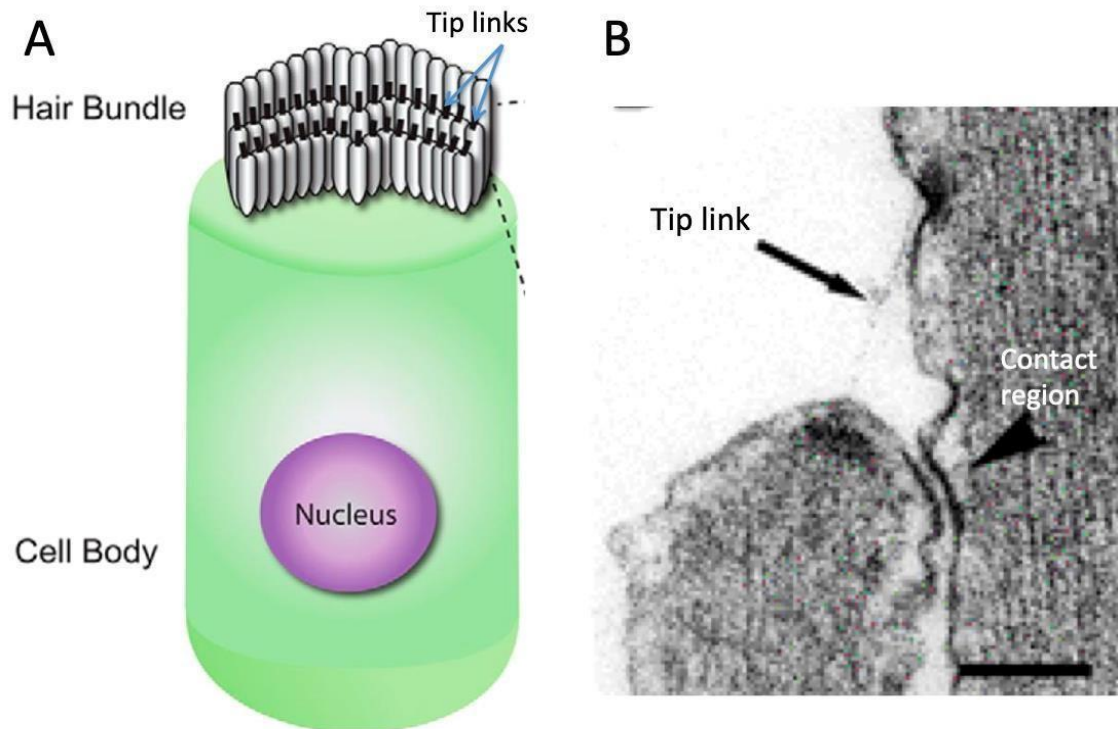


Figure 3: The hair cell bundle and tip-link filaments.

(A) Schematic of the hair cell stereocilia bundle arrangement on the apical domain of the hair cell body and the tip-links connecting the stereocilia in the direction of their mechanical sensitivity. Figure adapted from (Wu and Muller, 2016). (B) Transmission electron microscopy (TEM) image of a tip-link filament (arrow) connecting stereocilia of different heights at the apical region of a guinea pig cochlear hair cell. The contact region found between stereocilia is also shown (arrowhead). Figure adapted from (Hackney and Furness, 2013).

The tension on tip-links allows for hair cell bundles to respond to very small deflections (Hacohen et al., 1989; Assad et al., 1991), increasing MET channel opening probability (Corey and Hudspeth, 1979). MET channels, located on the tips of the shorter stereocilia rows (Beurg et al., 2009) are non-selective cation channels formed of the proteins TMC1 and

TMC2 (Pan et al., 2013), and exhibit a significant Ca^{2+} permeability (Vélez-Ortega et al., 2017), though the majority of the transduction current is carried by K^+ (Fettiplace and Ricci, 2006).

As well as mechanoelectrical transduction, the cochlea has the function of separating the frequencies that comprise a sound stimulus, known as frequency tuning (Fettiplace, 2017).

Frequency tuning is critical for sound recognition and localisation (Fettiplace, 2020).

Different subsets of hair cells encode different frequencies of sound, and along the cochlea the sound frequency the subsets of hair cells encode is graded in an arrangement called the tonotopic map (Fettiplace, 2020). At the base of the cochlea, hair cells respond to high frequencies of sound, while at the apex the hair cells respond to low frequencies (Warren et al., 2016). In mammals, this tonotopic map is produced by graduation in basilar membrane stiffness and mass along the cochlea (Naidu and Mountain, 1998; Teudt and Richter, 2014; Emadi et al., 2004), whereby a sound frequency generates a travelling wave that peaks at a specific location along the cochlear partition (Bekeşy, 1960).

1.4 The supporting cells

Supporting cells of the cochlea include inner and outer pillar cells, Hensen's cells, Deiters' cells, Claudius cells and Boettcher cells (Li-dong et al., 2008) (Figure 2). Cochlear supporting cell types each have a specific morphology and anatomical location within the OC (Raphael and Altschuler, 2003). Supporting cells are important for the development, function and maintenance of the inner ear sensory epithelia (Wan et al., 2013). In contrast to hair cells,

which make contact solely with the luminal surface of the epithelium, supporting cells span the entire depth of the epithelium (Wan et al., 2013).

1.4.1 Fibrocytes

Fibrocytes are embedded in the vascularised extracellular matrix of the spiral ligament, localised within the lateral wall of the cochlea (Furness, 2019). They have a homeostatic role within the cochlea, including in the development of the endolymphatic potential (Furness, 2019).

1.4.2 Hensen's cells

Hensen's cells are found as a layer of tall cells arranged in several rows contacting the cochlea basilar membrane (Merchan et al., 1980). The shape of the Hensen's cells differ depending on their position within the cochlea, varying from tall to cuboidal in shape (Merchan et al., 1980), with a tapering width from the apical to basal surface (Li-dong et al., 2008). Previous research has suggested that Hensen's cells (and Claudius' cells) may function as macrophages (Hayashi et al., 2020).

1.4.3 Boettcher cells

Boettcher cells are located only in the basal portion of the cochlea (the lower turn of the cochlea, which responds to high-frequency sound) and are found in rows based directly on the vestibular surface of the basilar membrane (Henson et al., 1982). The cytoplasm of Boettcher cells is dense and organelle-rich, relative to other SC types (Bruns and Schmieszek, 1980). Very little is known about this supporting cell type (Cloes et al., 2013), however specialised structures, such as microvilli that project into the intercellular space,

suggest a specific role within the cochlea (Kanazawa, A. et al., 2004). In rats, gap junctions have been observed between Boettcher cells and neighbouring supporting cells, suggesting that these cells may be involved in K⁺ recycling into the endolymph (Cloes et al., 2013).

1.4.4 Pillar cells

Within the OC inner and outer pillar cells function to maintain the structure of the tunnel of Corti- a space that upholds the structure of the OC. They provide this scaffold despite the pressure that is formed by the movement of the OC during acoustic stimulation which puts pressure on either side of the tunnel. Pillar cells are specialised for this role through their distinct cytoskeletal filaments known as microtubule stalks (also expressed by Deiters' cells (DCs)) that support the hair cells and therefore allow for the OC to carry out mechanotransduction (Slepecky et al., 1996; Wan et al., 2013). The first row of OHCs are located directly adjacent to the outer pillar cells at the apical surface. The sensory epithelium is anchored onto the basal lamina through the basal surfaces of pillar and DCs. Commonalities in the functioning of pillar cells and DCs also includes that both cell types have been suggested to influence frequency tuning (Geisler and Sang, 1995; Russell and Nilsen, 1997; Tolomeo and Holley, 1997; Mellado Lagarde et al., 2013).

1.5 Deiters' cells

Deiters' cells are a type of supporting cell that are known to perform important functions within the cochlea and will be the subject of this thesis. Deiters' cell morphology and function will be described in more detail below.

1.5.1 Morphology

Deiter's cells have an elongated body which spans from the basilar membrane to the reticular lamina (Slepecky, 1996). The bases and apices of all DCs span the entire sensory epithelium (Zetes et al., 2012). Deiters' cells possess a straight phalangeal process, which extends obliquely along the length of the cochlea and passes two or three OHCs (Li-dong et al., 2008). Deiters' cell bodies vary from 60–50 μm in length (Zetes et al., 2012). The apical region of the DC is a thin phalangeal process or phalangeal 'head' that fills the space between the OHCs by extending this branch-like process to the reticular lamina (Parsa et al., 2012; Li-dong et al., 2008), forming tight junctions with the apical surface of the OHC (Dulon et al., 1994). The mid-portion of the DCs are distinctly cup-shaped, and surround the base of the OHCs (Figure 4) (Slepecky, 1996).

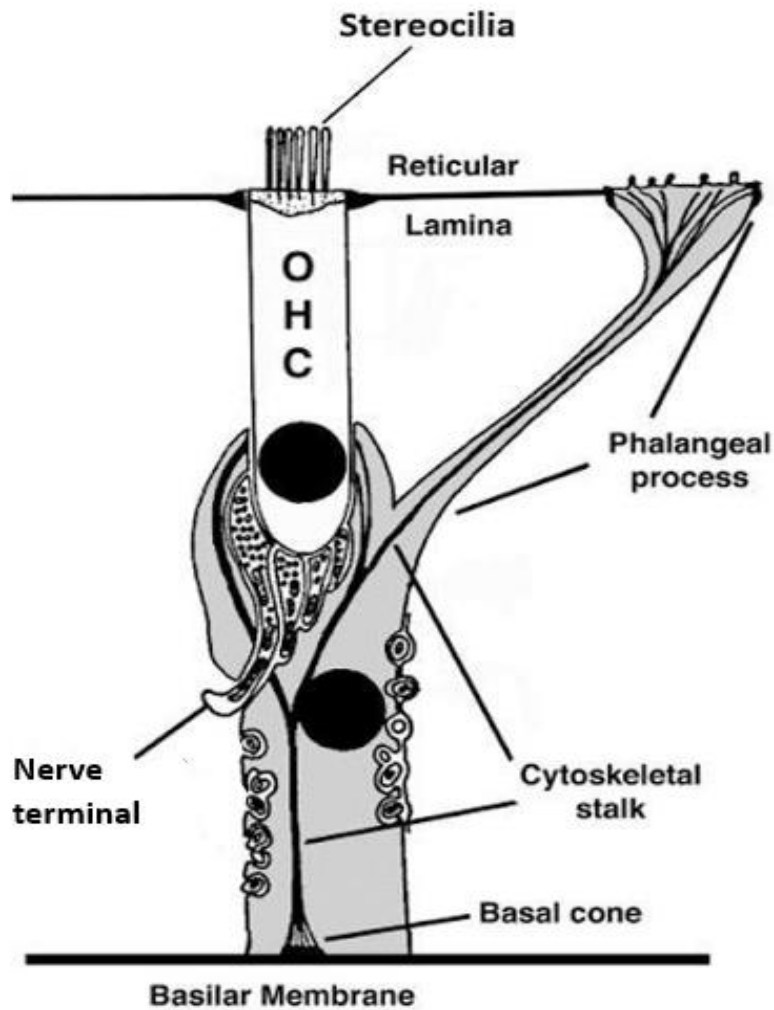


Figure 4: Diagram of Deiters' cell morphology (shown in grey).

Deiters' cells exhibit a basal cone, which forms the cell's foundation and directly contacts the basilar membrane. Also shown are afferent nerve terminals, the stalk-like structure of the Dieter cell's cytoskeleton, the phalangeal process, which extends to the reticular lamina, and the cell body, which cups the base of an outer hair cell. Figure adapted from Engström and Wersäll (1958).

The cytoskeleton of the DCs extends from a conical structure contacting the basilar membrane known as the basal cone, to the reticular lamina (Smith and Dempsey, 1957;

Engström and Wersäll, 1953). The cytoskeletal structure within the DC is mostly comprised of long bundles of microtubules that are interdigitated with actin filaments (Saito and Hama, 1982; Slepecky, 1996; Angelborg and Engström, 1972), and the axis of the basal portion of the DC cytoskeleton is aligned with the OHC it supports (Zetes et al., 2012).

Where the DCs and Pillar cells contact the basilar membrane is known as a 'footplate' (Angelborg and Engström, 1972). This 'Deiters' stalk' cytoskeletal structure is unique to DCs and Pillar cells (a supporting cell type observed to possess a similar structure) (Angelborg and Engström, 1972). It has been noted that DCs possess relatively few organelles such as lysosomes, mitochondria and rough endoplasmic reticulum (Zhixian and Yitong, 1988).

1.5.2 Variability in Deiters' cell morphology

Depending on their location along the Organ of Corti, DCs present differential expression of proteins. Nakazawa et al. (1995) described how DCs located at the extreme base of the gerbil cochlea do not express actin and vimentin (another protein component of the cytoskeleton), although the lack of these proteins may be due to the chemicals used in staining not effectively being administered to the base of the cochlea. Furness et al. (2001) found differences in the expression of the glutamate/aspartate transporter 'GLAST' in DCs, with expression being higher in cells of the apical region than in the basal region in guinea pigs. Differences in mitochondria of DCs in different regions have also been noted (Spicer and Schulte., 1994).

There is some variability in the structure of the DCs lower limb, seen along the Organ of

Corti- the first row DCs in the basal part of the mouse cochlea are positioned upright to a higher degree than in the apex, and in more apical cochlear regions, the DCs appeared to be more slanted (Parsa et al., 2012). The exact morphology and cell shape of a DC is determined by the length of the OHC that it is attached to (Szűcs et al., 2006; Laffon and Angelini, 1996; Nakazawa et al., 1995; Spicer and Schulte, 1994). In an electrophysiological study, Szűcs et al. (2006) noted that the longer the DC shape, the larger the recorded potassium current amplitude. It is yet to be determined as to what function this difference could play in Organ of Corti functioning.

1.5.3 Deiters' cells: OC location and function

There are three rows of DCs, which are there to support the three rows of OHCs present at the sensory epithelium (Zetes et al., 2012) (Figure 5).

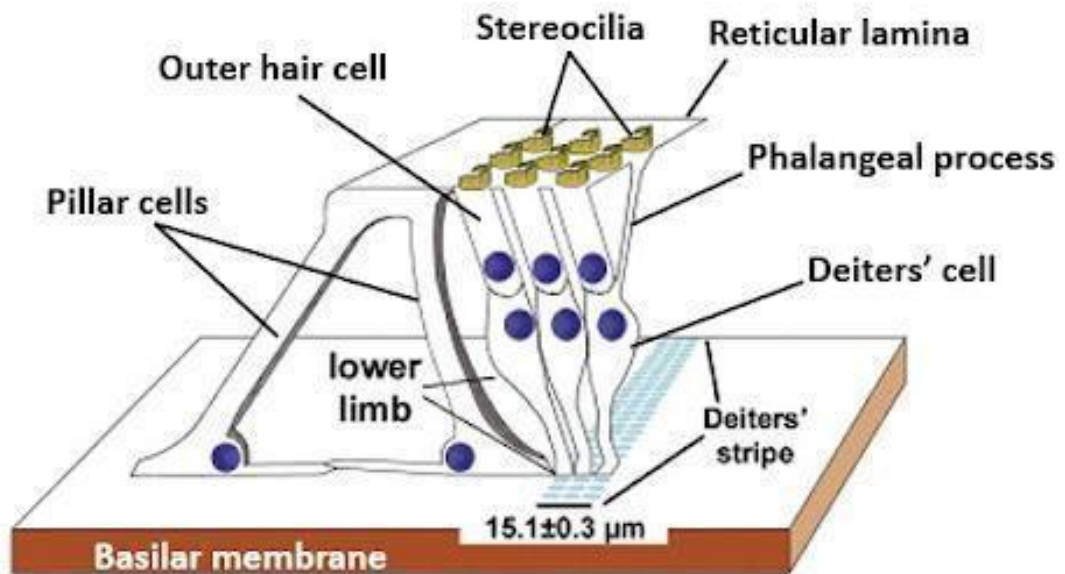


Figure 5: Schematic diagram of the organ of Corti.

Organ of Corti schematic depicting the three rows of outer hair cells with the three rows of Deiters' cells that support them. This figure shows the phalangeal process of the Deiters' cell that extends to the reticular lamina and the lower limb of the Deiters' cells, which end in Deiters' feet that contact the basilar membrane at a very close range. The location of the Pillar cells, an important supporting cell of the OC is also depicted. Figure adapted from Para et al. (2012).

Deiters' cells are mostly immersed in the cochlear perilymph, while the apical membrane of the phalangeal process is exposed to endolymph (Chung et al, 2013). Deiters' cells as supporting cells are known to perform critical functions within the cochlea, including some involvement in transducing basilar membrane motion into reticular lamina motion, transmitting the forces generated by OHCs to the basilar membrane (Parsa et al., 2012) and acting as mechanical equalisers to the forces of their respective OHCs (a cell type they are in

direct contact with) through passively regulating cell stiffness (Zhou et al., 2022). Deiters' cells have been found to clear cellular debris following the death of neighbouring OHCs (Abrashkin et al., 2006; Forge, 1985; Taylor et al., 2008). Moreover, there is evidence for a role of DCs in hearing sensitivity, as when the inner ear is exposed to a loud sound the third row DCs, along with other OC cells (including OHCs and Hensen's cells) form a protective response by gradually, over a few hours, moving closer to the centre of the cochlear turn. This reduces sensitivity to the potentially damaging sound (Flock et al., 1999). Deiters' cells are also critical for cochlear development, and without DCs present during development, hearing is drastically impaired (Mellado Lagarde et al., 2013).

1.6 Development of the auditory system

Research on hearing development in humans comes from evidence derived from those individuals with congenital mutations that affect hearing (with hereditary hearing loss accounting for over 50% of all congenital sensorineural hearing loss cases (Egilmez and Kalcioglu, 2016)), from neuroimaging techniques or histological postpartum labelling of neural connections in cadavers (Litovsky, 2015), as well as from inferences derived from studies on other vertebrates including the developing chick and rodents (Giraldez and Fritsch, 2007). Through the utilisation of single cell RNA sequencing on developing dissociated human and mouse cochleae, Yu et al. (2019) found that the overall architecture of the human and mouse cochlear cell populations were extremely similar, with them showing similar populations of mesenchyme, epithelium, neural crest and developing hair cells. It has also been found that the human and mouse cochlea epithelial floors show similar developmental trajectories. These similarities were noted through observation of the

similar expression patterns of genes involved in development shown in both the human and mouse cochlea (Yu et al., 2019).

Yu et al. (2019) analysed how the life stages of the mouse and human align in terms of early hearing development. The researchers were able to determine, through the comparison of levels of expression of developmental marker genes, that human hair cells 15-weeks into gestation correspond roughly to E16.5 mouse hair cells, that 17-week gestation human hair cells correspond to E18.5 mouse hair cells, and 23-week gestation human hair cells equate to past P2 in mice. The mouse is a good model for cochlear development in humans, as despite the differences in timing of developmental events, there are no vast differences in the characteristics of the events themselves (Yu et al., 2019). There has been extensive research on auditory system development utilising mice as models, a developmental timeline from which will be summarised in this section and in Figure 6.

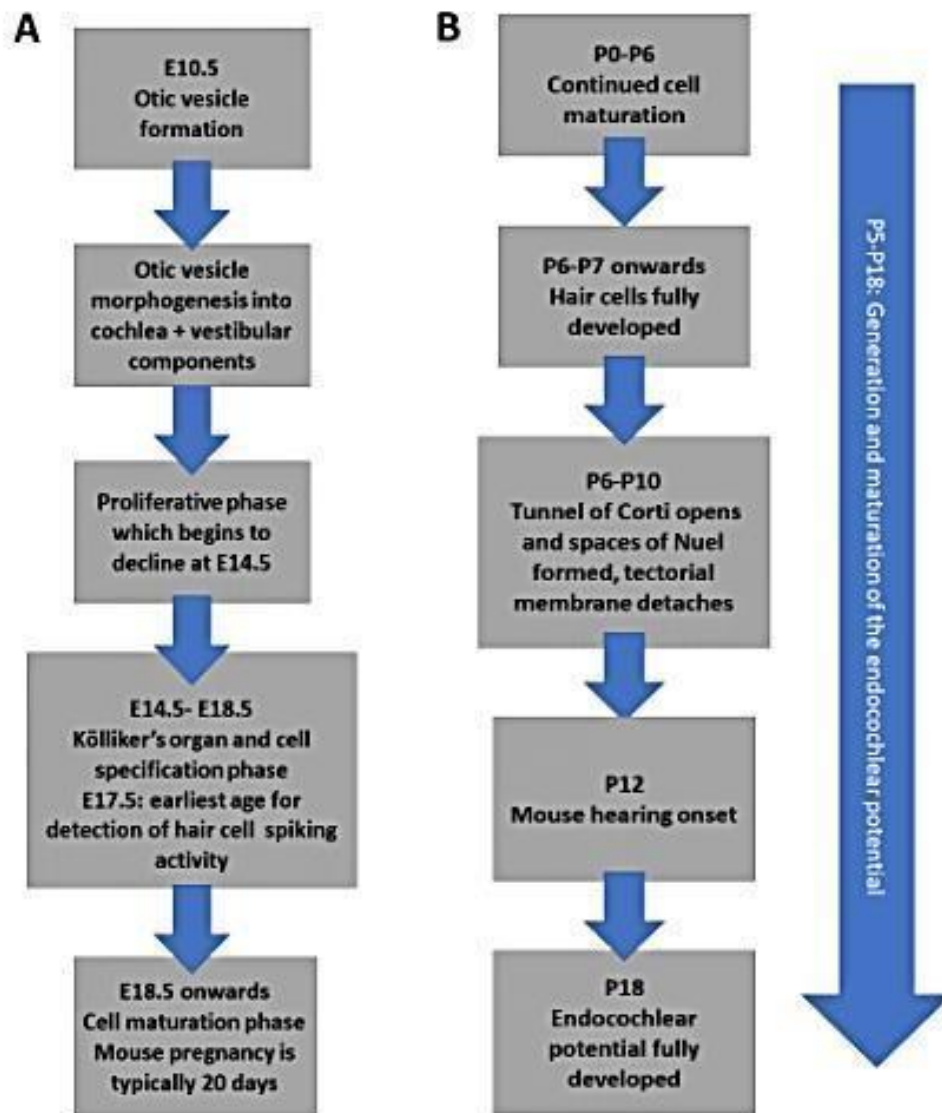


Figure 6: timelines of key developmental events.

Timelines of key developmental events that occur during embryonic (A) and postnatal (B) auditory system development in mice. The guinea pig has been a commonly used model animal for hearing research, with the depicted events occurring during auditory development over a longer period- due to guinea pigs possessing a longer life span than most other rodents. Most current hearing research utilises mice due to their shorter developmental time course that reduces laboratory costs as well as the way they are genetically tractable (Naert et al., 2019).

1.6.1 Mouse auditory system development

Mouse hearing development occurs both pre- and postnatally (Walters and Zuo, 2013). The inner ear is derived from the ectoderm and is the first of the three constituents of the ear to form (the others being the external and middle ear). This ectoderm thickens and gives rise to the otic placode at around embryonic day 8-9, which invaginates to form the otic vesicle at E10.5 (Figure 7) (Hartman et al., 2015). Therefore, the otic placode is the first structure that arises during the development of the auditory system. The elaborate structures of the inner ear, as well as the ganglion that innervates its sensory organs, almost all arise from the otic vesicle, which is a hollow sphere of epithelium (Morsli et al., 1998).

Early otic lineage populations of the mouse embryo

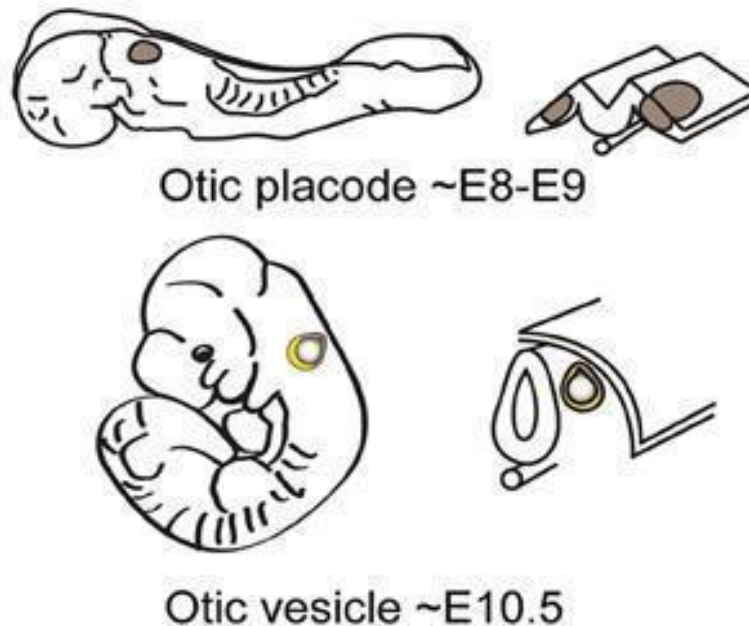


Figure 7: Locations of the otic placode and vesicle.

Schematic depicting the locations of the otic placode (above) and otic vesicle (below) on the mouse embryo, with corresponding days into embryonic development. Figure adapted from Hartman et al. (2015).

The otic vesicle later undergoing morphogenesis to form the inner ear labyrinth, which is composed of the vestibular components (endolymphatic duct, semicircular canals, utricle and saccule), and the cochlea (the auditory component) (Morsli et al., 1998). All OC cells are thought to arise from a common prosensory progenitor population (Groves and Fekete, 2012). A proliferative phase of these relatively undifferentiated cells then begins. Morphological evidence of hair cell differentiation is first seen throughout this period (Lim and Anniko, 1985). This differentiation begins to rapidly decline in magnitude after E14.5 in

mice (Groves and Fekete, 2012), with the putative sensory epithelium becoming visible around E14 (Simonneau et al., 2003). This putative sensory epithelium tissue gives rise to the sensory IHCs and is commonly known as “Kölliker's organ” (Figure 8) (Simonneau et al., 2003).

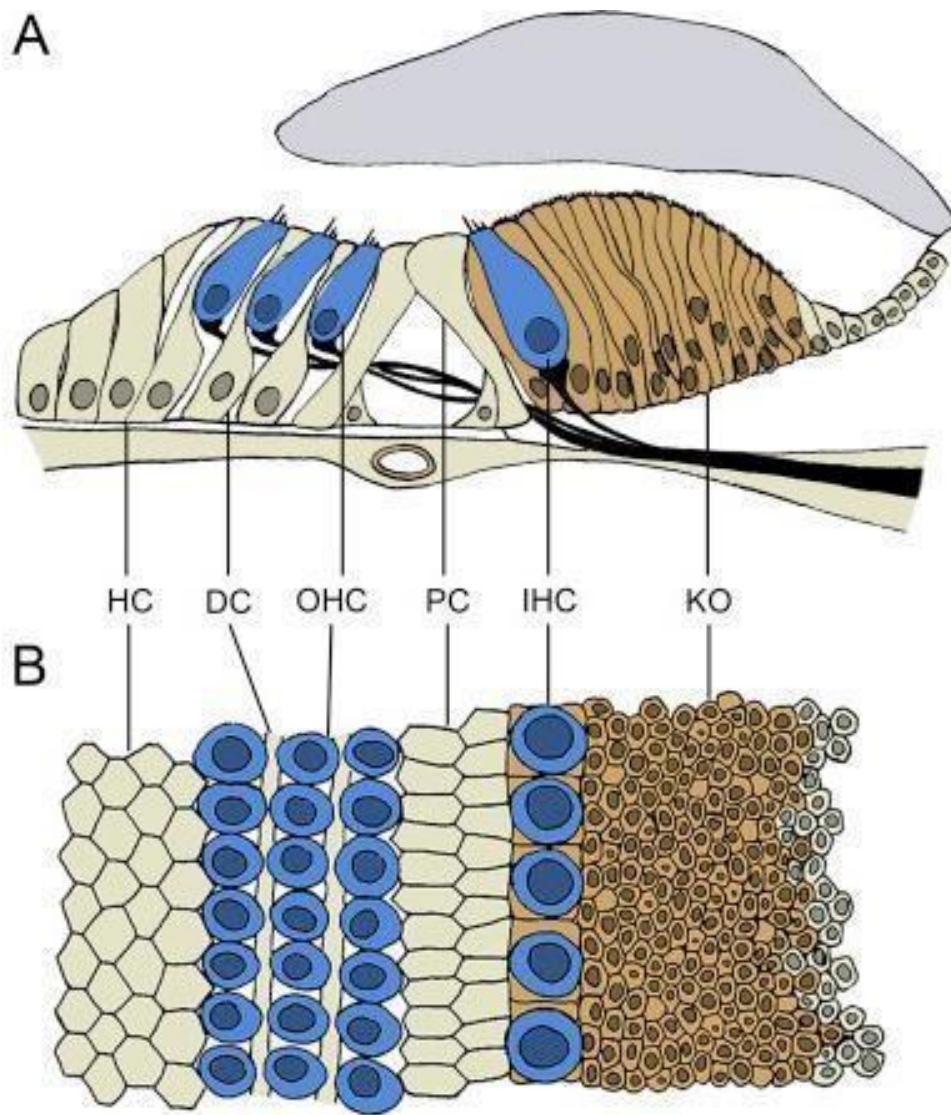


Figure 8: The immature Organ of Corti and Kölliker's organ.

Depiction of the mouse OC and Kölliker's organ at approximately 10 days old. (A) Schematic of the OC in cross section. This figure shows the cells of Hensen (HC), cells of Deiters' (DC), outer hair cells (OHC), pillar cells (PC), inner hair cells (IHC) and cells of the Kölliker's organ (KO). (B) The same cells of the OC in surface view. Figure from (Dayaratne et al., 2015).

The Kölliker's organ undergoes vast developmental changes from this embryonic stage onwards to early postnatal development, eventually becoming the inner sulcus region of the

OC (Dayaratne et al., 2014). From E14.5 to 18.5, following the rapid decline in progenitor proliferation, there is a specification phase where multiple distinct lineages are specified (Yu et al., 2019). Initially, sensory cells and non-sensory cells of the cochlea are indistinguishable by visual observation, while nerve fibres invade the greater epithelial ridge (Pujol et al., 1998; Majumder et al., 2010). From E16 onwards the putative sensory epithelium contains the IHCs and OHCs, that are present as transcriptionally distinct cells (Wiwatpanit et al., 2018)- the majority of sensory and non-sensory cells being formed during embryonic development in the mouse cochlea (Lee et al., 2006; Ruben, 1967).

The sensory epithelium is made up of two domains at this point- the greater epithelial ridge that contains the Kölliker's organ, and the lesser epithelial ridge in the lateral portion of the epithelium (Dayaratne et al., 2014). The cells that end up separating these two epithelia later become the inner and outer pillar cells (Lim and Anniko, 1985). The OHCs originate from the lesser epithelial ridge, while IHCs are theorised to develop from the greater epithelial ridge (Simonneau et al., 2003). The supporting cells known as Hensen's cells also derive from the lesser epithelial ridge (Simonneau et al., 2003). Kola et al. (2020) observed that transcriptionally unique classes of supporting cells are present as early as E16 in mice- these being the inner pillar cells and inner phalangeal cells. Beyond E18.5 there was shown to be a maturation phase, where cell gene expression continues to change, but cells retain the identities assigned during the specification phase (E14.5 to 18.5) (Yu et al., 2019).

The first postnatal week in mice is thought to represent a critical window, after which, hair cells cannot regenerate to the same degree following damage (Cox et al., 2014). Beyond postnatal day (P)6, no new hair cell addition is seen during mouse cochlear development

(Jan et al., 2013) and after P6-7 hair cells do not regenerate in response to damage (Cox et al., 2014). The $I_{k,n}$ current in OHCs is still maturing between P9 and P12 (Marcotti and Kros, 1999). At P7, the cochlear sensory epithelium is not yet fully developed (Kolla et al., 2020). During the first postnatal week, the mouse cochlea sees vast anatomical and structural changes- for example, between P6 and 10 the tunnel of Corti opens and the spaces of Nuel are formed (Kikuchi and Hilding, 1965). The spaces of Nuel being the spaces between the bodies of the OHCs, and the tunnel of Corti consisting of the arch formed by the angled phalangeal processes of the outer and inner pillar cells (Taylor et al., 2012). These structural changes are dependent on maturation of microtubule bundles (Taylor et al., 2012). Expression of gap junction proteins Cx26 and Cx30 show drastic changes during the postnatal developmental period, with their expression increases rapidly and substantially between P0-P12 (Jagger and Forge, 2006). Both of these gap junction proteins are important for the passage of a variety of small molecules between their intercellular channels as well as other functions within the inner ear (Veenstra, 1996; Harris, 2001; Goldberg et al., 2004; Valiunas et al., 2005).

1.6.2 Auditory system development: spontaneous action potentials

Refining of auditory circuits during development, prior to any external sensory experience, critically depends on the firing of spontaneous action potentials or spiking activity (Kros et al., 1998; Katz and Shatz, 1996; Blankenship and Feller, 2009; Feller, 1999; O'Donovan, 1999). Spontaneous action potentials have been found to occur in the auditory nerve during the developmental stages prior to hearing onset (Gummer and Mark, 1994; Lippe, 1994), and this activity originates in the cochlea (Tritsch et al., 2007; Lippe, 1994; Jones et al., 2001; Jones et al., 2007). Spontaneous action potentials are present in sensory cells of the cochlea

at pre-hearing stages (Kros et al., 1998; Tritsch et al., 2007), and direct auditory pathway maturation through providing stimulation (Eckrich et al., 2018).

Throughout development, a group of supporting cells termed inner supporting cells spontaneously release regular doses of a molecule called ATP (Babola et al., 2020). The supporting cells detect their own ATP release through activation of their purinergic 'P2RY1' auto-receptors, and this initiates a metabotropic purinergic cascade that ultimately results in release of K^+ from the supporting cells, IHC depolarization and subsequent burst firing of the spiral ganglion neurons (SGNs) and auditory neurons (Babola et al., 2020). Currently, it is not known whether DCs are also involved in the generation of developmental spiking activity. Spontaneous action potentials in mouse IHCs can be observed as early as E16 (Babola et al., 2020), with this activity continuing until P12. Spiking frequency is at its highest in mouse IHCs from P1-8 (Marcotti et al., 2003b).

Mouse hearing onset is at P12 (Mikaelian and Ruben, 1965) and development continues after this age, in particular with the development of the endocochlear potential (Anniko, 1985). In mice, an initial potential is first seen at around P5, subsequently increasing in a progressive manner until P18 when it reaches that seen in adult mice (excess of +100 mV) (Sadanaga and Morimitsu, 1995).

1.6.3 Deiters' cells and auditory system development

Mellado Lagarde et al. (2013) found that selective ablation at P0 of the Deiters' and Pillar cells had a marked impact on the postnatal development of the cochlea and subsequent hearing ability in mice. The researchers found that apoptosis of OHCs began to occur at around P14–P15, with remaining OHCs showed disrupted development. Because this study ablated both Pillar and DCs, it is unclear exactly what subsequent abnormalities can be attributed to which specific supporting cell type. Overall, DCs and pillar cells were found to be vital for not only development, but also in performing critical roles within the cochlea. For example, Mellado Lagarde and colleagues demonstrated that DCs and Pillar cells are necessary for OHC survival and development of OC neural connections.

The importance of DCs in cochlear development was also found through previous research that indicated that DCs (along with Pillar cells) change their shape during normal cochlear development in a manner that is critical for the ability of the OC to transduce auditory stimuli. Specifically, the DCs and pillar cells acquire slimmer columnar shapes through the maturation of their microtubule bundles, forming phalangeal processes that lead to an opening of the fluid-filled tunnel of Corti and the spaces of Nuel around the OHCs (Colvin et al., 1996; Souter et al., 1997; Shim et al., 2005; Vater et al., 1997; Inoshita et al., 2008).

1.7 *OC Physiology*

1.7.1 Ion homeostasis in the cochlea

The cochlea contains three fluid-filled compartments, known as the scala tympani and scala vestibuli, which both contain perilymph (and consist of similar ion concentrations to the body's extracellular fluid) and the scala media (Figure 9) (Table 2), containing the

endolymphatic fluid (endolymph), which is similar to intracellular fluid ionic concentration (Dobie and Van Hemel, 2004).

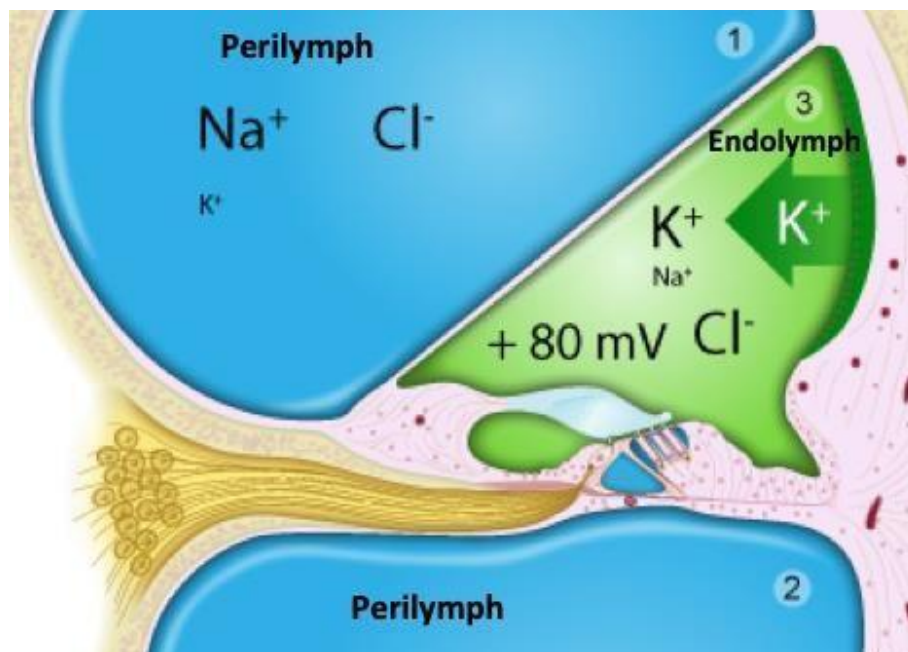


Figure 9: The fluid filled compartments of the cochlea.

The scala vestibuli (1) and the scala tympani (2) contain perilymph, which has a high concentration of sodium (Na⁺) (140mM) and low concentration of potassium (K⁺) (5mM) and calcium (Ca²⁺) (1.2mM). The scala media (3) contains endolymph, which is characterised by a high K⁺ concentration, a low Na⁺ concentration, and a positive potential (+80mV) when compared to the perilymph. Endolymph also shows a very low Ca²⁺ concentration of 20–30 μM. The Organ of Corti is bathed in endolymph. Figure adapted from (Delprat, 2016).

Composition	Perilymph	Endolymph
Na ⁺ (mM)	140	1
K ⁺ (mM)	4-5	150
Cl ⁻ (mM)	110	130
Ca ²⁺ (mM)	1.2	0.02-0.03
Osmolarity mosm/l	290	315
Potential	0	80
pH	7.4	7.4

Table 2: Composition of the perilymph and endolymph.

The two contrasting compositions function to regulate potassium flow while saving energy, since potassium ions enter hair cells passively from the endolymph across a concentration gradient, as concentration within the hair cell is lower than in the endolymph. Furthermore, potassium ions leave the hair cell passively via the perilymph, also due to a concentration gradient (Delprat and Irving, 2016).

1.7.2 Ion channels of the cochlea

Ion channels are grouped into categories based on what process initiates their opening.

Voltage-gated ion channels, such as potassium channels, are regulated by changes in transmembrane voltage (Kornreich, 2007). There are also ion channels regulated by the binding of ligands (ligand-gated), as well as channels with other gating mechanisms such as neurotransmitter-gated ion channels, ion-gated ion channels, nucleotide-gated ion channels and mechanically-gated ion channels (Alberts et al., 2002). Ligand-gated and voltage-gated channels both allow for the passage of ions, which is caused by ligand- or voltage-induced

conformational changes in channel protein structure. This change in structure, whereby the open channel allows ion passage, is referred to as activation (Kornreich, 2007) (Figure 10). The ion channel is closed when the channel protein structure does not allow for ion passage (referred to as the closed or inactivated state in relation to voltage-gated channels). The transition from the open state to the inactivated state is inactivation, and the transition from the inactivated state to the closed state is referred to as recovery from inactivation. It is important to note that the closed and inactivated states of a channel involve different conformational channel protein changes within the ion channel, despite both resulting in preventing ion passage (Kornreich, 2007).

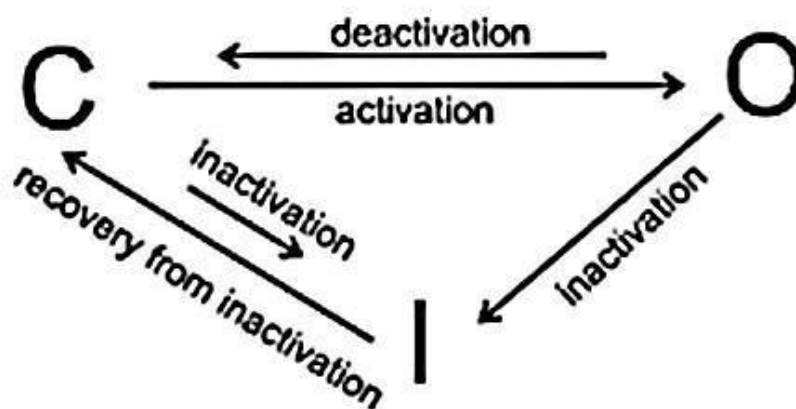


Figure 10: Channel conformational state transitions.

Schematic of gating transitions of voltage-dependent ion channels. Letters O, C and I represent the open state, closed state and inactivated state respectively. Voltage-dependent ion channels are expressed by excitable cells, these being potassium, sodium, calcium and chloride channels. From (Karmažínová and Lacinová, 2010).

In order for excitable cells to send impulses, the cells selectively change their permeability to different ions through voltage-gated channels. Voltage-gated sodium, potassium and calcium channels are composed of four main components. In the case of sodium and calcium channels, these are four linked domains. These four components are arranged surrounding a central pore that functions to conduct ions (Börjesson and Elinder, 2008). Such voltage-gated channels are all activated by membrane depolarisation. Voltage-gated channels possess activation and inactivation gates (Lousouarn and Tarek, 2021).

As of yet, only potassium currents have been studied in Deiters' cells (Chung et al., 2013; Nenov et al., 1998; Yang and Wang 2002). A summary of all channel types found on Deiters' cells can be found in Table 3.

Channel type	Channel name	Known function
Potassium channel	Outward and inward rectifying voltage-gated K ⁺ channel	<p>Of outward rectifying potassium channels:</p> <p>Possibly to buffer extracellular K⁺ between DCs and OHCs or neural fibres (Yang and Wang, 2002).</p> <p>Possibly to participate in the diffusion of K⁺ from the endolymph to the perilymph (Yang and Wang, 2002).</p> <p>To restore DC resting potential after the cells have been exposed to depolarising influences (Nenov et al., 1998).</p> <p>Of the inward rectifying potassium channel (Kir4.1):</p> <p>To set the resting membrane potential and regulate neurotransmitter release, as well as potassium homeostasis critical to hearing and hearing development (Chen and Zhao, 2014).</p>

	Big Conductance Ca ²⁺ -activated potassium channel	Involved in hearing development (Pyott et al., 2004; Kros, 2007). Hypothesised to have role in development of cochlear organisation and hearing function following P12 (age of mouse hearing onset) (Sakai et al., 2011).
Cation channels	ATP gated cation channels (P2X2)	Permeable to Ca ²⁺ and Na ⁺ (Bean, 1992; Nakagawa et al., 1990). This permeability is thought to allow DC adjustment of tension applied to the OHC during changing levels of sound (Chen and Bobbin, 1998).

Table 3: Summary of all known channels known to be present on Deiters' cells.

1.7.3 Voltage-gated sodium channels

In the mature and developing cochlea, voltage-gated sodium channels are essential for cochlear action potential generation and propagation. Voltage-gated sodium channels are the first channels to open in response to depolarisation, allowing for the flow of sodium ions across a concentration gradient into the excitable cell- with depolarisation being critical for the transformation of electrical signals into an action potential (Hernandez and Richards, 2022). Voltage-gated sodium channels are transiently expressed in cochlear hair cells before hearing onset, with all known subtypes of the channel being expressed in mouse cochlear sensory epithelia before the onset of hearing (Zhou et al., 2019). The subtypes of the voltage-gated sodium channels include nine Na_v1 channel subtypes named Na_v1.1 through Na_v1.9 (Chahine, 2018).

It is theorised that multiple sodium channel variants play roles in spiking activity seen in the pre-hearing cochlea, as these variants would be able to adapt to the unique physiological environment the developing organ presents. A large Na^+ current (I_{Na}) expressed during auditory system development can shape action potentials and to facilitate firing frequency by speeding up the time necessary for the membrane potential to reach threshold (Eckrich et al., 2012). I_{Na} has been observed in IHCs from E16.5 onwards, and this current increases in size significantly from P0 (Marcotti et al., 2003a), regulating the frequency of spiking activity (Eckrich et al., 2012). I_{Na} shows steady-state inactivation, and its contribution to spiking activity action potentials depends on the IHC resting membrane potential- which in spontaneously active IHCs (P0–P7) has been found to be between -55 mV and -60 mV (Eckrich et al., 2012). The resting potential of mature mouse cochlear hair cells is kept at around -72 mV (Oliver et al., 2003).

Voltage-gated calcium channels

Voltage gated calcium channels are expressed abundantly in the inner ear (Pangrsic et al., 2018), and they are also potentially expressed on the DCs (Shen et al., 2006; Nenov et al., 1998), although Nenov et al. (1998) suggested a potential low density or complete absence of them on DC membranes. Voltage-gated calcium channels activate upon depolarisation, opening to produce a rapid intracellular calcium flux (Cooper and Dimri, 2022).

External and internal Ca^{2+} regulates a multitude of diverse functions within the developing and mature cochlea (Ceriani and Mammano, 2012). In the cochlea, Ca^{2+} is an important regulator of sound-independent spiking activity (which is mostly mediated by L-type Ca^{2+} channels that contain the Cav1.3 subunit) (Platzer et al., 2000; Brandt et al., 2003), which is

critical to cochlear development (Eckrich et al., 2018; Burbridge et al., 2014; Marcotti et al., 2003a). Moreover, Ca^{2+} is one of the regulators of the MET current (Ricci and Fettiplace, 1998) and brings about a process known as MET current adaptation (Mammano et al., 2007). Intracellular Ca^{2+} signalling also regulates synaptic transmission and modulates receptor potential in the cochlea (Castellano-Muñoz and Ricci, 2014). Lastly, fine frequency tuning in the non-mammalian cochlea occurs through an interplay between voltage-gated calcium current and potassium current through neighbouring large conductance, calcium and voltage-activated potassium (BK) channels (Lewis and Hudspeth, 1983; Art and Fettiplace, 1987; Hudspeth and Lewis, 1988).

Cochlear Ca^{2+} homeostasis in the lymphatic fluids is essential for maintaining normal hearing function (Ceriani and Mammano, 2012). The concentration of endolymphatic Ca^{2+} is tightly controlled at a level that is unusually low (0.017–0.133 mmol/l) (Salt et al., 1989). Several *in vivo* studies have indicated that maintenance of low concentration of Ca^{2+} within the endolymph is essential for normal hearing (Wood et al., 2004), including evidence that scala media application of Ethylenediaminetetraacetic acid, which acts as a Ca^{2+} chelating agent, results in suppression of cochlear microphonics (Tanaka et al., 1979; Marcus et al., 1982). For the hair cells, Ca^{2+} influx through voltage-gated calcium channels supports the release of neurotransmitter (Parsons et al., 1994; Beutner and Moser, 2001; Robertson and Paki, 2002) and also functions to activate calcium-dependent potassium channels (Lewis and Hudspeth, 1983; Art and Fettiplace, 1987; Fuchs et al., 1988). Mature Ca^{2+} concentration in the endolymph is reached at P8 (Anniko and Wroblewski, 1981) and the strongly positive endocochlear potential (Table 2) drives cations out of the endolymph and into the hair cells

during mechanotransduction, and Ca^{2+} is actively transported out of the endolymph (Ikeda et al., 1988; Wood et al., 2004). Disrupted cochlear Ca^{2+} homeostasis is associated with the pathogenesis of Ménière's disease, a disease characterised by hearing loss, vertigo and tinnitus (Koenen and Andaloro, 2023). Investigating the calcium dependence of Deiters' cell potassium currents therefore adds necessary novel knowledge to the understanding of how Deiters' cells might be affected in cases of pathologically disrupted Ca^{2+} homeostasis within the cochlea.

1.7.4 Voltage-gated potassium channels

Potassium ions and channels perform a variety of roles such as excitable cell functioning, regulation of apoptosis, cell growth and differentiation (Grizel et al., 2014), and in the cochlea they play a key role in the cochlea's response to sound.

Voltage-gated potassium channels in excitable cells are responsible for regulating cellular excitability, with potassium channel opening causing membrane potential hyperpolarisation, and their closing producing depolarisation and excitation (Edwards and Weston, 1995) (Figure 11). Potassium channels are also responsible for the electrochemical gradient within the cochlea that results in the passive flow of K^+ into cells (Zdebik et al., 2009). IHCs express at least two different types of potassium channel, while OHCs express at least three (Kros and Crawford, 1990).

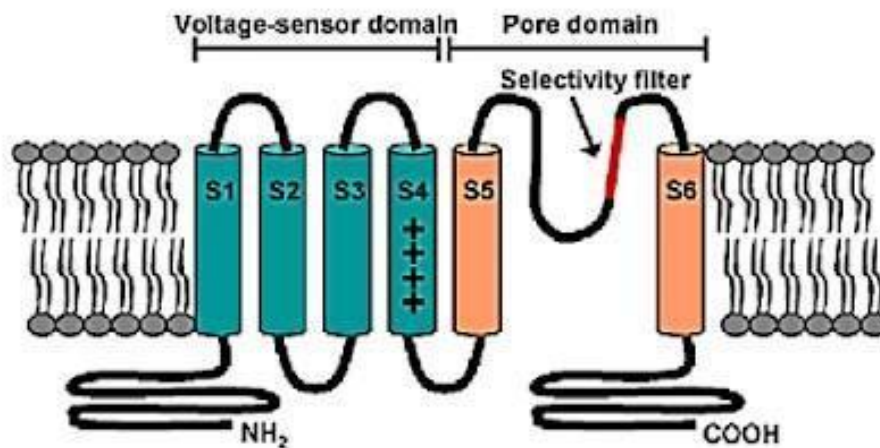


Figure 11: Voltage-gated potassium channel structure.

Voltage-gated potassium channels are tetramers, composed of subunits that consist of 6 transmembrane segments. The first to the fourth transmembrane segments form the voltage sensor domain, and the fifth and sixth form the channel pore. Figure adapted from Priest et al., 2008.

Changes in potassium ion conductance are key to the maturation of the postnatal cochlea (Kros et al., 1998; Marcotti et al., 2003b). Helyer et al (2004) investigated mouse embryonic expression of outward K^+ currents during hearing development in mouse embryos from E16 to birth. It was found that a conductance similar to $I_{k_{neo}}$ (a slow outward K^+ current expressed during the first postnatal week (Marcotti and Kros, 1999)) was present in basal IHCs from E16, and in apex OHCs from E18 onwards (Helyer et al., 2004).

The appearance of $I_{k_{neo}}$ is an important developmental stage within the first postnatal week for IHCs and OHCs (Kros, 1996). Changes in ionic conductances also continue through earlier

neonatal development. Marcotti et al. (2003b) noticed a distinct difference in the ionic conductances recorded from OHCs during the first postnatal week compared to conductances from P9 onwards. It was noted that before P9, when exposed to depolarising voltage steps, OHC ionic conductances showed slowly activating and partially inactivating voltage-dependent outward currents which were found to increase in amplitude over the first postnatal week (Marcotti et al., 2003b). From P9 onwards the slowly activating outward currents were still present in the mouse OHCs, but they did not show the same decay of currents seen in recordings taken prior to this age (Marcotti et al., 2003b). In IHCs, $I_{k_{neo}}$ persists until around the age of hearing onset (P12) (Mikaelian and Ruben, 1965; Shnerson and Pujol, 1981), after which a faster component of the current develops (Kros et al., 1998; Marcotti et al., 2003b). $I_{K,n}$ is a current that occurs after around P8-P9 in mature OHCs that is characterised by instantaneous inward currents activated at the holding potential and deactivates upon hyper-polarisation (Housley and Ashmore, 1992; Mammano and Ashmore, 1996; Nenov et al., 1998). $I_{K,n}$ contributes in part to the development of OHC excitability (Marcotti et al., 2003b).

The K^+ concentration of cochlear endolymph in mammals is maintained at around 150 mM (Wangemann, 2002). The endolymph has an endocochlear potential of +80 mV relative to perilymph, which has a lower concentration of K^+ (5mM) (Bekesy, 1952; Hibino and Kurachi, 2006). The endocochlear potential is maintained by K^+ transport across the lateral cochlear wall (Adachi et al., 2013). Fibrocytes and strial marginal cells (both cochlear supporting cell types) contribute indirectly to the generation of the endocochlear potential, by maintaining a low K^+ concentration in the fluid filled intrastrial spaces of the stria vascularis, and a high

K⁺ concentration in the intermediate cell cytosol (Wangemann, 2002). The stria vascularis is medially located within the lateral wall of the cochlea (Raphael and Altschuler, 2003) and made up of marginal cells, intermediate cells and basal cells (Furness, 2019). It is a heavily vascularised structure and fulfils the same homeostatic functions as the fibrocytes (Furness, 2019; Liu et al., 2016) as well as being critical for maintaining the ionic gradients and endocochlear potential (Hibino et al., 2009; Marcus et al., 1983; Salt et al., 1987).

Deiters' cells, like other supporting cells, are not excitable. Excitable referring to a cell's ability to signal via action potentials, generated through voltage-gated ion channels (Brady et al., 2005). Rather, DCs express spontaneous inward currents, during which, DCs depolarise from the cell resting potential (Ceriani et al., 2019). Deiters' cells express voltage-gated potassium channels and have been found to exhibit large outwardly rectifying K⁺ currents in response to depolarization (Zhao et al., 2000; Nenov et al., 1998; Chung et al., 2013; Yang and Wang, 2002). Voltage-gated potassium channels in DCs have been theorised to be involved in the diffusion of K⁺ from the endolymph to the perilymph (Yang and Wang, 2002) and in restoring DC resting potential after the cells have been exposed to depolarising influences (Nenov et al., 1998).

1.7.5 Calcium-dependence of the Deiters' cell potassium current

Kv channels as a group make up the largest grouping of potassium channels- with a total of twelve families (from Kv1 to Kv12) (Shah et al., 2006). There exist outwardly rectifying (Kv) and inwardly rectifying (Kir) type voltage-gated potassium channels (Hibino et al., 2010). The

Kir channels allow K^+ to move more easily into rather than out of the cell, while Kv channels bring about the opposite effect (Hibino et al., 2010; Shah et al., 2006). Nenov et al. (1998) found that the predominant voltage-dependent currents in DCs were outward rectifying and K^+ -selective. Following on from Nenov et al. (1998), Yang and Wang (2002) characterised potassium channel currents in DCs also, finding, through manipulating K^+ concentration in the extracellular solution, that potassium channels were the primary channel contributing to recorded DC currents.

Tetraethylammonium (TEA), which blocks voltage-gated potassium channels (Simmons, 2007), has been found to suppress outwardly rectifying currents in a concentration-dependent manner in adult guinea pig DCs (Nenov et al., 1998). Furthermore, Szűcs et al. (2006) also found that at higher mM TEA concentrations, both components of the DC outward current were inhibited significantly by the potassium channel blocker.

Chung et al. (2013) also found a TEA-sensitive current component in DCs. The researchers observed Deiters' cell ionic conductances when exposed to increasing concentrations of TEA, and when exposed to the potassium channel blocker Clofilium, which blocks outward rectifying potassium channels (Chung et al. 2013). The researchers hypothesised, based on the presence of a TEA-sensitive current component, that voltage-gated potassium channels Kv1.4 and Kv3.4 (Kv denoting voltage-gated potassium channel) are likely present on DCs (Chung et al., 2013). This is due to these channels being particularly sensitive to block by TEA, and the DCs showing sensitivity to exposure (Rudy et al., 1991).

Moreover, further evidence for the presence of multiple voltage-gated potassium channels on DCs was found by the researchers, in the finding that there was a biphasic time course of inactivation, revealed through pharmacological separation (Chung et al., 2013). Nenov et al. (1998) isolated the outward rectifying currents and attributed them to the Kv1.5 type channel. Szűcs et al. (2006) used Charybdotoxin, which is a blocker of voltage-dependent potassium channels Kv1.2 and Kv1.3 and of high-conductance calcium-activated potassium channels (Garcia et al., 1995). The researchers concluded, after finding a ChTx-sensitive, relatively rapidly inactivating current component in DCs, that the channel responsible for this current component was Kv1.3. This study is the only study of the three electrophysiological DC studies that attributes a current component to the channel Kv1.3 (the other studies being Chung et al. (2013) and Nenov et al. (1998)).

Nenov et al. (1998) was an important seminal paper in many aspects, one of those being that it was the first to examine the effect of the absence of external Ca^{2+} on the outward K^+ currents recorded in DCs. The researchers recorded outward currents from DCs in Ca^{2+} -free extracellular solution and found that almost half the cells presented a depolarising shift of the resting potential and smaller potassium currents. The researchers also noted a change in the current-voltage (*I-V*) curve of the cells in Ca^{2+} -free external solution, where it was seen that these cells exhibited a peak at a membrane potential of -60 mV while the rest of the cells showed a linear *I-V* curve without such a peak.

1.8 Aims and Objectives

There is currently a very limited understanding of the effect of extracellular calcium on DCs throughout neonatal development (Wan et al., 2013; Mellado Lagarde et al., 2013).

Investigating the effect of changing extracellular calcium concentration on neonatal DC potassium currents is important as disrupted calcium homeostasis in the inner ear is associated with various pathologies, including Ménière's disease (Koenen and Andaloro, 2023; Wood et al., 2004; Minakata et al., 2019). Moreover, understanding potential changes in the effect of calcium on DC potassium currents on different days during neonatal development would allow for the understanding of the development of DC potassium currents throughout this important period of development, as in other cells of the auditory system, namely the hair cells, the development of various potassium currents are key developmental processes (Kros, 1996; Kros et al., 1998; Marcotti et al., 2003b). Moreover, the first two postnatal weeks represent a critical developmental period as during this time, some key processes occur, such as the maturation and pruning of OHC synapses and spontaneous action potentials (Delacroix and Malgrange, 2015; Berekméri et al., 2019).

The present study will investigate mouse apical DC ionic conductances during a period of neonatal cochlear development (from postnatal day [P] 6 - P10). The range of ages examined are during a critical period of mouse postnatal cochlear development which involves many key developmental events (Berekméri et al., 2019). Ionic conductances will be investigated using the patch clamp technique in null-Ca²⁺ extracellular solution and Ca²⁺-containing extracellular solution to investigate the sensitivity of DC potassium currents to external Ca²⁺. Patch clamp recordings of potassium currents made in DCs and isolated by gap junction blocker 1-Heptanol-containing extracellular solution will also be investigated.

Finally, the potential effects of postnatal age on potassium currents investigations will be established. Therefore, the aims of this study are:

1. To investigate possible changes in expression of calcium-modulated channels in mouse DCs during a narrow window of neonatal cochlear development,
2. To investigate the effect of gap junction block/ DC isolation on recorded DC ionic conductances during a narrow window of neonatal cochlear development,

This investigation will make an important contribution to literature on Deiters' cells.

Moreover, with human and mouse auditory systems sharing similar cellular components and developmental events, this research can contribute to understanding of hearing development and therefore, potentially to the understanding of conditions that derive from abnormal auditory system development.

Chapter 2

Methodology

2.1.1 Ethics statement

All animal studies were performed in the UK and licensed by the Home Office under the Animals (Scientific Procedures) Act 1986 and were approved by the University of Brighton and University of Sussex Ethical Review Committees. Personal licence number: I35844177.

2.1.2 Tissue preparation

The mice were heterozygous for a recessive missense mutation in *Gna11* (D195G) (Source: MRC Harwell Institute) and therefore phenotypically wild type. Apical coil DCs of WT mice were studied in acutely dissected Organ of Corti, derived from animals of ages P6-P10, where the day of birth (P0) corresponds to E19.5. All mice were killed using Schedule 1 cervical dislocation. Organ of Corti dissection was carried out while the tissue was immersed in normal extracellular solution (Table 4). The dissection consisted of removing the bone, revealing the cochlea tissue spiralled around the modiolus. The modiolus and tectorial membrane were then removed. The apical portion of the cochlea was cut away and flattened under a holder. Increased magnification was used to identify the sensory epithelium under the patch clamp, and Hensen's cells were removed to reveal the DCs. Apical coil preparations were then added to the microscope chamber, in a bath containing extracellular solution components that depended on one of the two utilised experimental procedures being carried out (Figure 12) (Figure 13). Deiters' cells were identified under the microscope through observation of their unique morphological characteristics and the thin curved neck that is attached to the OHCs at their base and apex.

	High Ca ²⁺ - containing extracellular	Null (0) Ca ²⁺ extracellular	Normal extracellular solution
Sodium chloride	110	140	135
Potassium chloride	5.8	5.8	5.8
Calcium chloride	10	0	1.3
Magnesium chloride	0.9	0.9	0.9
Monosodium phosphate	0.7	0.7	0.7
D-glucose	5.6	5.6	5.6
HEPES	10	10	10
Sodium pyruvate	2	2	2

Table 4: Composition of extracellular solutions (in mM).

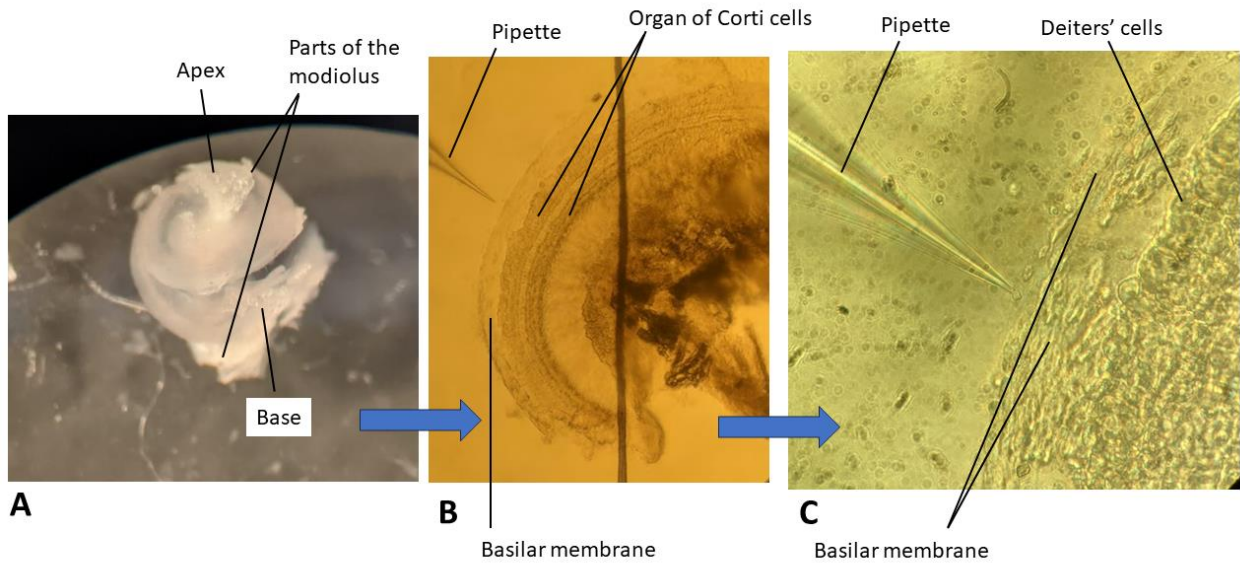


Figure 12: Images of the cochlear tissue during dissection and at different magnifications.

(A) Mouse cochlear during the dissection, showing the cochlear tissue (apex and base labelled), as well as parts of the modiolus that remained intact after dissection. The apical portion was cut from the rest of the cochlea and used for patch clamp experiments. (B) The apical cochlear tissue at 20X magnification, with the basilar membrane and various cells of the organ of Corti visible. (C) The apical cochlear tissue at 40X magnification, showing the outer layer of the Deiters' cells that were approached with the pipette and recorded from in experiments.

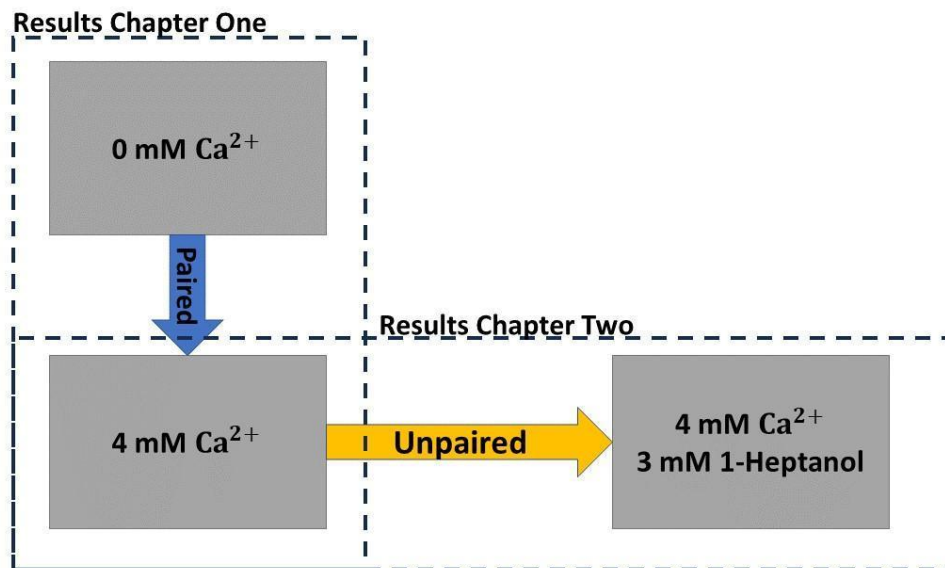


Figure 13: Flow diagram showing two experimental conditions

(A) Paired experiment that began with 2.5 ml of null-Ca²⁺ extracellular solution in the chamber, then 1ml of high Ca²⁺ extracellular solution was added, forming a dilution of 4 mM Ca²⁺ overall. (B) Unpaired experiment that involved comparing the 4mM high Ca²⁺ extracellular solution condition with a condition comprised of high Ca²⁺ extracellular solution containing 5mM 1-Heptanol, forming a dilution of 3 mM 1-Heptanol and 4 mM Ca²⁺ in the extracellular solution (2.5ml).

The present study utilised two experimental procedures to investigate DCs. One of these experimental procedures involved the OC tissue being transferred into a microscope chamber bath containing 'nominally zero' Ca²⁺ (null-Ca²⁺) extracellular solution (obtained by omitting Ca²⁺ from the extracellular solution, compensating for the reduced osmolarity (Table 5), then making patch-clamp recordings before raising the extracellular solution Ca²⁺ concentration to 4 mM and continuing recording.

The second experimental procedure involved an unpaired experiment in which patch-clamp recordings taken in 4 mM Ca²⁺ extracellular solution was compared with those taken in extracellular solution containing 4 mM Ca²⁺ concentration and 3 mM 1-Heptanol (Sigma Aldrich) (Table 5).

1-Heptanol- containing extracellular solution	
Components	mM
Sodium chloride	140
Potassium chloride	5.8
Calcium chloride	0
Magnesium chloride	0.9
Monosodium phosphate	0.7
D-glucose	5.6
HEPES	10
Sodium pyruvate	2
1-heptanol	5

Table 5: composition of 5 mM 1-Heptanol- containing extracellular solution (in mM).

In all electrophysiological experiments, only cells of healthy appearance were selected for electrophysiological recordings. Criteria for cell health included cell membranes with a smooth surface, absence of vacuoles in the cytoplasm and lack of Brownian motion of mitochondria.

2.1.3 Electrophysiological recording

Voltage- and current-clamp recordings were performed at room temperature (22-25°C) by the whole-cell patch clamp technique using Axon Digidata 1550B Low-Noise Data Acquisition System and HumSilencer digitiser system (Molecular Devices, LLC. San Jose, California) and a Multiclamp 700B amplifier (Molecular Devices, LLC. San Jose, California) (Figure 14). Patch pipettes were pulled from soda glass capillaries (Sutter Instrument, California, USA) using the PC-10 puller (Narishige group. Tokyo, Japan), and electrode resistances in the microscope chamber extracellular solution were between 2–13 MΩ. Electrodes were fire-polished using the MF-830 Microforge (Narishige group. Tokyo, Japan) in order to reduce pipette resistance. Patch pipettes were fitted into the Axon Instruments CV-7B voltage clamp head-stage (Molecular Devices, LLC. San Jose, California). Electrophysiological recordings were made using whole-cell capacitance compensation. Values of series resistance and whole-cell capacitance were obtained from readings from the Multiclamp 700B amplifier. Moreover, series resistance compensation was used on recordings and was typically in the range of 25-40 MΩ.

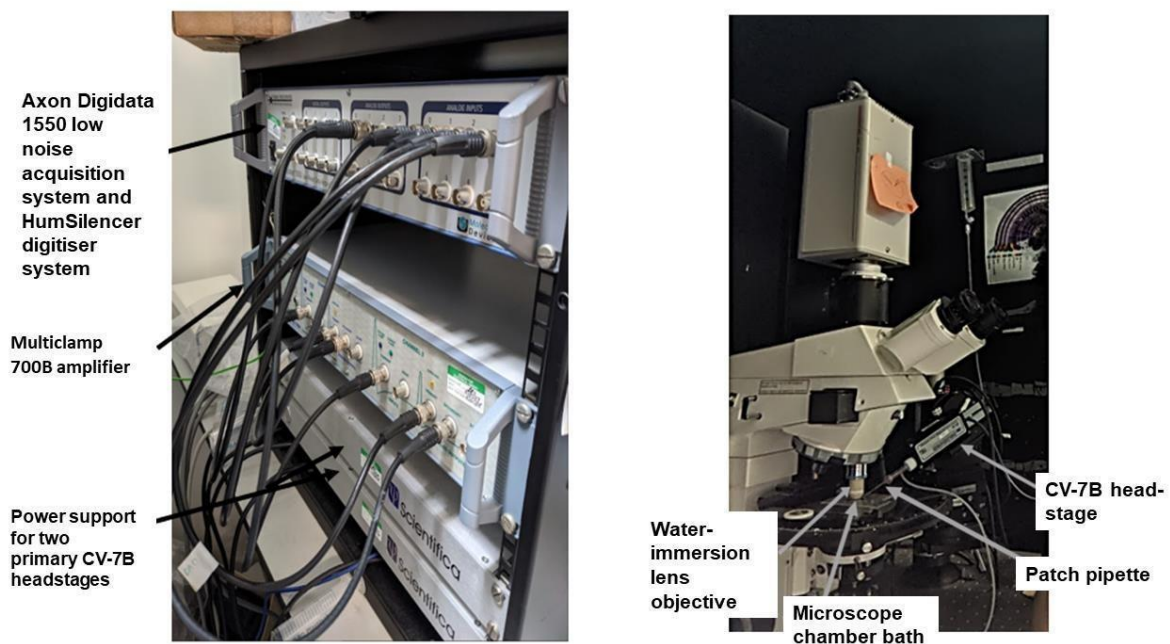


Figure 14: Photograph of the equipment set-up used for electrical recording.

The two photographs depict the Axon Digidata 1550 low noise acquisition system, Multiclamp 700B amplifier and the power support for the two primary CV-7B head-stages, as well as the head-stage itself, patch pipette, water immersion objective lens and microscope chamber bath.

Currents were recorded under voltage-clamp conditions using a pipette-filling intracellular solution containing (in mM) 131 KCl, 3 MgCl₂, 5 Na₂ATP, 10 Na₂- phosphocreatine, 1 EGTA, 5 HEPES and 0.3 Na₂GTP (Table 6). The pH of the pipette filling solution was adjusted to 7.5 using NaOH. The Organ of Corti preparations were observed with Nomarski differential interference contrast optics (×40 water-immersion objectives).

Intracellular solution	
Components	mM
Potassium chloride	131
Magnesium chloride	3
Adenosine 5'-triphosphate disodium	5
Sodium phosphocreatine	10
EGTA	1
HEPES	5
Guanosine 5'-triphosphate sodium salt hydrate	0.3

Table 6: composition of pipette-filling intracellular solution (in mM).

Data acquisition was performed using pClamp software (Axon Instruments, Union City, CA, USA). Data was filtered at 10 kHz (eight-pole Bessel), sampled at 50 kHz and stored on a computer.

2.1.4 Whole-cell patch clamp recording

Voltage clamp recordings were made in the whole-cell configuration (Figure 15). This configuration involves approaching the cell with the patch pipette, and when in contact with the membrane, applying sudden negative pressure. This pressure causes the cell membrane closest to the opening of the pipette to rupture, allowing for a seal to be made between the pipette and pipette filling solution and the cell's cytosol. Whole-cell voltage clamp configuration allows for the recording of cell currents flowing through the membrane, or for

the recording of the membrane potential and allows for the characterisation of various ion channels under controlled experimental conditions (Steinert, 2023).

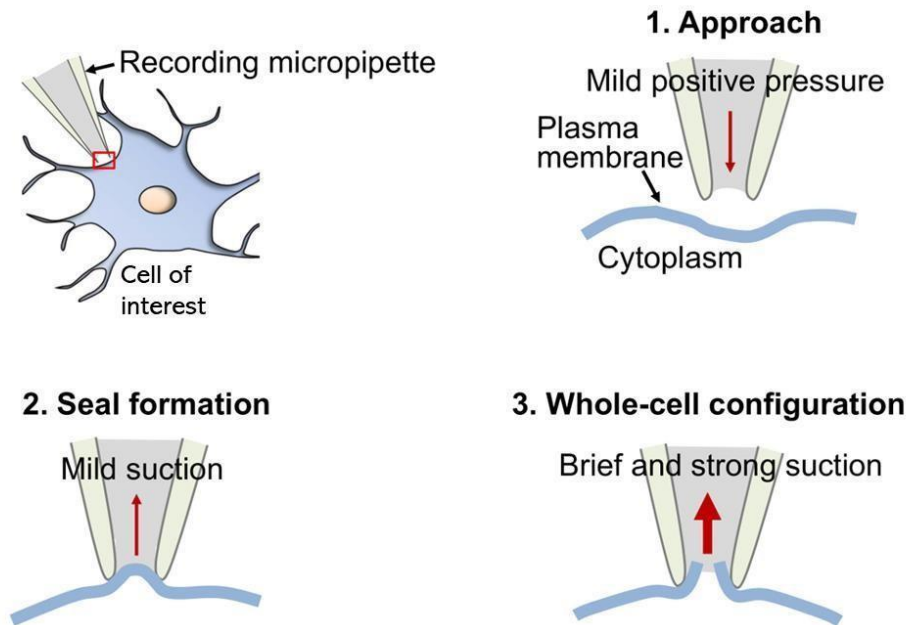


Figure 15: Schematic showing the steps involved in obtaining a whole-cell patch configuration.

This figure breaks the stages of obtaining whole-cell patch configuration into three key steps. The first is when the patch pipette approaches the cell of interest, a mild positive pressure is applied in the patch pipette at this stage. The second stage is when a sudden negative pressure is applied through the patch pipette, with mild suction applied at first. The third stage involves a strong suction that causes the cell membrane to rupture and form a strong seal with the patch pipette, forming a direct contact between the liquid environments of both the cell's cytosol and the pipette intracellular solution. Figure adapted from Segev et al., (2016).

2.1.5 Data analysis

Data analysis was computed using GraphPad Prism version 9 (GraphPad Software, California, USA). All analyses were considered statistically significant when the p value was <0.05 . Some data analysis was done using Clampfit software (Axon Instruments, Union City, CA, USA). Holding currents are plotted as zero current. Where relevant, data is presented with mean values and standard error of the means.

Current density and amplitude:

Current (I) was converted to current density by dividing the current amplitude (pA) at each membrane voltage step by the cell capacitance (pF). Current density and I-V relationships were also investigated using two-Way and one-Way ANOVA, depending on the number of independent variables. The Greenhouse-Geisser correction was used to adjust for lack of sphericity when utilising two-way repeated measures ANOVA, due to small sample sizes. Multiple comparisons were corrected for using the Bonferroni test, which adjusts the p -values because of the increased risk of a type I error.

Input resistance:

Input resistance was calculated through Ohm's law (Resistance= Voltage (mV)/ Current (pA)).

Passive membrane properties:

The passive cell membrane properties (cell properties that allow for the conduction of electrical impulses without the use of voltage-gated ion channels (Al-muhtasib, 2023)) of input resistance and cell capacitance were investigated using paired t-tests and One-Way ANOVA. Multiple comparisons were corrected for using the Bonferroni test.

Nernst potential

The Nernst potential was calculated according to the following formula:

$$V_{Eq.} = \frac{RT}{zF} \ln\left(\frac{[X]_{out}}{[X]_{in}}\right)$$

Where V_{Eq} is the equilibrium potential (Nernst potential) for a given ion, R is the universal gas constant, T is the temperature in Kelvin, z is the valence of the ionic species, F is the Faraday's constant, $[X]_{out}$ is the concentration of the ionic species X in the extracellular fluid and $[X]_{in}$ is the concentration of the ionic species X in the intracellular fluid.

Inactivation kinetics:

Percentage inactivation was calculated by subtracting the C-statistic (a percentage estimate of current amplitude if the protocol had measured the rate of inactivation over a longer time period) from 100.

Chapter 3
Potassium channel
activation in
neonatal Deiters'
cells

3.1 Introduction:

Voltage-gated potassium (Kv) channels are considered to be the most significant contributors to ionic conductances in DCs (Yang and Wang, 2002; Nenov et al., 1998; Chung et al., 2013). Despite this contribution, electrophysiological properties of DCs during neonatal development have not yet been investigated. As previously described in this thesis, Nenov et al. (1998) investigated the effects of null calcium and a calcium containing extracellular solution on DC activation and found that in a subset of 11 cells tested, 6 did not show any effect of Ca^{2+} while the rest of the cells in elevated Ca^{2+} exhibited a reduction in current amplitudes and a depolarizing shift of the resting potential, with an *I-V* curve presenting a peak at 60 mV. Further investigation in DCs would allow for a clearer understanding of whether Ca^{2+} potentially modulates activation, and it should be noted that in a previous study there was no difference in DC activation properties when recording in null-calcium extracellular solution (Chung et al., 2013).

In the present study, investigation of the activation of voltage-gated channels in DCs was conducted through eliciting depolarising voltage steps (Figure 16). Channel activation properties were investigated in DCs in null-calcium extracellular solution, and again after raising extracellular Ca^{2+} to 4 mM ('high calcium' extracellular solution (Table 4)). The possible impact of neonatal age on activation properties was also investigated, with age groups P7, P8 and P9 compared. This was initially investigated through analysing the peak of the activation trace. Because, in the present study, the Nav and Cav channels were not blocked, and Kv channels have a comparatively slower time of inactivation compared to other voltage-gated channels (Lacroix et al., 2013), recordings were also analysed by measuring from the later pseudo steady-state at the end of the activation trace.

3.2 Aims:

The experiments in this chapter aimed to characterise the potentially unique activation properties of DCs during neonatal development. Mouse DC activation recordings were grouped into two age groups: a P7 group (n=3) and a P8 group (n=3). The aims were:

- To investigate the potential effect of extracellular calcium concentration on DC activation when measuring peak activation
- To investigate the potential effect of extracellular calcium concentration on DC activation when measuring pseudo steady-state activation

3.3 Results

Typical examples of ionic currents recorded from DCs at age postnatal day (P) 7 in null calcium and high calcium extracellular solution are shown in Figure 17A. Depolarizing voltage steps from the holding potential of -80 mV caused slowly activating and modestly inactivating voltage-dependent outward currents in P7 and P8 aged mouse DCs, with the reversal potential (E_{rev}) of around -80 mV.

Peak voltage-activated potassium current amplitude is not modulated by extracellular calcium in neonatal Deiters' cells

The I - V curve in both extracellular solutions was nonlinear and outwardly-rectifying at hyperpolarised membrane voltages. The most depolarising membrane voltage of $+40$ mV should elicit the greatest extent of activation.

There was found to be no statistically significant interaction between the change in membrane voltage and calcium concentration on the recorded current amplitudes: $F(1.21, 6.07) = 3.05$ ($p=0.13$, $n=6$), (repeated-measures two-way ANOVA) (Figure 17B). Main effects describe the relationship between one independent variable, while interaction effects describe the relationship between two independent variables and the dependent response variable. The main effect of calcium concentration on recorded current amplitudes was not statistically significant: $F(1.00, 5.00) = 2.55$ ($p=0.17$, $n=6$). Furthermore, the main effect of changing membrane voltage was statistically significant $F(1.01, 5.04) = 36.96$ ($p=0.0017$, $n=6$).

Neonatal Deiters' cell input resistance is not modulated by calcium

Some potassium channels in excitable cells contribute to the leak conductance, which typically has a linear I - V , affects the cells input resistance and contributes to currents measured during voltage steps. Input resistance is a quantification of the total cell resistance and is a measure that depends on the number of open channels in the cell membrane (Almuhtasib, 2023). To establish whether the leak conductance at -80 mV was sensitive to changes in extracellular calcium, the DC input resistance was measured from test pulses performed at the start of the protocol. The input resistance when comparing that measured between the two extracellular solution conditions was not statistically significant $t(4) = 1.74$, $p = 0.16$, (Paired t-test) (Figure 17C).

Neonatal Deiters' cell capacitance is slightly lower in high calcium

The cell capacitance (pF) was measured to observe potential structural cell membrane surface area/ size change when changing extracellular calcium (Figure 17D). The difference in cell capacitance when comparing that measured between the two extracellular solution conditions was statistically significant $t(4) = 2.93$, $p = 0.043$, (Paired t-test).

Current density of neonatal Deiters' cells is not modulated by calcium

There were some small but significant changes in cell capacitance, which may reflect changes in cell size or specific membrane capacitance. Thus, currents were normalised to the cell capacitance to determine if the factors, age and calcium, affected current density (Kula et al., 2020). The difference in absolute current density when comparing that measured between the two extracellular solution conditions was not statistically significant, $t(5) = 0.95$, $p = 0.38$ (Paired t-test) (Figure 17F).

There was found to be no statistically significant interaction between the change in membrane voltage and calcium concentration on the recorded absolute mean current densities: $F(1.22, 6.11) = 0.53$ ($p = 0.53$, $n = 6$), (repeated-measures two-way ANOVA) (Figure 17E). The main effect of calcium concentration on absolute mean current densities was not statistically significant: $F(1.00, 5.00) = 0.083$ ($p = 0.78$, $n = 6$). Further, the main effect of changing membrane voltage was statistically significant $F(1.02, 5.11) = 59.21$ ($p = 0.0005$, $n = 6$).

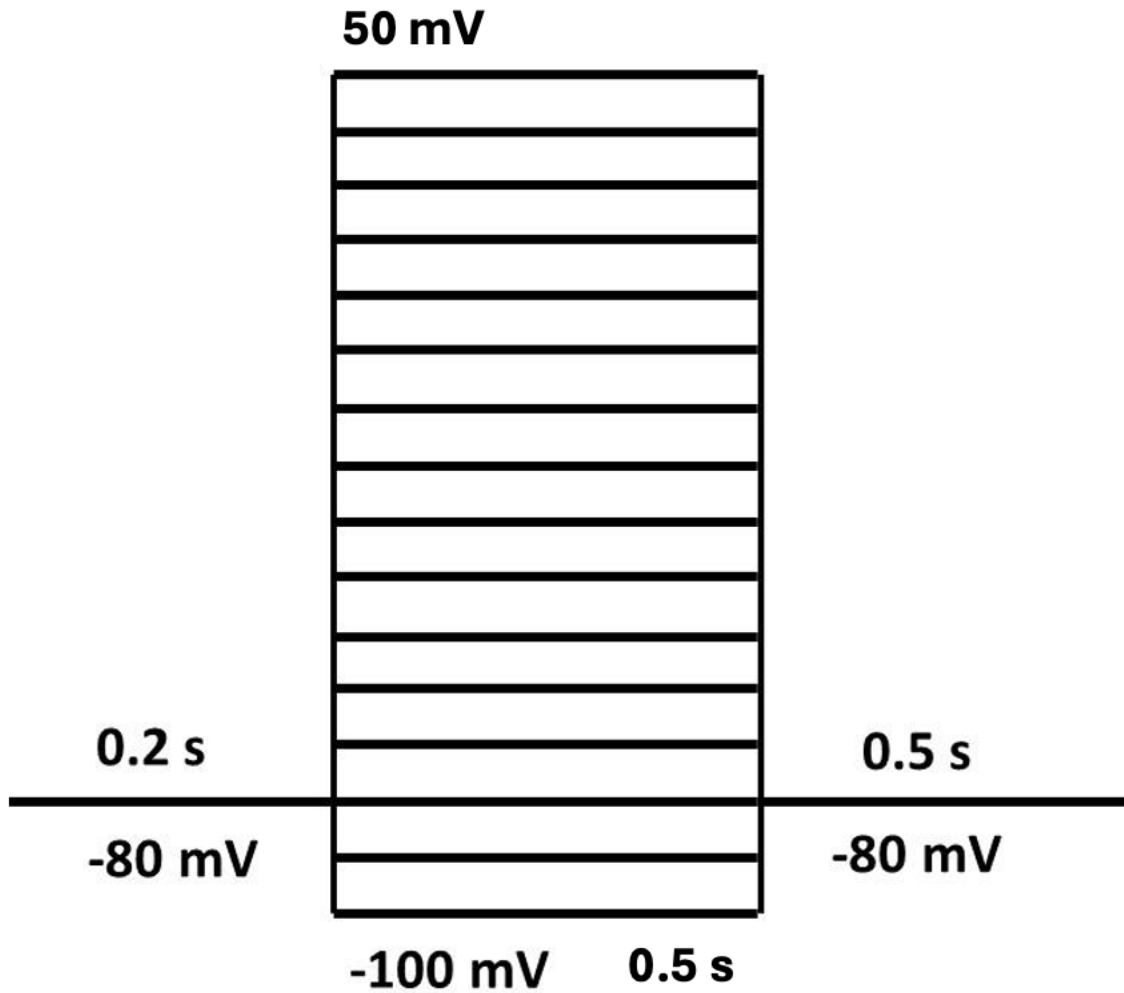


Figure 16: Activation protocols utilised.

For investigation of DC Kv channel activation, current traces were elicited using 0.5 second depolarising voltage steps in 10-mV increments from -100 to +50 mV, the holding potential was -80 mV.

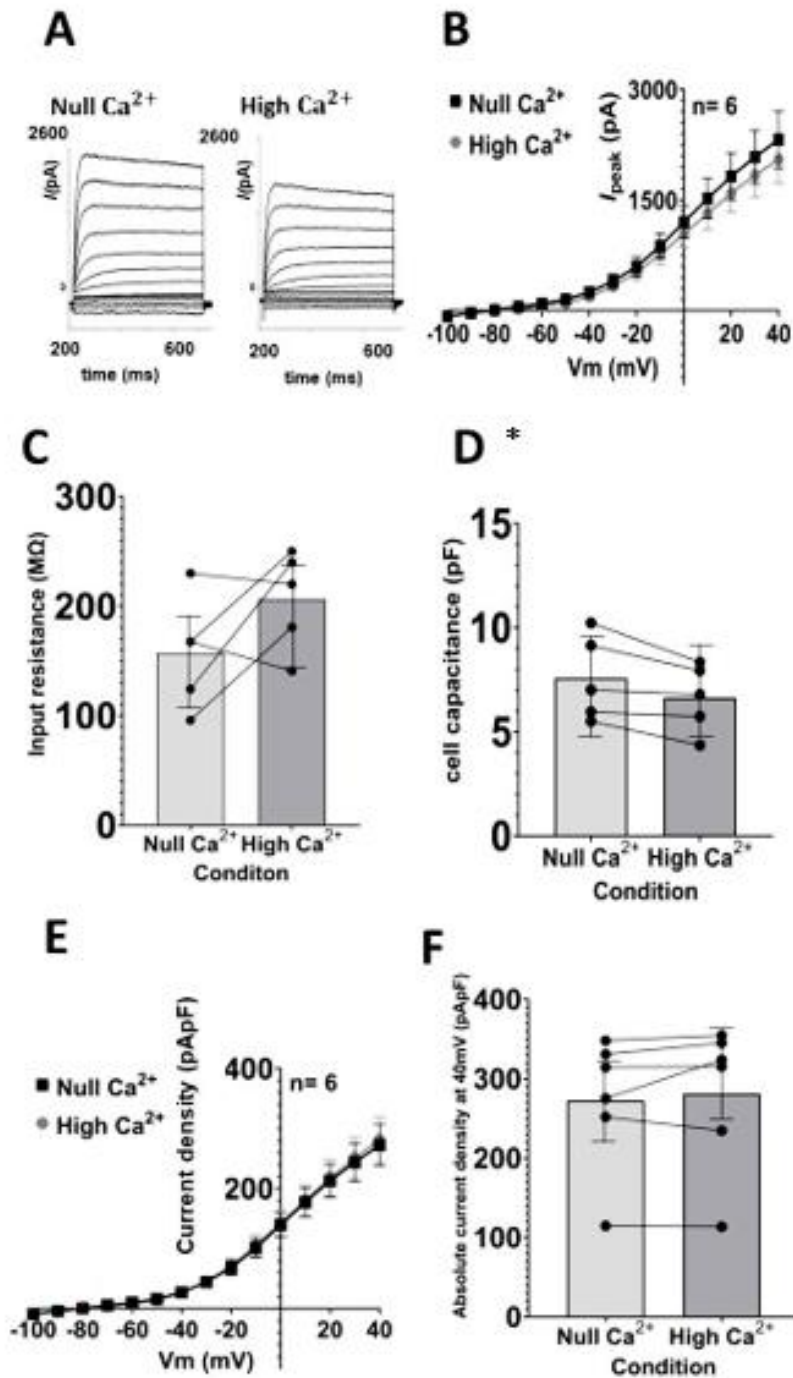


Figure 17: Graphs for ages postnatal day (P) 7 to P8 using peak of activation trace.

(A) Examples of current traces recorded at P7 from apically located Deiters' cells when in null calcium extracellular solution and high calcium extracellular solution. Current traces were elicited using 550-ms depolarising voltage steps in 10-mV increments from -80 to 40 mV. The holding potential was -80 mV. (B) Plot of the mean current-voltage relationships,

corresponding to changes in the magnitude of the transient current when in the two extracellular solution conditions for P7 (n= 3) and P8 (n= 2) (+/- SEM; mean). The mean current amplitude activated during steps to +40mV for all cells (P7-8) in null-calcium extracellular solution was 2317.33 pA (n=6, SEM= 391.01 pA). The same in high-calcium extracellular solution was 2049.59 pA (n=6, SEM= 327.51 pA). (C) Input resistances for both extracellular solution conditions for P7 and P8 (+/- SEM; mean) = 157.00 M Ω (SEM: 22.77 M Ω) in the null calcium extracellular solution, and 206.30 M Ω (SEM: 20.20 M Ω) in the high calcium containing extracellular solution). (D) Cell capacitance in both extracellular solution conditions for P7 and P8, the mean = 7.54 pF (SEM= 0.91 pF) in the null-calcium extracellular solution and the mean = 6.64 pF (SEM= 0.73 pF) in the high calcium containing extracellular solution ($p= 0.043$, (Paired t-test). (E) Mean current density for P7 and P8 in both extracellular solution conditions (+/- SEM). (F) Absolute current density (pA/pF) recorded at membrane potential of +40 mV in both extracellular solution conditions for the pooled P7 and P8 group (+/- SEM; mean). Mean= 272.58 pA/pF (SEM= 34.73 pA/pF) in null-calcium extracellular solution and the mean= 281.21 pA/pF (SEM= 37.71 pA/pF) in high calcium extracellular solution. Individual data points are shown on bar-chart graphs- (C), (D) and (F). Bars represent group means.

The observed reversal potential (-80 mV) of the peak depolarization-dependent current is consistent with the activation of potassium channels. Potassium channels tend to inactivate more slowly than sodium and calcium channels. As such, to rule out any contribution other

channels contributing to the currents, the effect of extracellular calcium on the pseudo steady-state currents was analysed at the end of the 0.5 s voltage steps. Pseudo steady-state currents were normalised to the capacitance measurements of the cells (Figure 17A) to give current densities as a function of voltage.

Voltage-activated potassium activation steady-state current density is not modulated by extracellular calcium in neonatal Deiters' cells

Current density is a parameter that characterises individual cell ionic membrane currents, by evaluating data with the presumption that the amplitude of membrane current is directly proportional to the cell's membrane capacitance (Kula et al., 2020). The relationship between current density and voltage was remarkably similar in null and high calcium across the ages of P7 and P8 (Figure 18A-C).

For the P7 age group (n= 4), there was found to be no statistically significant interaction between the change in membrane voltage and calcium concentration on the recorded mean current densities: $F(1.42,4.27)= 0.80$ ($p= 0.47$), (repeated-measures two-way ANOVA) (Figure 18A). The main effect of calcium concentration on the recorded mean current densities was not statistically significant: $F(1.00, 3.00)= 0.77$ ($p=0.45$). Further, the main effect of changing membrane voltage was statistically significant $F(1.12, 3.35)= 196.30$ ($p=0.00040$).

For the P8 age group (n= 2), there was found to be no statistically significant interaction between the change in membrane voltage and calcium concentration on the recorded mean current densities: $F(1.42,4.27)= 1.05$ ($p= 0.49$), (repeated-measures two-way ANOVA)

(Figure 18B). The main effect of calcium concentration on the recorded mean current densities was not statistically significant: $F(1.00, 1.00) = 0.10$ ($p=0.50$). Further, the main effect of changing membrane voltage was not statistically significant $F(1.00, 1.00) = 4.06$ ($p=0.29$).

Since the lack of statistical significance could arise from the small sample sizes, the P7 and P8 age groups were pooled to better observe any differences. For the pooled P7 and P8 age group ($n=6$), there was found to be no statistically significant interaction between the change in membrane voltage and calcium concentration on the recorded mean current densities: $F(1.24, 6.20) = 0.44$ ($p=0.57$), (repeated-measures two-way ANOVA) (Figure 18D). The main effect of calcium concentration on the recorded mean current densities was not statistically significant: $F(1.00, 5.00) = 0.0035$ ($p=0.96$). Further, the main effect of changing membrane voltage was statistically significant $F(1.002, 5.12) = 53.56$ ($p=0.0007$).

Investigating steady-state current density at +40 mV across age groups and conditions

There was found to be no statistically significant interaction between calcium concentration and neonatal age on the mean current densities at +40 mV: $F(1,4) = 1.45$ ($p=0.29$), (repeated-measures two-way ANOVA). The main effect of calcium concentration on the mean current densities at +40 mV was not statistically significant: $F(1.00, 3.05) = 4.11$ ($p=0.081$). Further, the main effect of changing membrane voltage was not statistically significant $F(1.00, 3.12) = 4.29$ ($p=0.075$).

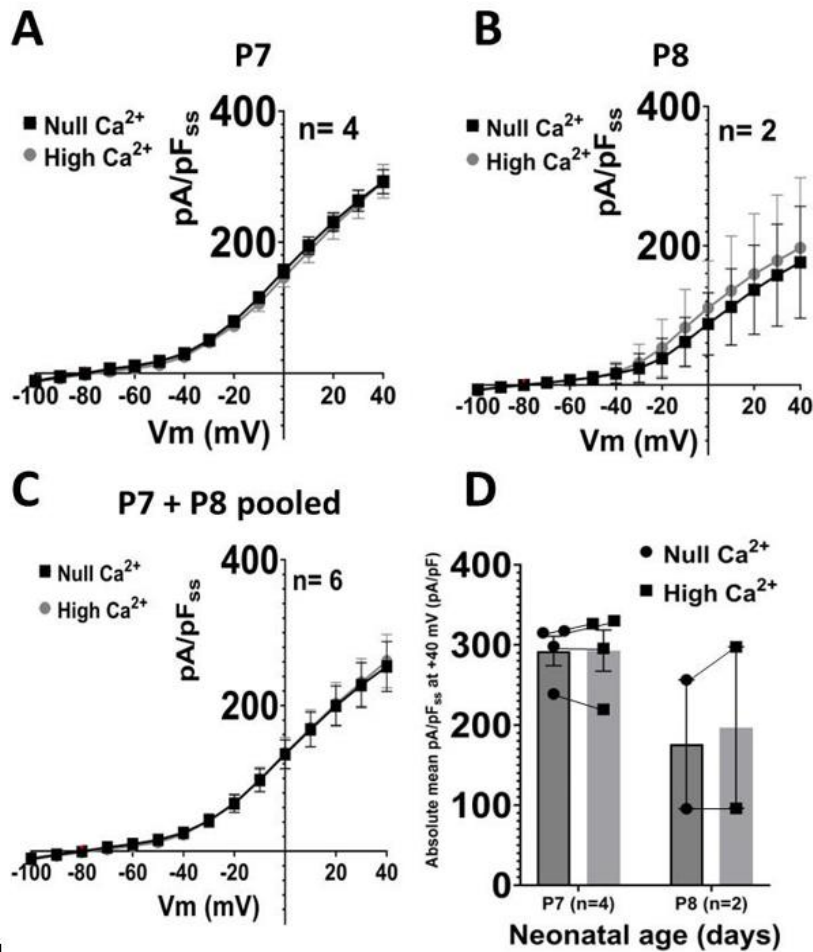


Figure 18: Graphs for ages postnatal day (P) 7 to P8 using the steady-state of the activation trace.

(A) Mean current density of P7 (n=4) from apically located Deiters' cells when in null calcium extracellular solution and high calcium extracellular solution (+/- SEM; mean) at +40 mV= 292.35 pA/pF in null-calcium extracellular solution, and 292.92 pA/pF (SEM= 25.67 pA/pF) in high calcium extracellular solution. (B) Mean current density of P8 (n=2) from apically located Deiters' cells when in the two extracellular solution conditions (+/- SEM; mean) at +40 mV= mV = 175.97 pA/pF in null-calcium extracellular solution, and 196.73 pA/pF in high calcium extracellular solution. (C) Mean current density (pA/pF) of pooled P7 and P8 apically located Deiters' cells when in the two extracellular solution conditions (+/- SEM; mean) at +40 mV= 253.56 pA/pF (SEM= 34.17 pA/pF, n= 6) in null-calcium extracellular solution, and 260.86 pA/pF (SEM= 36.77 pA/pF) in high calcium extracellular solution. (D) Mean current density at +40 mV in both

extracellular solution conditions for P7 and P8 plotted separately, including individual data points and SEM. Bars represent group means.

3.4 Main findings

In recordings made from DCs, depolarisation-activated currents that were slowly inactivating and outwardly rectifying, as well as being reversed at -80 mV were detected. It was found that changing extracellular solution calcium concentration from 0 mM to 4 mM has no statistically significant effect on the peak or steady-state depolarisation-activated current amplitude or current density in neonatal DCs aged P7-P8. Moreover, input resistance measured at resting membrane potential (and therefore leak conductance) in neonatal DCs is not modulated by extracellular calcium concentration. A small, but significant effect of extracellular calcium on cell capacitance was observed, but even accounting for this, no significant effect of calcium on potassium current density was detected.

3.5 Discussion

Depolarising voltage steps from the holding potential of -80 mV (Activation protocol shown in (Figure 16)) caused slowly developing voltage-dependent outward currents in P7 and P8 aged mouse DCs, with E_{rev} of ~ -80 mV suggesting that the main channel type contributing to this current is the Kv channel, since K^+ ions are expected to have a Nernst potential (E_K) of ~ -80 mV, based on the composition of intracellular and extracellular solutions used. This was also a finding seen when analysing the activation trace steady-state. There are 12 families of

Kv channels that form the most diverse group of potassium channels (Kv1-Kv12) (Gutman et al., 2005). Previous findings suggest the presence of Kv1.5 channels on DC membranes, as well as potentially Kv1.4 or Kv3.4 expression (Nenov et al., 1998; Chung et al., 2013). The Kv channel possesses two gates- gates being spaces through which ion passage occurs (Figure 19). The first gate is the lower gate, which is made up of six transmembrane helices, crossing on the intracellular side of the channel. The second gate is the upper gate, which is composed of the pore-loop (P-loop)- a structure that houses the channel selectivity filter that determines what specific type of ions the channel conducts, located on the extracellular side of the channel (Gutman et al., 2005).

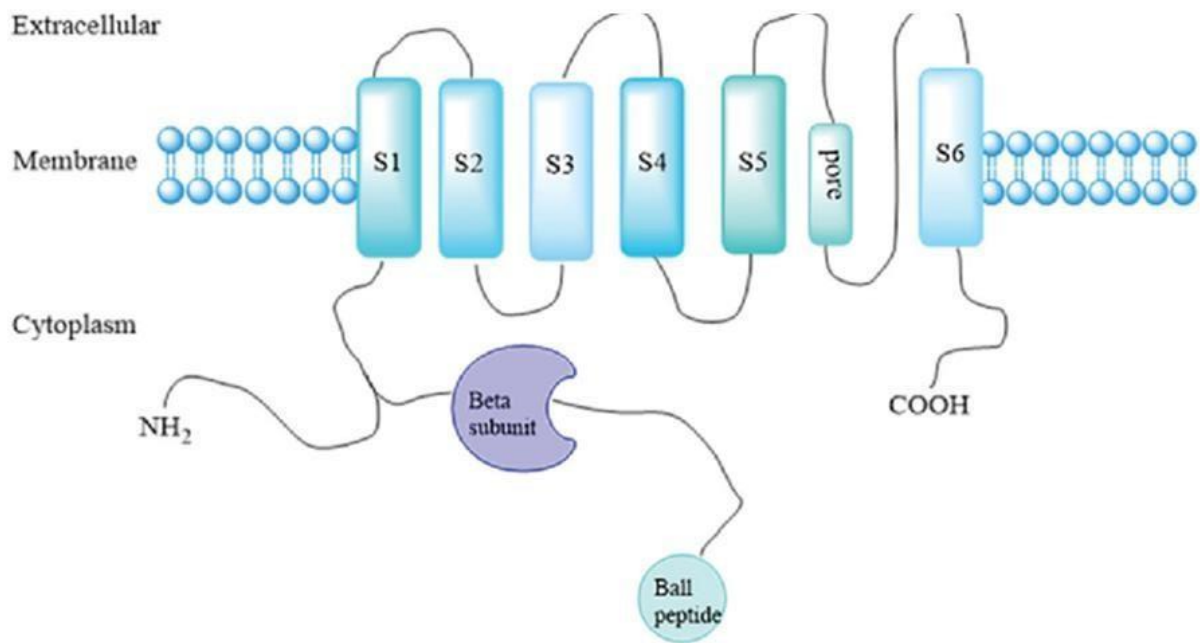


Figure 19: Schematic of the structure of voltage-gated potassium channel Kv1.5.

Shown are the six transmembrane segments or helices (S1-S6), the channel pore in the form of a pore-loop that is located between S5 and S6. Also shown is the linker to the N-terminus of a B-subunit, which are structures that connect to the channel ball peptide-this being a structure that plugs the open channel pore during inactivation. Figure from (Zhao et al., 2022).

The Kv1.5 channel has been found to exhibit features of activation that are sensitive to extracellular calcium concentration, with elevated extracellular calcium shifting the activation curve to the right- leading to the theory that the channel likely possesses calcium binding sites (Trapani and Korn, 2003). Considering this channel is potentially present on DCs (Nenov et al., 1998), it is interesting that there was no effect of changing extracellular calcium concentration on neonatal DC current amplitudes and densities. However, if the

Kv1.5 channel is expressed on DCs, it could be possible that this channel is not matured or expressed on DCs until a later stage in development. Changing channel configuration is important during cochlear development, as it is important for the mediation of spontaneous activity that refines the auditory system during this time (Moody and Bosma, 2005).

In excitable cells, depolarisation of the cell membrane also activates Cav channels, leading to influx of calcium into the cell (Catterall, 2011). Cav channels are subdivided based on their activation properties into two groups, the low and high threshold-activated channels- high threshold meaning the channels are distinguished by a high voltage of activation, and low threshold meaning activation occurs at a relatively lower membrane voltage (Catterall, 2011). Taking this into account, it is interesting that changing calcium concentration did not significantly change current density and current amplitudes, even at more depolarised voltages. It is possible that there is limited expression of BK channels on DCs between ages P7-P8, as BK channel expression and distribution on neonatal DCs has not yet been investigated.

In regard to the reduction in cell capacitance in 4mM calcium (Figure 17D), this could be due to the large amount of variation that exists between various animals, since individual differences, even within the same litter, can contribute to differences in cell capacitance. For example, differences in intrauterine environment, sex, maternal care and litter size can contribute to large differences in cell vitality and size (Crews et al., 2009; Golub and Sobin, 2020). Moreover, variations in the postnatal environment may impact critical periods of

early development (Valiquette et al., 2023). Therefore, this variation greatly obscures the potential link between high calcium extracellular solution and changes in cell capacitance. Moreover, the DCs, having been exposed to the null calcium extracellular solution, will be undergoing necrosis, in the high calcium condition, and therefore swelling in size, which will affect measurements of cell capacitance (Park et al., 2023). This is a result of sodium toxicity in the null calcium condition the cells, caused by the initial increased concentration gradient of calcium found within the cell when compared to the extracellular space (0 Ca outside the cell). This change in gradient adjusts the functioning of the Na/Ca ATPase, which resultantly pumps excess sodium into the cytoplasm (Skou, 1990). The toxicity of 1-heptanol would also be a contributor to cell swelling and death.

Current trace peak measurements were compared with steady-state measurements since Kv channels activate relatively slower than Nav channels, with the steady-state currents representing currents at a later time scale than peak measurements (Lacroix et al., 2013). The lack of significant differences between conditions when using the peak and when using the steady-state currents suggests that changing the extracellular calcium concentration does not affect current density or amplitude. The results of the present study are in contrast to the study by Nenov et al. (1998) who found that DCs in null calcium extracellular solution presented a depolarising shift of the resting potential and a decrease in current amplitude. The researchers also noted a change in the *I-V* relation curve of cells in null calcium extracellular solution, where it was seen that some DCs exhibited a current amplitude peak at a membrane potential of -60 mV (Nenov et al., 1998). In the present study, peak current amplitudes were seen at the more depolarised membrane voltage of +40 mV (Figure 17B).

The lack of difference in mean current density across ages and conditions for both peak and steady-state measurements when comparing P7 and P8 cells may be due to how close they are in age, as ion channel number and distribution may not have changed significantly over that short time. However, the absence of any significant effect of extracellular calcium concentration is in line with previous research that suggests extracellular calcium concentration may not affect DC functioning, as in just over half of cells in the dataset, Nenov et al. (1998) found that comparing activation in null calcium to that in calcium showed no evidence of modulation of DC activation by extracellular calcium.

Chapter 4

Effects of gap junction block on measurements of potassium currents in Deiters' cells

4.1 Introduction:

Extracellular calcium concentration is a major regulator of the connexin proteins, which form gap junctions (Lopez et al., 2016). Gap junctions are located between cochlear supporting cells and are critical during cochlear development as they maintain homeostasis of the microenvironment found within the organ (Wang et al., 2009; Johnson et al., 2016).

The faithful representation of the ionic currents across cell membranes in whole-cell recordings depends crucially on how effectively the membrane potential can be voltage clamped. Moreover, the membrane potential in parts of the cell that are more distal from the patch pipette tip are under less adequate voltage control - a factor that affects the size of the whole cell currents (Bar-Yehuda and Korngreen, 2008). Deiters' cells are coupled with other DCs and supporting cells via gap junctions (Zhao, 2000) therefore effectively extending the amount of membrane to be voltage clamped and thereby introducing this type of space-clamp issue. Both Deiter's cells that are coupled via gap junctions and uncoupled/isolated DCs exhibit large outward potassium currents in response to depolarisation (Zhao, 2000). The present study investigates the effect of gap junction block on these potassium currents.

One-Heptanol has been widely used as an efficient gap junction blocker in research conducted on cardiac cells (Garcia-Dorado et al., 1997; Moysan et al., 2023; Kimura et al., 1995; Bastiaanse et al., 1993). There is, as of time of writing, no published research utilising 1-Heptanol to block gap junctions between neighbouring DCs. However, there are studies that use a closely structurally related gap junction blocker called Octanol (Moysan et al., 2023; Lagostena and Mammano, 2001). Octanol has been found to inhibit intercellular Ca^{2+}

waves propagated by gap junctions between DCs, and in these studies, 1 mM concentrations of Octanol have been found to be effective at causing this intended connexin gap junction block (Sirko et al., 2018; Lagostena and Mammano, 2001). Investigating DC activation ionic conductances when the gap junctions are blocked, and therefore the cell is electrically isolated, is important in this study as gap junctions are modulated by extracellular calcium (Peracchia, 2020). Therefore, investigating the contribution that gap junctions make to activating ionic conductance can further elucidate the effect of extracellular calcium on DC functioning.

In previous studies utilising 1-heptanol, it has been added to the extracellular solution. In a historical paper using it to block sodium channel currents in cardiac Purkinje cells, the peak blocking effect of 1-heptanol was observed at 2 minutes after 1-heptanol addition, with the extent of the block being slightly increased by increasing the temperature at which the cell were kept at from 10°C to 27°C. (Nelson and Makielski, 1991). There is evidence that Cx26/Cx30 gap junction channels underlie key features of current flow observed in DCs, with gap junctions between DCs favouring K⁺ passage (Zhao et al., 2000). Isolated and coupled DCs have been found to exhibit large outwardly rectifying K⁺ currents in response to depolarization (Zhao et al., 2000; Nenov et al., 1998; Chung et al., 2013; Yang and Wang, 2002). This would be the first study to investigate isolated DCs during neonatal development.

4.2 Aims:

- To Investigate the effect of 1-heptanol induced electrical isolation on DC activation ionic conductances, hypothesising that blocking gap junctions would reduce recorded potassium currents due to the reduction of space-clamp issues.

4.3 Results

Deiters' cell capacitance is not significantly affected by 1-heptanol across ages P7-P8

If there is significant electrical coupling between DCs, then one would expect that blocking gap junctions using 1-heptanol would reduce the effective cell membrane surface area/size, and therefore cell capacitance, under voltage clamp (Figure 20A). Measurements of cell capacitance were made at the two different ages (P7 and P8) and 1-heptanol concentrations (0 and 3 mM) were made, all in high extracellular calcium (4 mM).

The interaction between the change from 0 to 3mM 1-heptanol extracellular solution and neonatal age was found to be not statistically significant when analysing the recorded cell capacitances: $F(1.00, 6.00) = 0.058$ ($p=0.82$), (two-way ANOVA) (Figure 20A). The main effect of 1-heptanol on cell capacitance was not statistically significant: $F(1.00, 8.00) = 0.053$ ($p=0.82$). Further, the main effect of neonatal age was also not statistically significant $F(2.00, 8.00) = 1.64$ ($p=0.25$).

No statistically significant differences between P7 and P8 input resistances across conditions

Input resistance is a quantification of the total cell resistance and is a measure that depends on the number of open channels in the cell membrane- with relatively higher membrane resistance and cell size resulting in relatively reduced input resistance (Al-muhtasib, 2023). Based on the gap junction-blocking effect of 1-heptanol, it would be expected that this electrical isolation would lead to an increase in input resistance.

The interaction between the change from 0 to 3mM 1-heptanol extracellular solution and neonatal age was found to be not statistically significant when analysing the recorded input resistances: $F(1.00, 6.00) = 0.067$ ($p=0.80$), (two-way ANOVA) (Figure 20C). The main effect of 1-heptanol on input resistance was not statistically significant: $F(1.00, 6.00) = 0.23$ ($p=0.65$). Further the main effect of neonatal age was also not statistically significant $F(1.00, 6.00) = 0.45$ ($p=0.53$).

Deiters' cell capacitance is not significantly different across ages P7-P9 in 1-heptanol

To examine more comprehensively the effect of neonatal age on the capacitance of putatively electrically isolated DCs, experiments in the presence of 1-heptanol were continued in P9 animals. The relationship between neonatal age and the cell capacitance in 1-heptanol extracellular solution was investigated. It was found that the effect of neonatal age on the cell capacitance was not statistically significant: $F(2.00,3.00) = 1.74$, $p = 0.32$, (Figure 20B) (One-way ANOVA).

Input resistance of electrically isolated DCs in 1-heptanol differed significantly across the ages P7-P9

The 1-heptanol recordings of DCs across the wider range of ages (P7, P8 and P9) were also analysed to determine whether input resistance varied in electrically isolated DCs.

The relationship between neonatal age and the input resistance in 1-heptanol extracellular solution was investigated. It was found that the effect of neonatal age on the cell capacitance was statistically significant: $F(2.00,3.00)= 11.46, p= 0.044$, (one-way ANOVA). However, pairwise post-hoc tests could not resolve statistically significant differences between any of the age groups in 1-heptanol (Figure 20D).

No statistically significant effects of age (P7 and P8) or 1-heptanol on mean current densities at +40mV in high extracellular calcium

The interaction between the change from high calcium to 3mM 1-heptanol extracellular solution and neonatal age was found to be not statistically significant when analysing the recorded mean current densities at +40 mV: $F(1.00, 6.00)= 0.00049 (p=0.98)$, (two-way ANOVA) (Figure 20E). The main effect of 1-heptanol on mean current densities at +40mV was not statistically significant: $F(1.05, 8.44)= 18.09 (p=0.055)$. Further, the main effect of membrane voltage was statistically significant $F(1.00, 6.00)= 0.45 (p=0.0023)$.

Current density at +40 mV in 1-heptanol was not statistically significant across P7-P9 The

1-heptanol recordings of DCs across the wider range of ages (P7, P8 and P9) were next analysed to determine whether the peak current density varied in electrically isolated DCs.

The relationship between neonatal age and the current density at +40 mV in 1-heptanol extracellular solution was investigated. It was found that the effect of neonatal age on the current density at +40 mV in 1-heptanol was not statistically significant: $F(2.00,3.00)= 0.27$, $p= 0.78$, (one-way ANOVA). (Figure 20F).

At P7, 1-heptanol significantly reduced current densities

Both the P7 and the P8 age group were analysed separately to understand whether the effect of 1-heptanol is different at different neonatal ages. The interaction between the change in membrane voltage and changing from high calcium to 3 mM 1-heptanol extracellular solution was found to be strongly statistically significant when analysing the recorded current densities: $F(14.00, 56.00)= 13.41$ ($p<0.0001$), (repeated-measures two way ANOVA). However, pairwise post-hoc tests with Bonferroni correction could not resolve statistically significant differences between any of the age groups in 1-heptanol (Figure 21A).

At P8, 1-heptanol did not significantly reduce current densities

Both the P7 and the P8 age group were analysed separately to understand whether the effect of 1-heptanol is different at different neonatal ages. The interaction between the change in membrane voltage and changing from high calcium to 3 mM 1-heptanol extracellular solution was found to be not statistically significant when analysing the

recorded current densities: $F(1.00, 1.00) = 3.27$ ($p=0.32$), (repeated-measures two-way ANOVA) (Figure 21B). The main effect of 1-heptanol on current densities was not statistically significant: $F(1.00, 1.00) = 3.78$ ($p=0.30$). Further, the main effect of membrane voltage was statistically significant $F(1.00, 1.00) = 3.43$ ($p=0.32$).

When P7 and P8 are grouped, 1-heptanol significantly reduced current densities, especially at more depolarised membrane voltages

The interaction between the change in membrane voltage and changing from high calcium to 1-heptanol extracellular solution was found to be strongly statistically significant when analysing the recorded current densities: $F(14.00, 112) = 5.76$ ($p < 0.0001$), (repeated measures two-way ANOVA). However, pairwise post-hoc tests with Bonferroni correction could not resolve statistically significant differences between any of the age groups in 1-heptanol (Figure 21C).

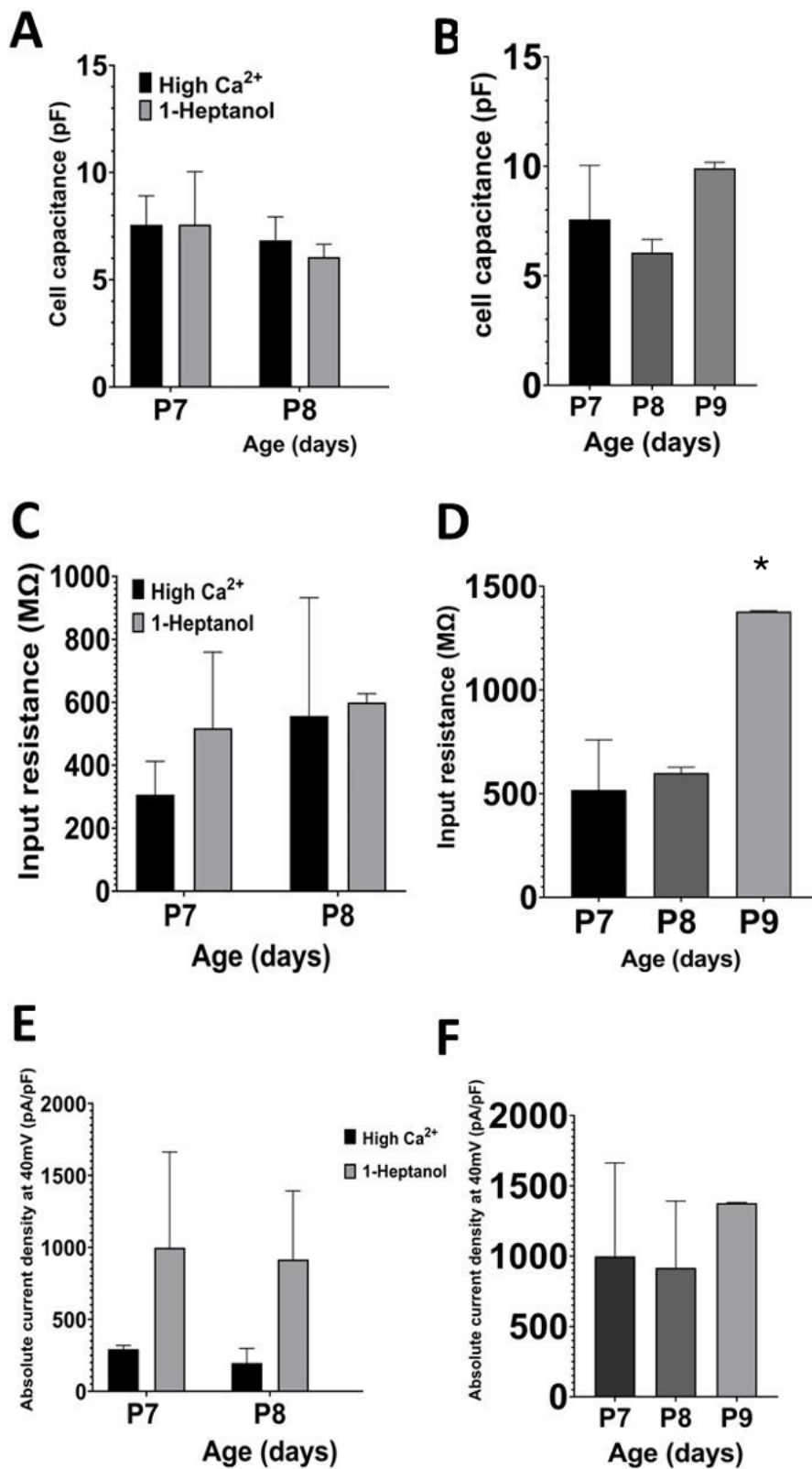


Figure 20: Absolute Deiters' cell current density at 40 mV and passive membrane properties for ages postnatal day (P) 7, P8 and P9 in high calcium (0 mM 1-heptanol) and 3 mM 1-heptanol

(A) Cell capacitances (pF) for P7 and P8 DCs in high calcium and 1-heptanol (+/- SEM). At P7, the mean cell capacitance was 6.50 pF (n=4, SEM= 1.16 pF), and 7.58 pF in 1-heptanol (n=2). At P8, the mean cell capacitance in high calcium extracellular solution was 6.84 pF (n=2), and 6.06pF in 1-heptanol was (n= 2). (B) Cell capacitances (pF) for P7, P8 and P9 DCs in 1-heptanol (+/- SEM). Compared to P7 (7.58 pF, n=2) and P8 (6.06pF, n= 2), the mean cell capacitance in 1-heptanol in P9 DCs was 9.91pF (n= 2). (C) Input resistances (MΩ) for P7 and P8 Deiters' cells in high calcium and 1-heptanol (+/- SEM). The mean input resistance in high calcium extracellular solution for P7 was 372.30 MΩ (n= 4, SEM: 107.40 MΩ). The same in 1-heptanol was 517.90 MΩ (n= 2). The mean input resistance measured in high calcium extracellular solution for P8 was 556.70 MΩ (n= 2). The same in 1-heptanol was 599.40 MΩ (n= 2). The same in 1-heptanol for P9 was 1378.00 MΩ (n= 2). (D) Input resistances (MΩ) for P7, P8 and P9 Deiters' cells in 1-heptanol (+/- SEM). It was found that the effect of neonatal age on the cell capacitance was statistically significant: $F(2.00,3.00)= 11.46$, $p= 0.044$, (one-way ANOVA). (E) Absolute mean current density (pA/pF) at 40 mV of P7 and P8 DCs in high calcium and 1-heptanol (+/- SEM). For P7, the mean current density at +40 mV was 2122.07 pA/pF (n=4, SEM= 232.94 pA/pF). The same in 1-heptanol was 998.29 pA/pF (n=2). For P8, the mean current density at +40 mV was 1456.47 pA/pF (n=2). The same in 1-heptanol was 916.09 pA/pF (n=2). (F) Absolute mean current density (pA/pF) at 40 mV of P7, P8 and P9 DCs in 1-heptanol (+/- SEM). For P7, the mean current density at +40 mV in 1-heptanol was 998.29 pA/pF (n=2). For P8, the mean current density at +40 mV in 1-heptanol was 916.09 pA/pF (n=2). For P9, the mean current density at +40 mV in 1-heptanol was 78.11 pA/pF (n=2).

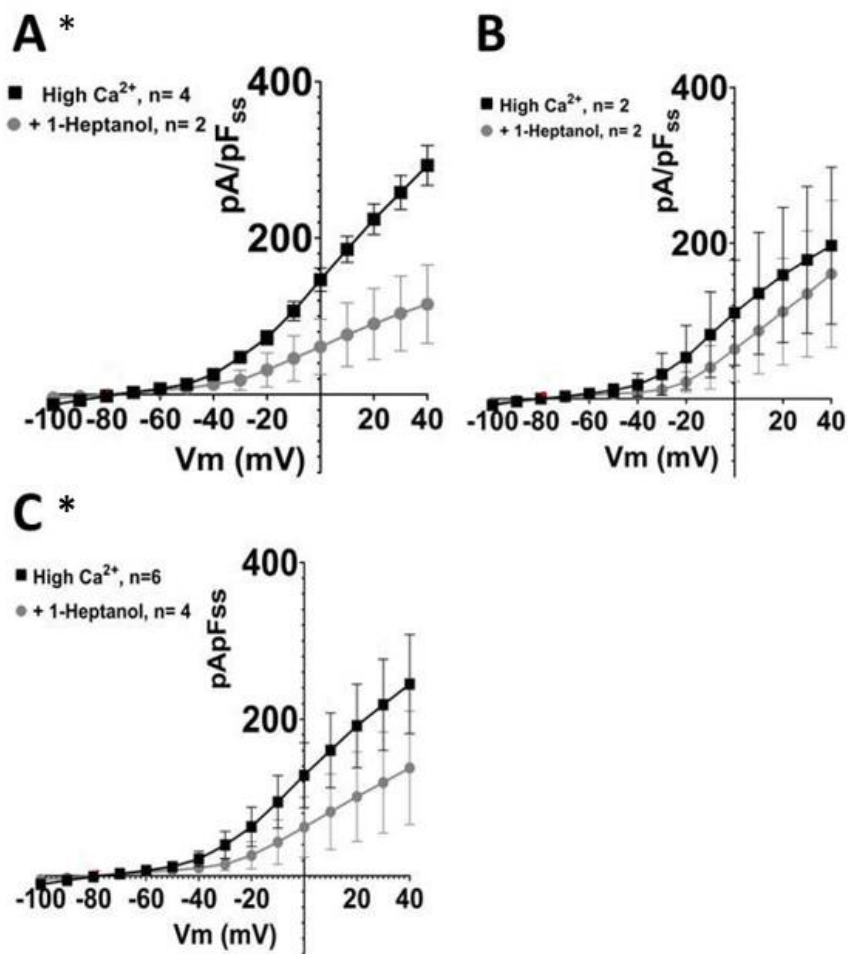


Figure 21: Graphs for ages postnatal day (P) 7 and P8, comparing high calcium (0 mM 1-heptanol) with 3 mM 1-heptanol condition.

(A) Mean current density (pA/pF) of P7 DCs in the high calcium extracellular solution compared with that in 1-heptanol extracellular solution (+/- SEM). The * symbol indicates a statistically significant difference between conditions. (B) Mean current density of P8 DCs in the high calcium extracellular solution compared with that in 1-heptanol extracellular solution (+/- SEM). (C) Mean current density of grouped P7 and P8 DCs in the high calcium extracellular solution compared with that in 1-heptanol extracellular solution (+/- SEM). The * symbol indicates a statistically significant difference between conditions.

Input resistance (MΩ)			
P7 High calcium	P7 +1-heptanol	P8 High calcium	P8 +1-heptanol
488.48	276.50	180.81	627.15
140.88	759.21	932.49	571.67
249.95			
609.98			

Table 7: Input resistances (MΩ) for P7 and P8 (n=6) Deiters' cells in high calcium and 1-heptanol extracellular solution. Grey blocks indicate an absence of available data.

4.4 Main findings

It was found that there was no statistically significant effect of 1-heptanol on cell capacitance, input resistance or current density at +40 mV. There were statistically significant interactions between the change in extracellular solution 1-heptanol concentration and changing membrane voltage for P7 current densities and pooled P7 and P8 current densities. There was no statistically significant interaction between these factors for the P8 age group. Moreover, the difference in input resistance in 1-heptanol across P7, P8 and P9 were statistically significant.

4.5 Discussion

The lack of statistically significant difference in cell capacitance and input resistance suggests that 1-heptanol does not affect cell size/ membrane surface area/number of open channels, as cell capacitance increases with cell surface area/ increases in open channels, and input resistance depends on the total number of open ion channels on a neuron's membrane and cell size (Al-muhtasib, 2023). This is a finding that is contradictory to the purpose of 1-heptanol and its historical use for blocking gap junctions and to previous findings in experiments that have electrically uncoupled DCs from their gap junctions that have resulted in decreases in input resistance and the amount of cell membrane able to contribute to measures of conductance (Blasits et al., 2000). However, it is possible that the gap junctions were already blocked in high calcium extracellular solution, as calcium ions have been found to be involved in gap junction hemichannel gating (Lopez et al., 2016).

It has been previously proposed that 1-heptanol is able to modify the activity of many different channel types, and that the general mechanism of action was through altering lipid-protein interaction within these channels (Nelson and Makielski, 1991). Therefore, in consideration of this block of gap junctions and potential broader effect, it is interesting that the present study found no effect on cell capacitances and input resistances.

In the previous results chapter, it was found that cell capacitance is statistically significantly reduced by high calcium extracellular solution when compared to the null calcium solution, and it is possible therefore that the cell capacitance in this solution, prior to adding 1-heptanol, was already reduced, especially due to the toxicity of 0mM calcium extracellular

solution (Figure 17D). It should be noted that the concentration of Ca^{2+} in the high calcium extracellular solution is higher than that found in perilymph (1.2mM), the cochlear fluid that DCs are immersed in (Chung et al., 2013). Therefore, if the present study utilised a starting extracellular solution that more closely resembled either natural perilymph concentrations, the effect of 1-heptanol on the cell capacitance and input resistance of these cells would potentially be more clearly observed (Delprat and Irving, 2016).

The possibility that 1-heptanol and neonatal age are factors that statistically significantly affect current density is an interesting and important finding. The differences in this effect, and also the interaction between these two factors being not statistically significant for P8 (Figure 21B) but significant for P7 (Figure 21A) potentially suggests that across neonatal age in DCs there may be significant variation in the number of gap junctions available to be blocked by 1-heptanol. This is supported by previous research that found that across development, DC expression of certain gap junctions changes considerably- with expression of Cx26 and Cx30 increasing gradually across neonatal development until reaching a level of saturation at P15 (Zhao and Yu, 2006; Qu et al., 2012). Therefore, it is possible that different age groups across the neonatal developmental period may require higher concentrations of 1-heptanol to provide a significant block, accommodating for increases in gap junction expression across this period. However, it also should be noted that the concentration of 1-heptanol utilised in the present study is markedly higher in concentration than that used in previous studies that report significant effects on cell types found in other areas of the body (Nelson and Makielski, 1991; Eckle and Todorovic, 2010). Overall, this data suggests

interesting potential variation across neonatal DCs that should be further explored in order to understand cochlear development.

Chapter 5

Potassium channel inactivation in neonatal Deiters' cells

5.1 Introduction:

Previously it has been found using potassium channel blockers including Clofilium and Tetraethylammonium (TEA) that mature DCs have a biphasic time course of inactivation with a fast and slow component, indicating the potential presence of different types of voltage-gated potassium channels (Chung et al., 2013). The researchers attributed the TEA-sensitive component of DC inactivation to the presence of either the Kv1.4 or Kv3.4 channel, as both channels have been shown to be sensitive to TEA (Rudy et al., 1991; Chung et al., 2013). Nenov et al. (1998) also found evidence of multiple Kv channels based on the multiple time constants of inactivation in mature DCs, and used drugs TEA and nimodipine, with the latter being used at a concentration that leads to the blocking of calcium channels. Interestingly, the researchers found that the block nimodipine brought about was not mediated by effects on calcium channels, as the blocking effect of the drug was also observed in null calcium extracellular solution (Nenov et al., 1998).

Like both Chung et al. (2013) and Nenov et al. (1999), Szűcs et al. (2006) also reported the existence of multiple Kv channels based on inactivation properties of DCs. They also made an interesting contribution to the literature in noting differences in inactivation properties based on the specific size and shape of a DC, since DCs that had a 'corpulent' shape showed mainly slow inactivating K⁺ current, while 'lanky' DCs had this slow component and a fast inactivating K⁺ current. The researchers determined that the shape of the DCs was linked to the shape of the OHCs they were attached to since DCs attached to shorter OHCs had more

voluminous, corpulent cell bodies while those attached to longer OHCs had lanky cell bodies. Interestingly, Szűcs et al. (2006) also noted that a portion of DCs investigated did not show biphasic, but monophasic inactivation kinetics. The researchers theorised that the Kv1.3 channel was probably the reason for the slow inactivation component observed in some DCs, based on previous research (Grissmer et al., 1994; Somodi et al., 2004).

Changing potassium channel currents have been found to be an important aspect of auditory system development in other OC cells (Marcotti and Kros, 1999). In this chapter, an investigation into the inactivation of voltage-gated channels in neonatal DCs was conducted to further understand the inactivation properties of DCs, as well as to potentially observe any functional changes in inactivation properties across neonatal auditory development, making an important contribution to literature that currently only focuses on mature DCs. This chapter will address this query through analysing the extent of inactivation when stepping to different membrane voltages. This was achieved through eliciting current traces using a protocol composed of a pre-pulse of 12 seconds (s) duration, consisting of depolarising voltage steps (Figure 21A). The peak current recorded during the 30 mV voltage step following the pre-pulse, where DC currents (mainly contributed to by voltage-gated potassium channels (Nenov et al., 1998; Yang and Wang, 2002; Chung et al., 2013)) are activated again but for a shorter duration, shows the extent of inactivation brought about by each pre-pulse.

Another aspect of this experiment was the analysis of the steady-state inactivation that occurred during the 12 s pre-pulse, allowing for characterisation of the rate of inactivation

seen in the DCs. The inactivation steady-state was analysed since Kv channels inactivate relatively slower than voltage-gated Na⁺ channels, with the steady-state currents representing currents at a later timescale when compared with the peak measurements (Lacroix et al., 2013). Inactivation recordings were made in extracellular solution containing 3 mM 1-heptanol to electrically isolate Deiters' cell currents.

5.2 Aims:

- To characterise the potentially unique inactivation properties of DC Kv channel rate of inactivation during neonatal development. The neonatal ages included in this investigation were P6 (n= 1), P7 (n= 2), P8 (n= 1), P9 (n= 2) and P10 (n= 1). Recordings were made in high calcium extracellular solution as well as in 3mM gap junction blocker 1-Heptanol, used to block gap junctions present between cells that could otherwise contribute to the currents recorded.

5.3 Results

There is possibly an effect of neonatal age on the features of inactivation, with inactivation current amplitudes seeming to reduce across P6-P10 (Figure 22). However, this needs further investigation to elucidate.

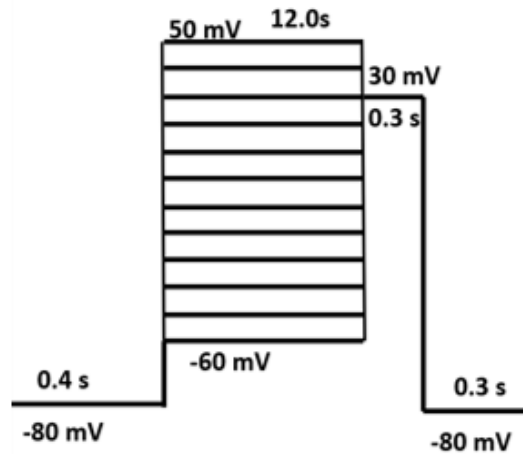
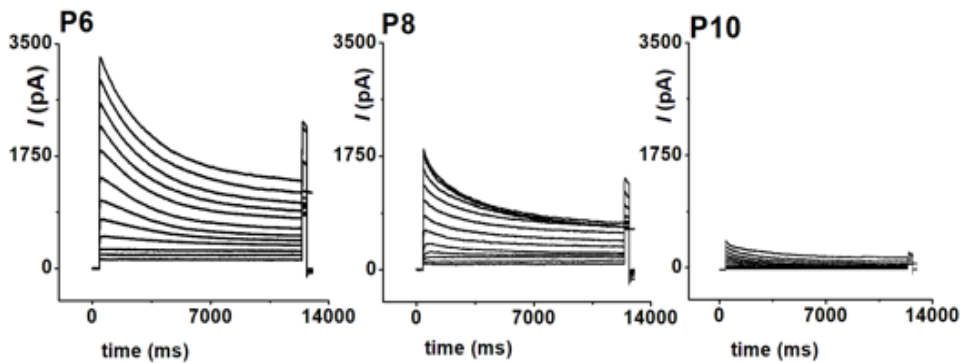
A**B**

Figure 22: Graphs for extent of inactivation during postnatal development

(A) Schematic of the inactivation protocol. Inactivation current traces were elicited using a protocol involving a pre-pulse of 12 seconds (s) in duration, eliciting depolarising voltage steps in 10-mV increments from -60 mV (line coloured in red) to 40 mV before stepping to 30 mV for 0.3 s. The holding potential was -80 mV. (B) Example inactivation traces from P6, P8 and P10.

The transition from the inactivated state to the closed state is referred to as recovery from inactivation (Kornreich, 2007). In Kv channels, recovery from inactivation takes place on a

timescale of up to several seconds, and the mechanism underlying it is not yet fully understood (Ostmeyer et al., 2013). Previously in mature DCs, the time course of recovery from inactivation has been described by double exponential time constants (Nenov et al., 1998). Properties of recovery from inactivation in DCs have not been characterised by any of the previously described key papers on DC electrophysiology (Chung et al., 2013; Yang and Wang, 2002; Szűcs et al., 2006), making this investigation relevant and pertinent. It is important to investigate recovery from inactivation properties, as recovery from inactivation is of functional significance for sensory systems and the nervous system in general (Jackson et al., 1991). This experiment was performed to characterise the recovery from inactivation properties of Deiters' cell Kv channels during neonatal development, using a protocol outlined in (Figure 23A).

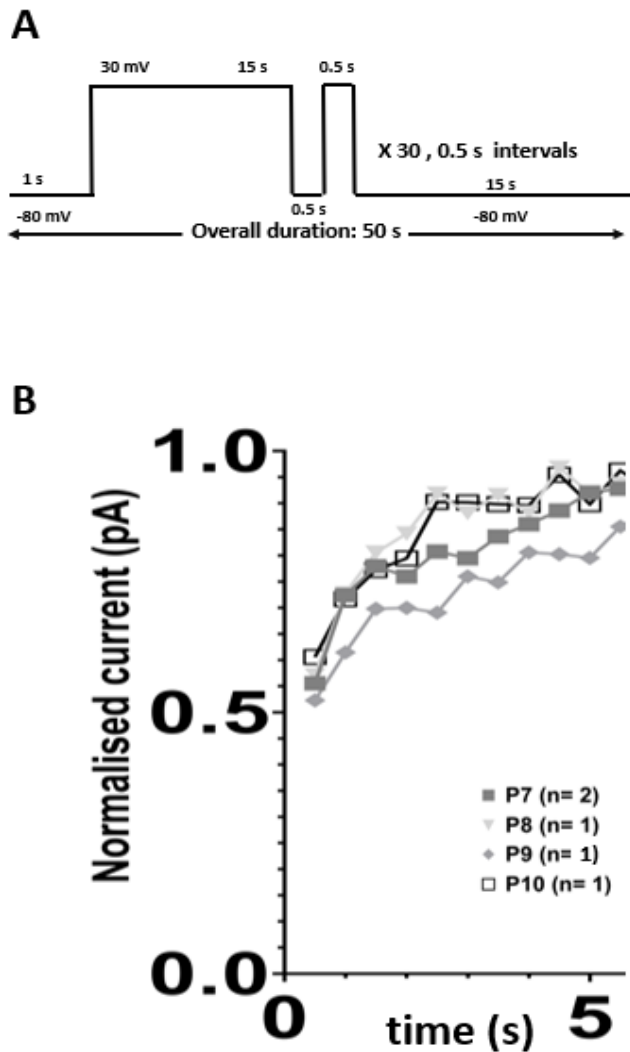


Figure 23: Graphs for recovery from inactivation during postnatal development

(A) Schematic of the recovery from inactivation protocol. Recovery from inactivation current traces were elicited using a protocol involving a pre-pulse of 15 seconds (s) in duration, eliciting a depolarising voltage step to 30 mV before a step to the holding potential for 0.5 s, after which occurred a test pulse to 30 mV for 0.5 s. This 0.5 s depolarising test pulse was repeated throughout the protocol at different time intervals per sweep, in intervals of 0.5 s across the 15 s allotted to the test pulses. The holding potential was -80 mV. (B) Plot of the normalised recovery from inactivation current-voltage relationship for each age group. Inactivation recordings were made in extracellular containing 3 mM 1-heptanol to isolate

Deiters' cell currents. The neonatal ages investigated are P6 (n= 1), P7 (n= 2), P8 (n= 1), P9 (n= 1) and P10 (n= 1).

5.4 Main findings

It was found that there might be an effect of neonatal age on inactivation and recovery from inactivation current amplitudes across development.

5.5 Discussion

Inactivation

In the present study that there might be an effect of neonatal age on inactivation current amplitudes across development, which is worth further investigation. Previous research into the features of inactivation in DCs over postnatal development have not been conducted, however in the first postnatal week, OHCs have been found to exhibit delayed rectifier K^+ currents that show slow inactivation. At the beginning of the second postnatal week, this current (called $I_{K,neo}$) was found to decrease in amplitude (Marcotti and Kros, 1999). It is possible that a similar process occurs in DCs across postnatal development, especially considering how they are intimately connected to the OHCs, and both cell types therefore share developmental milestones such as a peak in spontaneous activity between P10-P11 (Berekméri et al., 2019). The finding that inactivation was best fit with double exponential time constants is also a finding reported in previous research on DCs (Nenov et al., 1998). This study therefore supports this previous finding and makes an important contribution to previous literature by finding evidence of two potassium channels on DCs across neonatal development.

In previous similar studies by Nenov et al. (1998) and Chung et al. (2013), inactivation protocols involved overall protocol durations of 4.1 s and 10 s respectively. Nenov et al. (1998)'s protocol involved a membrane voltage varying step of 2 s duration, with voltage steps in 10 mV increments from -80 mV to 40 mV. Then a step to 70 mV for 1 ms was applied, and following this, a step to 50 mV for 2 s. Chung et al (2013) investigated the steady-state inactivation through applying 10 s pre-pulses from -100 mV to 50 mV in 5 mV increments. Nenov et al. (1998) depolarised to a greater extent with the subsequent voltage steps to 70 mV and 50 mV, inactivating the Kv channels to a greater extent and potentially resulting in more accurate recordings of the inactivation steady-state in DCs.

To further characterise DC inactivation and recovery from inactivation, Nenov et al. (1998) utilised a double pulse voltage protocol with an increasing time interval between the two pulses to determine the time course of these processes. The Kv channels, Nav channels and Cav channels exhibit fast and slow inactivation (Mitrovic et al., 2000). In the present study, a longer depolarising step duration to inactivate more channels (a 12 s step duration was utilised) would have allowed for more detailed characterisation of inactivation properties, as Nav channel slow inactivation occurs over a timescale of seconds to minutes after cell membrane depolarisation. The mechanism of this is still largely unknown but is theorised to involve the channel pore and selectivity filter regions of Nav channels (Payandeh, 2018). Moreover, slow inactivation initiates in Cav channels after depolarisations lasting over a minute and occurs over a timescale of seconds. Like Nav channel slow inactivation, this process for Cav channels is still poorly understood (Shi and Soldatov, 2002).

Recovery from inactivation

In the present study it was found that there might be an effect of neonatal age on recovery from inactivation current amplitudes across development (Figure 23B), but further investigation is required to determine this. A difference across P7-P9 would be an interesting finding, as the expression of potassium currents changes throughout ages. P8 OHCs show the first sign of the mature potassium current $I_{K,n}$, which replaces the previous $I_{K,neo}$ (Marcotti and Kros, 1999). Again, as DCs are closely connected to the OHCs (Berekméri et al., 2019), the DCs may show a similar maturation in potassium currents at this age that potentially leads to differences in recovery from inactivation current amplitude.

Moreover, any potential change in recovery from inactivation across this period of development could be influenced by the still maturing endocochlear potential, as the rate of recovery from slow inactivation is modulated by the concentration of extracellular K^+ , with increased concentrations increasing recovery rate at relatively more hyperpolarized membrane voltages (Levy and Deutsch, 1996). Intracellular cation concentration has also been shown to modulate recovery from slow inactivation in Kv channels (Ray and Deutsch, 2006). The endocochlear potential is maturing from P5 until P18 (Sadanaga and Morimitsu, 1995), and this maturation process involves a steady increase in concentration of K^+ in the endolymph (Raphael et al., 1983). Based on this developmental trajectory, it might therefore be expected that the rate of recovery from inactivation potentially increases as a product of increasing K^+ concentration, due to K^+ being intrinsic to membrane repolarisation. Moreover, increasing extracellular concentration of K^+ leads to acceleration of slow inactivation recovery speed (Levy and Deutsch, 1996; Kim and Nimigean, 2016). Further investigation of this is therefore required and utilising a broader range of neonatal ages

would allow for an understanding of changes in inactivation recovery rate across neonatal development in DCs.

Chapter 6

Discussion

The present study explored neonatal DC activation and inactivation, investigating the effect of extracellular calcium concentration and gap junction block on the former. The findings were in alignment with previous research that suggests the main currents exhibited by DCs upon depolarisation are outwardly rectifying potassium channel currents (Nenov et al., 1998; Yang and Wang, 2002; Szűcs et al., 2006; Chung et al., 2013). Previously, the effect of null-calcium and calcium-containing extracellular solution on these potassium currents have been investigated by Nenov et al. (1998), a study that found no significant effect of extracellular Ca^{2+} concentration on DC activation *I-V* curves. Therefore, the lack of significant effect of extracellular Ca^{2+} concentration in the present study bolsters this previous finding, with the added novel discovery that this is also the case for DCs during neonatal development.

This study found potential differences in the extent of gap junction block brought about by 3 mM 1-heptanol during neonatal development, with P7 aged DCs displaying a significant reduction of current density in 1-heptanol (Figure 21A), while P8 DCs did not show a significant effect (Figure 21B). As previously described, gap junctional intercellular communication is critical for cochlear development (Jagger and Forge, 2014), and the expression of gap junction proteins Cx26 and Cx30 show drastic changes during the neonatal developmental period. It has been noted that their levels of expression increase rapidly and substantially between P0-P12 (Jagger and Forge, 2006). Therefore, this difference seen across P7 and P8 is potentially a highly interesting finding, as it suggests that there could possibly be a significant difference in expression levels between these ages, and it is a finding made especially interesting that these age groups are only separated by one day.

Although there are confounding factors that contributed to this result, to be explored further in this section.

Future studies should further investigate these ages to establish whether this difference is of developmental significance. The investigation of inactivation in the present study included a broader range of neonatal ages (P6-P10) than the investigations of activation, including ages both during OHC development and after OHC developmental maturity. Therefore, it would be interesting to determine whether the developmental timeline of OHCs could also be a factor that affects the timescale of inactivation in DCs.

It is already known that OHCs and DCs, being closely connected, share certain developmental milestones, such as both cell types displaying peaks in spontaneous action potentials between P10-P11 (Berekméri et al., 2019). Moreover, although at P7 the OHCs are fully mature, the cochlear sensory epithelium is not yet fully developed, and this may also affect the currents recorded from DCs after P12 (hearing onset), as DCs have been found to be involved in cochlear amplification mechanics by acting as mechanical equalisers to the OHCs (Zhou et al., 2022). Therefore, further investigation that compares earlier neonatal development to P12 (hearing onset) would be a fascinating future direction. Moreover, studies that evaluate whether the conductances of neonatal DCs are affected by the different stages of spontaneous action potential firing observed across neonatal development in OHCs, which fire up until just before the onset of functional OHC maturation at around P7 (Jeng et al., 2020), would also be fascinating. Whether developmental changes in OHC morphology impacts the ionic conductances of DCs across

neonatal development would also be an interesting future study, considering the finding by Szűcs et al. (2006) that the longer the DC shape, the larger the recorded potassium current amplitude.

6.1 Limitations

A limitation of the inactivation protocol utilised in the present study is that rather than beginning the inactivation voltage steps at -60 mV, a more negative starting voltage step of around -100 mV (at least below resting potential of -80 mV) would allow for a broader and more detailed picture of DC inactivation, as in the present study, a substantial amount of inactivation is already seen at the starting membrane voltage step of -60 mV (Figure 22). Key papers that investigated DC inactivation by Nenov et al. (1998) and Chung et al. (2013) chose initial voltage steps of -80 mV and -100 mV respectively. This limitation also means that for the present study, characterising the inactivation through implementation of a Boltzmann equation was not possible, as this equation requires the maximum inactivation conductance. Therefore, how rapidly inactivation current is changing with membrane potential is not possible to characterise (Dubois et al., 2009).

A potential limitation to the recovery from inactivation protocol used in the present study is that each 0.5 s interval depolarising step was to a membrane voltage of +30 mV, while Nenov et al. (1998) depolarised to a more positive potential of +80 mV. Stepping to a more positive and therefore more depolarising potential may have allowed for a clearer picture of recovery from inactivation in the DCs over the protocol duration, as previously inactivated Kv channels would have been activated to a greater extent. Nenov et al. (1998)'s recovery

from inactivation protocol involved a 5 s depolarising pulse followed by 0.1 s test pulses with increasing time intervals from 0 s to 0.2 s, 0.6 s, 2.4 s and 3.2 s. Increasing the time interval between the test pulses over a shorter period overall when compared to the present study. Increasing the interval time allows for more Kv channels to recover from inactivation between each interval, and therefore a strength of the present study is that it could be argued that the 0.5 s intervals used allows for a more detailed and broader representation of recovery from inactivation in the neonatal DCs.

A limitation for both the inactivation and activation investigations of this study is that recordings for each day alone were limited and sample sizes were very low. This may have been a contributing factor to the lack of statistically significant differences at certain ages, as the small sample size available for cells of certain age groups and conditions has resulted in the study being underpowered, resulting in the strong possibility of reporting falsely negative results (Nayak, 2010). For example, this may be the reason for the lack of significant difference in P8 DC current densities when comparing high calcium and 1-heptanol extracellular solution conditions, as this group had a much lower sample size (n=2) when compared to the P7 age group (n=4).

Moreover, a limitation of all three-results chapter investigations is that the concentration of Ca^{2+} in the high calcium extracellular solution is higher than that found naturally in perilymph (Ca^{2+} concentration of 1.2mM) (Delprat and Irving, 2016). The high calcium extracellular solution used in the present study, at a Ca^{2+} concentration of 4 mM, contained a considerably higher concentration of Ca^{2+} than naturally occurs in the cochlea. Future

studies that compare DC functioning when in extracellular solution resembling perilymph as separate investigations would allow for a clearer understanding of whether DC ionic conductances are modulated by extracellular calcium concentration. Moreover, it would allow for the possible identification of any differences in calcium modulation and gap junctional block that might occur along the length of the cell, depending on what cochlear fluid it is exposed to. Other key studies investigating DC physiology have utilised Ca^{2+} concentrations that don't resemble either lymphatic fluid, using concentrations of 2 mM, 2.5 mM and 2 mM respectively (Chung et al., 2013; Nenov et al., 1998; Yang and Wang, 2002).

Furthermore, another key limitation in this study is the toxicity brought about by 1-heptanol exposure, which may have caused cells to die, which would inevitably affect patch clamp recordings. Toxicity could have been limited by utilising rapid perfusion, in order to expose the DCs to 1-heptanol within a narrower time window. Moreover, because of the tight junctions present between DCs and OHCs, it is difficult to ensure that the 1-heptanol reached every DC in the preparation, since these tight junctions insulate the cells and extracellular spaces below them (Farquhar, 1963).

Another limitation of this study is that the developmental period investigated (P6-P10) encompasses a time in which the inwardly rectifying K^+ channels (Kir channels) are active. These channels are essential for cochlear development and endocochlear potential generation. For example, the Kir4.1 channel, which is encoded by the *KCNJ10* gene, plays a critical role in development and maintenance of the endocochlear potential (Bazard et al., 2021). The Kir channels can be blocked using barium (Alagem et al., 2001; Hsieh et al., 2015).

If a later developmental period was investigated, more information about developmental potassium channels and conductances within the DCs could have been elucidated, since Kir channels simply allow K^+ to passively traverse the cell membranes and are not involved in cell signalling. Moreover, considering the expression of various potassium channels on DCs across cochlear development, blocking certain channels in order to study select potassium channels would have been a more detailed approach to this investigation.

6.2 Future directions

Deiters' cells are an important and critical supporting cell, during both development and maturity (Mellado Lagarde et al., 2013). Further research into a broader range of ages representing neonatal development would further elucidate the diverse functions of these cells. The present study investigated DCs that were located on the apical turn of the cochlea. Previous studies that point to differences in DC morphology and functioning across the length of the cochlea (Furness et al., 2001; Spicer and Schulte., 1994; Parsa et al., 2012; Szűcs et al., 2006; Laffon and Angelini, 1996; Nakazawa et al., 1995), as well as the finding that cochlear development starts at the basal portion of the cochlea (Polley et al., 2013) make it evident that DCs located at different portions of the cochlea should be investigated and compared. Moreover, there is possibly location-based differences in DC ionic conductances, as for example, the distribution of BK channels changes along the cochlear turn (Szűcs et al., 2006). Investigating the neonatal ages included in the present study further (the present study having investigated DCs located in the apical turn of the cochlea) by comparing with DCs in other locations would allow for identification of any potential differences in conductances that may be important for cochlear development. Moreover, a

future focus on elucidating the role that DCs play in the modulation of spontaneous action potentials during cochlear development would help determine the role of DCs in this critical period.

This research will also potentially shed light on how abnormal DC development may be a major factor in disorders/ genetic mutations that result in hearing loss, as further understanding DC functioning at every point during neonatal hearing development would aid in understanding potential issues that may occur during this time. It is already known that loss of DCs during auditory development results in hearing loss, making them a critical cell to research further, especially in regard to cochlear development (Mellado Lagarde et al., 2013).

6.3 Concluding remarks

The cochlear supporting cells have not been the primary focus of hearing research until recent years- during which time much of the multitude of important functions they serve have been elucidated (Wan et al., 2013), supporting the necessary course of action that is further research into these fascinating and important unique cochlear cells. Deiters' cells are of particular interest due to their close connection to the sensory OHCs, as well as because there is evidence that DCs are essential for the development of hearing (Mellado Lagarde et al., 2013). The present study represents an important first step into research focussed upon Deiters' cell functioning during cochlear development. This study therefore makes an important contribution to the literature on DCs and highlights the pertinence of further research to elucidate the functioning of DCs during auditory development.

Chapter 7

References

Abrashkin, K.A. *et al.* (2006) 'The fate of outer hair cells after acoustic or ototoxic insults', *Hearing Research*, 218(1–2), pp. 20–29. doi:10.1016/j.heares.2006.04.001.

Adachi, N. *et al.* (2013) 'The mechanism underlying maintenance of the endocochlear potential by the K⁺ transport system in fibrocytes of the inner ear', *The Journal of Physiology*, 591(18), pp. 4459–4472. doi:10.1113/jphysiol.2013.258046.

Alberti, P. W. (2001). The anatomy and physiology of the ear and hearing. In B., Goelzer, C. H., Hansen, G. A. Sehrndt, (Eds.), *Occupational exposure to noise: Evaluation, prevention and control* (pp. 53-62). Bremerhaven, Germany: World Health Organization.

Alberts, B., Johnson, A., Lewis, J., Raff, M., Roberts, K. and Walter, P. (2002). Ion Channels and the Electrical Properties of Membranes. *Molecular Biology of the Cell*. 4th edition, [online] 4(1). Available at: <https://www.ncbi.nlm.nih.gov/books/NBK26910/>.

Anniko, M. and Wroblewski, R. (1981) 'Elemental composition of the developing inner ear', *Annals of Otology, Rhinology & Laryngology*, 90(1), pp. 25–32.
doi:10.1177/000348948109000107.

Anniko, M., (1985). 'Histochemical, Microchemical (Microprobe) and Organ Culture Approaches to the Study of Auditory Development', *Acta Oto-Laryngologica*, 99(sup421), pp.10-18.

Angelborg, C. and Engström, H. (1972) 'Supporting elements in the Organ of Corti I. Fibrillar structures in the supporting cells of the Organ of Corti of mammals', *Acta Oto-Laryngologica*, 73(sup301), pp. 49–60. doi:10.3109/00016487209122689.

Antz, C. and Fakler, B. (1998) 'Fast inactivation of voltage-gated K⁺ channels: From cartoon to structure', *Physiology*, 13(4), pp. 177–182. doi:10.1152/physiologyonline.1998.13.4.177.

Assad, J.A., Shepherd, G.M.G. and Corey, D.P. (1991) 'Tip-link integrity and mechanical transduction in vertebrate hair cells', *Neuron*, 7(6), pp. 985–994.

doi:10.1016/08966273(91)90343-x.

Ashmore, J.F. (1987). A fast motile response in guinea-pig outer hair cells: the cellular basis of the cochlear amplifier. *The Journal of Physiology*, 388(1), pp.323–347.

doi:https://doi.org/10.1113/jphysiol.1987.sp016617.

Art, J.J. and Fettiplace, R. (1987) 'Variation of membrane properties in hair cells isolated from the turtle cochlea', *The Journal of Physiology*, 385(1), pp. 207–242.

doi:10.1113/jphysiol.1987.sp016492.

Babola, T.A. *et al.* (2020) 'Purinergic signaling controls spontaneous activity in the auditory system throughout early development', *The Journal of Neuroscience*, 41(4), pp. 594–612. doi:10.1523/jneurosci.2178-20.2020.

Bar-Yehuda, D. and Korngreen, A. (2008) 'Space-clamp problems when voltage clamping neurons expressing voltage-gated conductances', *Journal of Neurophysiology*, 99(3), pp.1127–1136. doi:<https://doi.org/10.1152/jn.01232.2007>.

Bastiaanse, E.M. *et al.* (1993) 'Heptanol-induced decrease in cardiac gap junctional conductance is mediated by a decrease in the fluidity of membranous cholesterol-rich domains', *The Journal of Membrane Biology*, 136(2), pp. 135–145. doi:10.1007/bf02505758.

Bazard, P., Frisina, R.D., Acosta, A.A., Dasgupta, S., Bauer, M.A., Zhu, X. and Ding, B. (2021). Roles of Key Ion Channels and Transport Proteins in Age-Related Hearing Loss. *International Journal of Molecular Sciences*, 22(11), p.6158. doi:<https://doi.org/10.3390/ijms22116158>.

Bean, B.P. (1992) 'Pharmacology and electrophysiology of ATP-activated Ion Channels', *Trends in Pharmacological Sciences*, 13, pp. 87–90. doi:10.1016/0165-6147(92)90032-2.

Bekeasy, G.V. (1952) 'Resting potentials inside the cochlear partition of the guinea pig', *Nature*, 169(4293), pp. 241–242. doi:10.1038/169241a0.

Bekesy Gv., (1960) 'Experiments in Hearing', *McGraw-Hill*.

Beutner, D. and Moser, T. (2001) 'The presynaptic function of mouse cochlear inner hair cells during development of hearing', *The Journal of Neuroscience*, 21(13), pp. 4593–4599. doi:10.1523/jneurosci.21-13-04593.2001.

Beurg, M. *et al.* (2009) 'Localization of inner hair cell mechanotransducer channels using high-speed calcium imaging', *Nature Neuroscience*, 12(5), pp. 553–558. doi:10.1038/nn.2295.

Berekméri, E. *et al.* (2019) 'Postnatal development of the subcellular structures and purinergic signaling of deiters' cells along the tonotopic axis of the cochlea', *Cells*, 8(10), p. 1266. doi:10.3390/cells8101266.

Blankenship, A.G. and Feller, M.B. (2009) 'Mechanisms underlying spontaneous patterned activity in developing neural circuits', *Nature Reviews Neuroscience*, 11(1), pp. 18–29. doi:10.1038/nrn2759.

Blake, R. and Shiffrar, M. (2007) 'Perception of Human Motion', *Annual Review of Psychology*, 58(1), pp. 47–73. doi:10.1146/annurev.psych.57.102904.190152.

Blasits, S., Maune, S. and Santos-Sacchi, J. (2000) 'Nitric oxide uncouples gap junctions of supporting deiters cells from corti's organ', *Pflügers Archiv - European Journal of Physiology*, 440(5), pp. 710–712. doi:10.1007/s004240000355.

Börjesson, S.I. and Elinder, F. (2008) 'Structure, function, and modification of the voltage sensor in voltage-gated ion channels', *Cell Biochemistry and Biophysics*, 52(3). doi:10.1007/s12013-008-9032-5.

Brady, S., Siegel, G., R Wayne Albers and Price, D. (2005). *Basic Neurochemistry : Molecular, Cellular and Medical Aspects*. [online] Academic Press. Available at: <https://www.elsevier.com/books/basic-neurochemistry/brady/978-0-12-088397-4>.

Brandt, A., Striessnig, J. and Moser, T. (2003) 'Cav1.3 channels are essential for development and presynaptic activity of cochlear inner hair cells', *The Journal of Neuroscience*, 23(34), pp. 10832–10840. doi:10.1523/jneurosci.23-34-10832.2003.

Bruns, V. and Schmieszek, E. (1980) 'Cochlear innervation in the Greater horseshoe bat: Demonstration of an acoustic fovea', *Hearing Research*, 3(1), pp. 27–43. doi:10.1016/03785955(80)90006-4.

Burbridge, T.J. *et al.* (2014) 'Visual circuit development requires patterned activity mediated by retinal acetylcholine receptors', *Neuron*, 84(5), pp. 1049–1064.

doi:10.1016/j.neuron.2014.10.051.

Casale, J. and Agarwal, A. (2023). Anatomy, Head and Neck, Ear Endolymph. In *StatPearls*. StatPearls Publishing.

Castellano-Muñoz, M. and Ricci, A.J. (2014) 'Role of intracellular calcium stores in hair-cell ribbon synapse', *Frontiers in Cellular Neuroscience*, 8. doi:10.3389/fncel.2014.00162.

Catterall, W.A. (2011) 'Voltage-gated calcium channels', *Cold Spring Harbor Perspectives in Biology*, 3(8). doi:10.1101/cshperspect.a003947.

Chahine, M. (2018). *Voltage-gated Sodium Channels: Structure, Function and Channelopathies*. Springer.

Ceriani, F. and Mammano, F. (2012) 'Calcium signaling in the cochlea – molecular mechanisms and physiopathological implications', *Cell Communication and Signaling*, 10(1), p. 20. doi:10.1186/1478-811x-10-20.

Ceriani, F., Hendry, A., Jeng, J.-Y., Johnson, S.L., Stephani, F., Olt, J., Holley, M.C., Mammano, F., Engel, J., Kros, C.J., Simmons, D.D. and Marcotti, W. (2019). Coordinated calcium signalling in cochlear sensory and non-sensory cells refines afferent innervation of outer hair cells. *The Embro Journal*, 38(9). doi:<https://doi.org/10.15252/embj.201899839>.

Chen, P. *et al.* (2002) 'The role of math1 in inner ear development: Uncoupling the establishment of the sensory primordium from hair cell fate determination', *Development*, 129(10), pp. 2495–2505. doi:10.1242/dev.129.10.2495.

Chen, C. and Bobbin, R.P. (1998) 'P2X receptors in cochlear deiters' cells', *British Journal of Pharmacology*, 124(2), pp. 337–344. doi:10.1038/sj.bjp.0701848.

Chen, J. and Zhao, H.-B. (2014). The role of an inwardly rectifying K⁺ channel (Kir4.1) in the inner ear and hearing loss. *Neuroscience*, 265, pp.137–146.
doi:<https://doi.org/10.1016/j.neuroscience.2014.01.036>.

Choi, C.-H. (2012) 'Mechanisms and treatment of blast induced hearing loss', *Korean Journal of Audiology*, 16(3), p. 103. doi:10.7874/kja.2012.16.3.103.

Colvin, J.S. *et al.* (1996) 'Skeletal overgrowth and deafness in mice lacking fibroblast growth factor receptor 3', *Nature Genetics*, 12(4), pp. 390–397. doi:10.1038/ng0496-390.

Corey, D. and Hudspeth, A. (1983) 'Kinetics of the receptor current in bullfrog saccular hair cells', *The Journal of Neuroscience*, 3(5), pp. 962–976. doi:10.1523/jneurosci.03-05-00962.1983.

Corey, D. and Hudspeth, A. (1979) 'Ionic basis of the receptor potential in a vertebrate hair cell'. *Nature*, 281(5733), pp.675-677.

Chung, J.W. *et al.* (2013) 'Potassium currents in isolated deiters' cells of Guinea pig', *The Korean Journal of Physiology & Pharmacology*, 17(6), p. 537.
doi:10.4196/kjpp.2013.17.6.537.

Cloes, M. *et al.* (2013) 'Differentiation of boettcher's cells during postnatal development of rat cochlea', *Cell and Tissue Research*, 354(3), pp. 707–716. doi:10.1007/s00441-013-1705-8.

Cooper, D. and Dimri, M. (2023) *Biochemistry, calcium channels, NCBI bookshelf*. Available at: <https://www.ncbi.nlm.nih.gov/books/NBK562198/> (Accessed: 25 September 2023).

Crews, D. (2009). Litter environment affects behavior and brain metabolic activity of adult knockout mice. *Frontiers in Behavioral Neuroscience*, 3.
doi:<https://doi.org/10.3389/neuro.08.012.2009>.

Cunningham, L.L. and Tucci, D.L. (2017) 'Hearing loss in adults', *New England Journal of Medicine*, 377(25), pp. 2465–2473. doi:10.1056/nejmra1616601.

Dayaratne, M.W.N. *et al.* (2015) 'Putative role of border cells in generating spontaneous morphological activity within Kölliker's organ', *Hearing Research*, 330, pp. 90–97. doi:10.1016/j.heares.2015.06.017.

de Lera Ruiz, M. and Kraus, R.L. (2015) 'Voltage-gated sodium channels: Structure, function, pharmacology, and clinical indications', *Journal of Medicinal Chemistry*, 58(18), pp. 7093–7118. doi:10.1021/jm501981g.

Delprat, B. and Irving, S. (2016) *Journey into the world of hearing, Cochlea*. Available at: <http://www.cochlea.eu/en/cochlea/cochlear-fluids>.

Desai, M. *et al.* (2001) 'Trends in vision and hearing among older Americans', *PsycEXTRA Dataset*, 2, pp. 1–8. doi:10.1037/e620682007-001.

Delacroix, L. and Malgrange, B. (2015) 'Cochlear Afferent Innervation Development', *Hearing Research*, 330, pp. 157–169. doi:10.1016/j.heares.2015.07.015.

Dobie, R. A., and Van Hemel, S., (2004). Hearing Loss: Determining Eligibility for Social Security *Benefits*. In: National Research Council (US) Committee on Disability Determination for Individuals with Hearing Impairments. National Academies Press (US).

Dubois, J.-M., Ouanounou, G. and Rouzaire-Dubois, B. (2009) 'The Boltzmann equation in molecular biology', *Progress in Biophysics and Molecular Biology*, 99(2–3), pp. 87–93.
doi:10.1016/j.pbiomolbio.2009.07.001.

Dulon, D., Blanchet, C. and Laffon, E. (1994) 'Photoreleased intracellular Ca²⁺ evokes reversible mechanical responses in supporting cells of the Guinea-pig organ of corti', *Biochemical and Biophysical Research Communications*, 201(3), pp. 1263–1269.
doi:10.1006/bbrc.1994.1841.

Eckrich, T., Blum, K., Milenkovic, I. and Engel, J., (2018). Fast Ca²⁺ Transients of Inner Hair Cells Arise Coupled and Uncoupled to Ca²⁺ Waves of Inner Supporting Cells in the Developing Mouse Cochlea. *Frontiers in Molecular Neuroscience*, 11.

Eckrich, T. *et al.* (2012) 'Development and function of the voltage-gated sodium current in immature mammalian cochlear inner hair cells', *PLoS ONE*, 7(9).
doi:10.1371/journal.pone.0045732.

Eckle, V.-S. and Todorovic, S.M. (2010) 'Mechanisms of inhibition of Cav3.1 T-type calcium current by aliphatic alcohols', *Neuropharmacology*, 59(1–2), pp. 58–69.

doi:10.1016/j.neuropharm.2010.03.016.

Edwards, G. and Weston, A.H. (1995) 'The role of potassium channels in excitable cells', *Diabetes Research and Clinical Practice*, 28. doi:10.1016/0168-8227(95)01080-w.

Egilmez, O.K. and Kalcioğlu, M.T. (2016) 'Genetics of nonsyndromic congenital hearing loss', *Scientifica*, 2016, pp. 1–9. doi:10.1155/2016/7576064.

Emadi, G., Richter, C. and Dallos, P., (2004) 'Stiffness of the Gerbil Basilar Membrane: Radial and Longitudinal Variations', *Journal of Neurophysiology*, 91(1), pp.474-488. doi: <https://doi.org/10.1152/jn.00446.2003>.

Engström, H. and Wersäll, J., (1958). The ultrastructural organization of the organ of corti and of the vestibular sensory epithelia. *Exp Cell Res*.14:460–492.

Engstrom, H., and Wersall, J. (1958) 'The ultrastructural organization of the organ of Corti and of the vestibular sensory epithelia', *Experimental cell research*, 14(Suppl 5), pp. 460–492.

Engström, H. and Wersall, J., (1953) 'Structure of the Organ of Corti: Supporting Structures and Their Relations to Sensory Cells and Nerve Endings', *Acta Oto-Laryngologica*, 43(4-5), pp. 323-334.

Faber, J. and Fonseca, L.M. (2014) 'How sample size influences research outcomes', *Dental Press Journal of Orthodontics*, 19(4), pp. 27–29. doi:10.1590/2176-9451.19.4.027-029.ebo.

Fábio Daumas Nunes, Lopez, L.N., Lin, H.W., Davies, C., Ricardo Bentes Azevedo, Gow, A. and Bechara Kachar (2006). Distinct subdomain organization and molecular composition of a tight junction with adherens junction features. *Journal of Cell Science*, 119(23), pp.4819–4827. doi:<https://doi.org/10.1242/jcs.03233>.

Farquhar, M.G. (1963). Junctional complexes in various epithelia. *The Journal of Cell Biology*, 17(2), pp.375–412. doi:<https://doi.org/10.1083/jcb.17.2.375>.

Feher, J. (2012b). Hearing. *Quantitative Human Physiology*, 2, pp.440–455. doi:<https://doi.org/10.1016/b978-0-12-800883-6.00040-9>.

Feller, M., (1999) 'Spontaneous Correlated Activity in Developing Neural Circuits'. *Neuron*, 22(4), pp.653-656.

Fettiplace, R. (2017) 'Hair cell transduction, tuning, and synaptic transmission in the mammalian cochlea', *Comprehensive Physiology*, pp. 1197–1227. doi:
<https://doi.org/10.1002/cphy.c160049>.

Fettiplace, R., Ricci, A.J., (2006) 'Mechano-electrical transduction in auditory hair cells'. In: *Vertebrate Hair Cells*, edited by Eatock RA, Fay RR, and Popper AN. New York: Springer Science, 2006, pp. 154–203.

Fettiplace, R., (2020) 'Diverse Mechanisms of Sound Frequency Discrimination in the Vertebrate Cochlea'. *Trends in Neurosciences*, 43(2), pp.88-102.

Flock, Å. *et al.* (1999) 'Supporting cells contribute to control of hearing sensitivity', *The Journal of Neuroscience*, 19(11), pp. 4498–4507. doi:10.1523/jneurosci.19-11-04498.1999.

Forge, A., (1985) 'Outer hair cell loss and supporting cell expansion following chronic gentamicin treatment'. *Hearing Research*, 19(2), pp.171-182.

Fuchs, P., Nagai, T. and Evans, M. (1988) 'Electrical tuning in hair cells isolated from the chick cochlea', *The Journal of Neuroscience*, 8(7), pp. 2460–2467. doi:10.1523/jneurosci.08-0702460.1988.

Furness, D., (2019) 'Forgotten Fibrocytes: A Neglected, Supporting Cell Type of the Cochlea

With the Potential to be an Alternative Therapeutic Target in Hearing Loss'. *Frontiers in Cellular Neuroscience*, 13.

Furness, D.N. *et al.* (2001) 'Distribution of the glutamate/aspartate transporter glast in relation to the afferent synapses of outer hair cells in the guinea pig cochlea', *Journal of the Association for Research in Otolaryngology*, 3(3), pp. 234–247. doi:10.1007/s101620010064.

Ganesan, P. *et al.* (2018) 'Ototoxicity: A challenge in diagnosis and treatment', *Journal of Audiology and Otology*, 22(2), pp. 59–68. doi:10.7874/jao.2017.00360.

Garcia, M.L. *et al.* (1995) 'Charybdotoxin and its effects on potassium channels', *American Journal of Physiology-Cell Physiology*, 269(1). doi:
<https://doi.org/10.1152/ajpcell.1995.269.1.c1>.

Garcia-Dorado, D. *et al.* (1997) 'Gap Junction uncoupler heptanol prevents cell-to-cell progression of hypercontracture and limits necrosis during myocardial reperfusion', *Circulation*, 96(10), pp. 3579–3586. doi:10.1161/01.cir.96.10.3579.

Geisler, C. and Sang, C., (1995) 'A cochlear model using feed-forward outer-hair-cell forces'. *Hearing Research*, 86(1-2), pp.132-146.

Geisler, C (1998). *From sound to synapse : physiology of the mammalian ear*. New York ; Oxford: Oxford University Press.

Gentet, L.J. *et al.* (2000) 'Direct measurement of specific membrane capacitance in neurons', *Biophysical Journal*, 79(1), pp. 314–320. doi:10.1016/s0006-3495(00)76293-x.

Gibson, J.R. *et al.* (1999). 'Two networks of electrically coupled inhibitory neurons in neocortex', *Nature*, 402(6757), pp. 75–79. doi:10.1038/47035.

Gillespie, P. and Müller, U., (2009) 'Mechanotransduction by Hair Cells: Models, Molecules, and Mechanisms'. *Cell*, 139(1), pp.33-44.

Giraldez, F. and Fritsch, B. (2007) 'The molecular biology of Ear Development - "twenty years are nothing"', *The International Journal of Developmental Biology*, 51(6–7), pp. 429–438. doi:10.1387/ijdb.072390fg.

Goldberg, G., Valiunas, V. and Brink, P., (2004) 'Selective permeability of gap junction channels', *Biomembranes*, 1662(1-2), pp.96-101.

Golub, M.S. and Sobin, C.A. (2020). Statistical modeling with litter as a random effect in mixed models to manage 'inralitter likeness'. *Neurotoxicology and Teratology*, [online] 77, p.106841. doi:<https://doi.org/10.1016/j.ntt.2019.106841>.

Gummer, A. and Mark, R., (1994). Patterned neural activity in brain stem auditory areas of a prehearing mammal, the tammar wallaby (*Macropus eugenii*). *NeuroReport*, 5(6), pp.685-688.

Gutman, G.A. *et al.* (2005). 'International Union of Pharmacology. LIII. nomenclature and molecular relationships of voltage-gated potassium channels', *Pharmacological Reviews*, 57(4), pp. 473–508. doi:10.1124/pr.57.4.10.

Grizel, A.V. *et al.* (2014) 'Mechanisms of activation of voltage-gated potassium channels', *Acta Naturae*, 6(4), pp. 10–26. doi:10.32607/20758251-2014-6-4-10-26.

Groves, A. and Fekete, D., (2012) 'Shaping sound in space: the regulation of inner ear patterning'. *Development*, 139(2), pp.245-257.

Hacohen, N., *et al.* (1989). 'Regulation of tension on hair-cell transduction channels: displacement and calcium dependence'. *The Journal of Neuroscience*, 9(11), pp.3988-3997.

Hackney, C. and Furness, D., (2013) 'The composition and role of cross links in mechano-electrical transduction in vertebrate sensory hair cells'. *Journal of Cell Science*, 126(8), pp.1721-1731.

Harris, A., (2001) 'Emerging issues of connexin channels: biophysics fills the gap'. *Quarterly Reviews of Biophysics*, 34(3), pp.325-472.

Hartman, B.H. *et al.* (2015) 'Identification and characterization of mouse otic sensory lineage genes', *Frontiers in Cellular Neuroscience*, 9. doi: <https://doi.org/10.3389/fncel.2015.00079>.

Hayashi, Y. *et al.* (2020) 'Cochlear supporting cells function as macrophage-like cells and protect audiosensory receptor hair cells from pathogens', *Scientific Reports*, 10(1). doi: <https://doi.org/10.1038/s41598-020-63654-9>.

Henson, M.M. *et al.* (1982) 'The cells of boettcher in the bat, *Pteronotus P. Parnellii*', *Hearing Research*, 7(1), pp. 91–103. doi: [https://doi.org/10.1016/0378-5955\(82\)90083-1](https://doi.org/10.1016/0378-5955(82)90083-1).

Helyer, R. *et al.* (2004) 'Development of Outward Potassium Currents in Inner and Outer Hair Cells from the Embryonic Mouse Cochlea', *Audiology and Neurotology*, 10(1), pp.22-34.

Hernandez, C. M., and Richards, J. R. (2023) 'Physiology, Sodium Channels', In *StatPearls*. StatPearls Publishing.

Hibino, H. *et al.* (2009) 'How is the highly positive endocochlear potential formed? the specific architecture of the stria vascularis and the roles of the ion-transport apparatus',

Pflügers Archiv - European Journal of Physiology, 459(4), pp. 521–533. doi:

<https://doi.org/10.1007/s00424-009-0754-z>.

Hibino, H., *et al.* 2010) 'Inwardly Rectifying Potassium Channels: Their Structure, Function, and Physiological Roles', *Physiological Reviews*, 90(1), pp.291–366.

doi:<https://doi.org/10.1152/physrev.00021.2009>.

Hibino, H. and Kurachi, Y. (2006) 'Molecular and physiological bases of the K⁺ circulation in the mammalian inner ear', *Physiology*, 21(5), pp. 336–345. doi:

<https://doi.org/10.1152/physiol.00023.2006>.

Housley, G.D. and Ashmore, J.F. (1992) 'Ionic currents of outer hair cells isolated from the guinea-pig cochlea', *The Journal of Physiology*, 448(1), pp. 73–98.

doi:10.1113/jphysiol.1992.sp019030.

Hsieh, C.-P., Kuo, C. and Huang, C.-W. (2015). Driving force-dependent block by internal Ba²⁺ on the Kir2.1 channel: Mechanistic insight into inward rectification. *Biophysical Chemistry*, 202, pp.40–57. doi:<https://doi.org/10.1016/j.bpc.2015.04.003>.

Hudspeth, A.J. and Lewis, R.S. (1988) 'Kinetic analysis of voltage- and ion-dependent conductances in saccular hair cells of the bull-frog- *Rana catesbeiana*', *The Journal of Physiology*, 400(1), pp. 237–274. doi: <https://doi.org/10.1113/jphysiol.1988.sp017119>.

Ikeda, K., *et al.* (1988) 'Ionic changes in cochlear endolymph of the guinea pig induced by acoustic injury', *Hearing Research*, 32(2–3), pp. 103–110. doi:10.1016/0378-5955(88)90081-0.

Inoshita, A., *et al.* (2008). 'Postnatal development of the organ of Corti in dominant-negative Gjb2 transgenic mice'. *Neuroscience*, 156(4), pp.1039-1047.

Jagger, D. and Forge, A. (2006) 'Compartmentalized and Signal-Selective Gap Junctional Coupling in the Hearing Cochlea'. *Journal of Neuroscience*, 26(4), pp.1260-1268.

Jackson, M. B., *et al.* (1991) 'Action potential broadening and frequency-dependent facilitation of calcium signals in pituitary nerve terminals', *Proc. Natl. Acad. Sci*, pp.380–384.

Jeng, J.-Y., *et al.* (2020) 'Hair cell maturation is differentially regulated along the tonotopic axis of the mammalian cochlea', 598(1), pp.151–170. doi:<https://doi.org/10.1113/jp279012>.

Jones, T., *et al.* (2001) 'Primordial Rhythmic Bursting in Embryonic Cochlear Ganglion Cells', *The Journal of Neuroscience*, 21(20), pp.8129-8135.

Jones, T., *et al.* (2007) 'Spontaneous Discharge Patterns in Cochlear Spiral Ganglion Cells Before the Onset of Hearing in Cats', *Journal of Neurophysiology*, 98(4), pp.1898-1908.

Johnson, S.L. *et al.* (2016) 'Connexin-mediated signaling in nonsensory cells is crucial for the development of sensory inner hair cells in the mouse cochlea', *The Journal of Neuroscience*, 37(2), pp. 258–268. doi:10.1523/jneurosci.2251-16.2016.

Kanazawa, A. *et al.* (2004) 'Probable function of Boettcher cells based on results of morphological study: Localization of nitric oxide synthase', *Acta Oto-Laryngologica*, 124(sup554), pp. 12–16, doi: <https://doi.org/10.1080/03655230410018444>.

Karabaliev, M. (2007) 'Effects of divalent cations on the formation and structure of solid supported lipid films', *Bioelectrochemistry*, 71(1), pp. 54–59.
doi:10.1016/j.bioelechem.2007.02.003.

Karmažínová, M. and Lacinová, Ľ. (2010) 'Measurement of cellular excitability by whole cell patch clamp technique', *Physiological Research* [Preprint]. doi:10.33549/physiolres.932000.

Katz, L.C. and Shatz, C.J. (1996) 'Synaptic activity and the construction of cortical circuits', *Science*, 274(5290), pp. 1133–1138. doi: <https://doi.org/10.1126/science.274.5290.1133>.

Kim, D.M. and Nimigean, C.M. (2016) 'Voltage-Gated Potassium Channels: A Structural Examination of Selectivity and Gating', *Cold Spring Harbor Perspectives in Biology*, 8(5).

doi:10.1101/cshperspect.a029231.

Kikuchi, K. and Hilding, D. (1965) 'The Development of the organ of Corti in the Mouse. *Acta Oto-Laryngologica*, 60(1-6), pp.207-221.

Kimura, H. *et al.* (1995) 'Reversible inhibition of gap junctional intercellular communication, synchronous contraction, and synchronism of intracellular Ca²⁺ fluctuation in cultured neonatal rat cardiac myocytes by Heptanol', *Experimental Cell Research*, 220(2), pp. 348–356. doi:10.1006/excr.1995.1325.

Koenen, L. and Andaloro, C. (2023) 'Meniere disease', *National Library of Medicine*. doi: at: <https://www.ncbi.nlm.nih.gov/books/NBK536955/>.

Kolla, L. *et al.* (2020) 'Characterization of the development of the mouse cochlear epithelium at the single cell level', *Nature Communications*, 11(1). doi:10.1038/s41467-020-16113-y.

Kollmeier, B. (2008) 'Anatomy, Physiology and Function of the Auditory System', In: Havelock,

D., Kuwano, S., Vorländer, M. (eds) *Handbook of Signal Processing in Acoustics*. Springer, New York, NY. doi: https://doi.org/10.1007/978-0-387-30441-0_10.

Kornreich, B.G. (2007) 'The patch clamp technique: Principles and technical considerations',

Journal of Veterinary Cardiology, 9(1), pp. 25–37. doi:

<https://doi.org/10.1016/j.jvc.2007.02.001>.

Korver, A.M. *et al.* (2017) 'Congenital hearing loss', *Nature Reviews Disease Primers*, 3(1).

doi:10.1038/nrdp.2016.94.

Kros, C.J. (2007) 'How to build an inner hair cell: Challenges for regeneration', *Hearing*

Research, 227(1-2), pp. 3–10. doi: <https://doi.org/10.1016/j.heares.2006.12.005>.

Kros, C., *et al.* (1998) 'Expression of a potassium current in inner hair cells during development of hearing in mice', *Nature*, 394(6690), pp.281-284.

Kros, C.J. and Crawford, A.C. (1990) 'Potassium currents in inner hair cells isolated from the guinea-pig cochlea', *The Journal of Physiology*, 421(1), pp. 263–291. doi:

<https://doi.org/10.1113/jphysiol.1990.sp017944>.

Kros CJ, (1996) 'Physiology of mammalian cochlear hair cells'. In: Dallos P, Popper AN, Fay RR, editors. *The Cochlea*. New York: Springer; pp. 318–385.

Kula, R. *et al.* (2020) 'Current density as routine parameter for description of ionic membrane current: Is it always the best option?', *Progress in Biophysics and Molecular Biology*, 157, pp. 24–32. doi:10.1016/j.pbiomolbio.2019.11.011.

Lacroix, J.J. *et al.* (2013) 'Molecular bases for the asynchronous activation of sodium and potassium channels required for nerve impulse generation', *Neuron*, 79(4), pp. 651–657. doi:10.1016/j.neuron.2013.05.036.

Laffon, E. and Angelini, E., (1996) 'On the Deiters cell contribution to the micromechanics of the organ of Corti', *Hearing Research*, 99(1-2), pp.106-109.

Lagostena, L. and Mammano, F. (2001) 'Intracellular calcium dynamics and membrane conductance changes evoked by deiters' cell purinoceptor activation in the organ of Corti', *Cell Calcium*, 29(3), pp. 191–198. doi:10.1054/ceca.2000.0183.

Lee, Y.-S., *et al.* (2006) 'A morphogenetic wave of p27kip1 transcription directs cell cycle exit during organ of Corti Development', *Development*, 133(15), pp. 2817–2826. doi: <https://doi.org/10.1242/dev.02453>.

Levy, D.I. and Deutsch, C. (1996) 'Recovery from C-type inactivation is modulated by extracellular potassium', *Biophysical Journal*, 70(2), pp. 798–805. doi:10.1016/s00063495(96)79619-4.

Lewis, R.S. and Hudspeth, A.J. (1983) 'Voltage- and ion-dependent conductances in solitary vertebrate hair cells', *Nature*, 304(5926), pp. 538–541. doi: <https://doi.org/10.1038/304538a0>.

Liberman, M.C. and Kujawa, S.G. (2017) 'Cochlear Synaptopathy in acquired sensorineural hearing loss: Manifestations and Mechanisms', *Hearing Research*, 349, pp. 138–147.

doi:10.1016/j.heares.2017.01.003.

Li-dong, Z. *et al.* (2008) 'Supporting cells—a new area in Cochlear Physiology Study', *Journal of Otolaryngology*, 3(1), pp. 9–17. doi: [https://doi.org/10.1016/s1672-2930\(08\)50002-x](https://doi.org/10.1016/s1672-2930(08)50002-x).

Lim, D. J., and Anniko, M. (1985) 'Developmental morphology of the mouse inner ear. A scanning electron microscopic observation', *Acta oto-laryngologica*, 422, pp.1–69.

Liu, H., *et al.* (2016) 'Organ of Corti and Stria Vascularis: Is there an Interdependence for Survival?', *PLOS ONE*, 11(12), p.e0168953.

Lippe, W., (1994) 'Rhythmic spontaneous activity in the developing avian auditory system'. *The Journal of Neuroscience*, 14(3), pp.1486-1495.

Litovsky, R. (2015) 'Development of the auditory system', *The Human Auditory System - Fundamental Organization and Clinical Disorders*, pp. 55–72. doi:

<https://doi.org/10.1016/b978-0-444-62630-1.00003-2>.

Lopez, W., *et al.* (2016) 'Mechanism of gating by calcium in connexin hemichannels', *Proceedings of the National Academy of Sciences*, 113(49).
doi:<https://doi.org/10.1073/pnas.1609378113>.

Loussouarn, G. and Tarek, M. (2021) 'Editorial: Molecular mechanisms of voltage-gating in ion channels', *Frontiers in Pharmacology*, 12. doi:[10.3389/fphar.2021.768153](https://doi.org/10.3389/fphar.2021.768153).

Majumder, P., *et al.* (2010) 'ATP-mediated cell–cell signalling in the organ of Corti: the role of connexin channels', *Purinergic Signalling*, 6(2), pp.167-187.

Mammano, F. *et al.* (2007) 'Ca²⁺ signalling in the inner ear', *Physiology*, 22(2), pp. 131–144.
doi:[10.1152/physiol.00040.2006](https://doi.org/10.1152/physiol.00040.2006).

Mammano, F. and Ashmore, J.F. (1996) 'Differential expression of outer hair cell potassium currents in the isolated cochlea of the Guinea-pig', *The Journal of Physiology*, 496(3), pp. 639–646. doi:[10.1113/jphysiol.1996.sp021715](https://doi.org/10.1113/jphysiol.1996.sp021715).

Marcotti, W., Johnson, S., Rüsçh, A. and Kros, C., (2003a) 'Sodium and calcium currents shape action potentials in immature mouse inner hair cells', *The Journal of Physiology*, 552(3), pp.743-761.

Marcotti, W., *et al.* (2003b) 'Developmental changes in the expression of potassium currents of embryonic, neonatal and mature mouse inner hair cells', *The Journal of Physiology*, 548(2), pp.383-400.

Marcotti, W. and Kros, C., (1999) 'Developmental expression of the potassium current $I_{K,n}$ contributes to maturation of mouse outer hair cells', *The Journal of Physiology*, 520(3), pp.653-660.

Marcus, D.C. *et al.* (1983) 'Response of cochlear potentials to presumed alterations of ionic conductance: Endolymphatic perfusion of barium, valinomycin and nystatin', *Hearing Research*, 12(1), pp. 17–30. doi: [https://doi.org/10.1016/0378-5955\(83\)90116-8](https://doi.org/10.1016/0378-5955(83)90116-8).

Marcus, D., Ge, X. and Thalmann, R., (1982) 'Comparison of the non-adrenergic action of phentolamine with that of vanadate on cochlear function', *Hearing Research*, 7(2), pp.233-246.

Marks, B. and McMahon, H.T. (1998) 'Calcium triggers calcineurin-dependent synaptic vesicle recycling in mammalian nerve terminals', *Current Biology*, 8(13), pp.740–749. doi:[https://doi.org/10.1016/s0960-9822\(98\)70297-0](https://doi.org/10.1016/s0960-9822(98)70297-0).

Mellado Lagarde, M., *et al.* (2013) 'Selective Ablation of Pillar and Deiters' Cells Severely Affects Cochlear Postnatal Development and Hearing in Mice', *Journal of Neuroscience*, 33(4), pp.1564-1576.

Merchan, M. A., *et al.* (1980) 'Morphology of Hensen's cells', *Journal of anatomy*, 131(Pt 3), pp.519–523.

Mikaelian, D. and Ruben, R.J. (1965) 'Development of hearing in the normal CBA-J mouse: correlation of physiological observations with behavioral responses and with Cochlear Anatomy', *Acta Oto-Laryngologica*, 59(2–6), pp. 451–461. doi:10.3109/00016486509124579.

Minakata, T. *et al.* (2019) 'Calcium-sensing receptor is functionally expressed in the cochlear perilymphatic compartment and essential for hearing', *Frontiers in Molecular Neuroscience*, 12. doi:10.3389/fnmol.2019.00175.

Mitrovic, N., *et al.* (2000) 'Role of domain 4 in Sodium Channel Slow inactivation', *The Journal of General Physiology*, 115(6), pp. 707–718, doi:10.1085/jgp.115.6.707.

Moody, W.J. and Bosma, M.M. (2005) 'Ion Channel Development, Spontaneous Activity, and Activity-Dependent Development in Nerve and Muscle Cells', *Physiological Reviews*, 85(3), pp. 883–941. doi:10.1152/physrev.00017.2004.

Morsli, H. *et al.* (1998) 'Development of the mouse inner ear and origin of its sensory organs', *The Journal of Neuroscience*, 18(9), pp. 3327–3335. doi:
<https://doi.org/10.1523/jneurosci.18-09-03327.1998>.

Moysan, L. *et al.* (2023) 'Ca²⁺ dynamics of gap junction coupled and uncoupled Deiters' cells in the organ of Corti in hearing BALB/C Mice', *International Journal of Molecular Sciences*, 24(13), p. 11095. doi:10.3390/ijms241311095.

Naert, G., *et al.* (2019) 'Use of the guinea pig in studies on the development and prevention of acquired sensorineural hearing loss, with an emphasis on noise', *The Journal of the Acoustical Society of America*, 146(5), pp. 3743–3769. doi:10.1121/1.5132711.

Naidu, R. and Mountain, D. (1998) 'Measurements of the stiffness map challenge a basic tenet of cochlear theories', *Hearing Research*, 124(1-2), pp.124-131.

Nakazawa, K., *et al.* (1995) 'The rosette complex in gerbil Deiters cells contains γ actin', *Hearing Research*, 89(1-2), pp.121-129.

Nakagawa, T. *et al.* (1990) 'ATP-induced current in isolated outer hair cells of guinea pig cochlea', *Journal of Neurophysiology*, 63(5), pp. 1068–1074. doi:10.1152/jn.1990.63.5.1068.

Nayak, B. (2010) 'Understanding the relevance of sample size calculation', *Indian Journal of Ophthalmology*, 58(6), p. 469. doi:10.4103/0301-4738.71673.

Nelson, W.L. and Makielski, J.C. (1991) 'Block of sodium current by heptanol in voltageclamped canine cardiac purkinje cells.', *Circulation Research*, 68(4), pp. 977–983. doi:10.1161/01.res.68.4.977.

Nenov, A., *et al.* (1998) 'Outward rectifying potassium currents are the dominant voltage activated currents present in Deiters' cells', *Hearing Research*, 123(1-2), pp.168-182.

Noga Alagem, Miri Dvir and Eitan Reuveny (2001). Mechanism of Ba²⁺block of a mouse inwardly rectifying K⁺channel: differential contribution by two discrete residues. *The Journal of Physiology*, 534(2), pp.381–393. doi:https://doi.org/10.1111/j.1469-7793.2001.00381.x.

O'Donovan, M., (1999) 'The origin of spontaneous activity in developing networks of the vertebrate nervous system', *Current Opinion in Neurobiology*, 9(1), pp.94-104.

Oliver, D., *et al.* (2003) 'Resting Potential and Submembrane Calcium Concentration of Inner Hair Cells in the Isolated Mouse Cochlea Are Set by KCNQ-Type Potassium Channels', *The Journal of Neuroscience*, 23(6), pp.2141-2149.

Ostmeyer, J. *et al.* (2013) 'Recovery from slow inactivation in K⁺ channels is controlled by water molecules', *Nature*, 501(7465), pp. 121–124. doi:10.1038/nature12395.

Pabst, G. *et al.* (2007) 'Rigidification of neutral lipid bilayers in the presence of salts', *Biophysical Journal*, 93(8), pp. 2688–2696. doi:10.1529/biophysj.107.112615.

Pan, B., Géléoc, Gwenaëlle S., Asai, Y., Horwitz, Geoffrey C., Kurima, K., Ishikawa, K., Kawashima, Y., Griffith, Andrew J. and Holt, Jeffrey R. (2013). TMC1 and TMC2 Are Components of the Mechanotransduction Channel in Hair Cells of the Mammalian Inner Ear. *Neuron*, 79(3), pp.504–515. doi:<https://doi.org/10.1016/j.neuron.2013.06.019>.

Pangrsic, T., *et al.* (2018) 'Voltage-gated calcium channels: Key players in sensory coding in the retina and the inner ear', *Physiological Reviews*, 98(4), pp. 2063–2096. doi:
<https://doi.org/10.1152/physrev.00030.2017>.

Parsa, A., *et al.* (2012) 'Deiters cells tread a narrow path—the Deiters' cells-basilar membrane junction—', *Hearing Research*, 290(1–2), pp. 13–20.
doi:10.1016/j.heares.2012.05.006.

Parsons, T.D. *et al.* (1994) 'Calcium-triggered exocytosis and endocytosis in an isolated presynaptic cell: Capacitance measurements in saccular hair cells', *Neuron*, 13(4), pp. 875–883. doi: [https://doi.org/10.1016/0896-6273\(94\)90253-4](https://doi.org/10.1016/0896-6273(94)90253-4).

Payandeh, J. (2018) 'Progress in understanding slow inactivation speeds up', *Journal of General Physiology*, 150(9), pp. 1235–1238. doi:10.1085/jgp.201812149.

Pérez-Armendariz, M. *et al.* (1991) 'Biophysical properties of gap junctions between freshly dispersed pairs of mouse pancreatic beta cells', *Biophysical Journal*, 59(1), pp. 76–92. doi:10.1016/s0006-3495(91)82200-7.

Peracchia, C. (2020) 'Calmodulin-mediated regulation of Gap Junction channels', *International Journal of Molecular Sciences*, 21(2), p. 485. doi:10.3390/ijms21020485.

Pickles, J., *et al.* (1984) 'Cross-links between stereocilia in the guinea pig organ of Corti, and their possible relation to sensory transduction', *Hearing Research*, 15(2), pp.103-112.

Platzer, J., *et al.* (2000) 'Congenital Deafness and Sinoatrial Node Dysfunction in Mice Lacking Class D L-Type Ca²⁺ Channels', *Cell*, 102(1), pp.89-97.

Polley, D.B. *et al.* (2013) 'Functional circuit development in the auditory system', *Neural Circuit Development and Function in the Brain*, pp. 21–39. doi:10.1016/b978-0-12-397267-5.00136-9.

Priest, B., *et al.* (2008) 'Role of hERG potassium channel assays in drug development', *Channels*, 2(2), pp. 87–93, doi:10.4161/chan.2.2.6004.

Pujol, R., *et al.* (1998) 'Development of Sensory and Neural Structures in the Mammalian Cochlea', *Development of the Auditory System*, pp.146-192.

Pyott, S., *et al.* (2004) 'Extrasynaptic Localization of Inactivating Calcium-Activated Potassium Channels in Mouse Inner Hair Cells', *Journal of Neuroscience*, 24(43), pp.9469-9474.

Qu, Y. *et al.* (2012) 'Early developmental expression of connexin26 in the cochlea contributes to its dominant functional role in the cochlear gap junctions', *Biochemical and Biophysical Research Communications*, 417(1), pp.245–250. doi:10.1016/j.bbrc.2011.11.093.

Raphael, Y. *et al.* (1983) 'Prenatal maturation of endocochlear potential and electrolyte composition of inner ear fluids in guinea pigs', *Archives of Oto-Rhino-Laryngology*, 237(2), pp.147–152. doi:10.1007/bf00463614.

Ray, E.C., and C. Deutsch. (2006) 'A trapped intracellular cation modulates K⁺ channel recovery from slow inactivation', *J. Gen. Physiol*, pp.128:203–217.

Ricci, A.J. and Fettkaplan, R. (1998) 'Calcium permeation of the turtle hair cell mechanotransducer channel and its relation to the composition of endolymph', *The Journal of Physiology*, 506(1), pp.159–173. doi:10.1111/j.1469-7793.1998.159bx.x.

Robertson, D. and Paki, B. (2002) 'Role of L-type Ca²⁺ channels in transmitter release from mammalian inner hair cells. II. single-neuron activity', *Journal of Neurophysiology*, 87(6), pp.2734–2740. doi:10.1152/jn.2002.87.6.2734.

Rudy, B., *et al.* (1991) 'Families of potassium channel genes in mammals: Toward an understanding of the molecular basis of potassium channel diversity', *Molecular and Cellular Neuroscience*, 2(2), pp.89–102. doi:10.1016/1044-7431(91)90001-5.

Russell, I.J. and Nilsen, K.E. (1997) 'The location of the cochlear amplifier: Spatial representation of a single tone on the guinea pig basilar membrane', *Proceedings of the National Academy of Sciences*, 94(6), pp.2660–2664. doi:10.1073/pnas.94.6.2660.

Russell, I.J. and Sellick, P.M. (1978) 'Intracellular studies of hair cells in the mammalian cochlea.', *The Journal of Physiology*, 284(1), pp.261–290.
doi:10.1113/jphysiol.1978.sp012540.

Ruben R. J. (1967) 'Development of the inner ear of the mouse: a radioautographic study of terminal mitoses'. *Acta oto-laryngologica*, pp.1–44.

Runge-Samuelson, C.L. and Friedland, D.R. (2016) *Anatomy of the auditory system*. Available at: <https://entokey.com/anatomy-of-the-auditory-system/> (Accessed: 26 September 2023).

Sadanaga, M. and Morimitsu, T. (1995) 'Development of endocochlear potential and its negative component in mouse cochlea', *Hearing Research*, 89(1–2), pp. 155–161.
doi:10.1016/0378-5955(95)00133-x.

Saito, K. and Hama, K. (1982) 'Structural Diversity of Microtubules in the Supporting Cells of the Sensory Epithelium of Guinea Pig Organ of Corti', *Journal of Electron Microscopy*, 3(31), pp.278-81.

Sakai, Y., *et al.* (2011) 'Identification and quantification of full-length BK channel variants in the developing mouse cochlea', *Journal of Neuroscience Research*, 89(11), pp.1747-1760.

Salt, A.N., *et al.* (1987) 'Mechanisms of endocochlear potential generation by stria vascularis', *The Laryngoscope*, 97(8). doi:10.1288/00005537-198708000-00020.

Salt, A., *et al.* (1989). 'Calcium gradients in inner ear endolymph', *American Journal of Otolaryngology*, 10(6), pp.371-375.

Schwander, M., *et al.* (2010) 'The cell biology of hearing', *Journal of Cell Biology*, 190(1), pp. 9–20. doi:10.1083/jcb.201001138.

Segev, A., *et al.* (2016) 'Whole-cell patch-clamp recordings in brain slices', *Journal of Visualized Experiments* [Preprint], (112). doi: <https://doi.org/10.3791/54024>.

Shah, V.N., Chagot, B. and Chazin, W.J. (2017) *Calcium-dependent regulation of ion channels, Calcium binding proteins*. Available at: <https://pubmed.ncbi.nlm.nih.gov/28757812/> (Accessed: 26 September 2023).

Shen, Y., *et al.* (2006) 'Alternative Splicing of the CaV1.3 Channel IQ Domain, a Molecular Switch for Ca²⁺-Dependent Inactivation within Auditory Hair Cells', *Journal of Neuroscience*, 26(42), pp.10690-10699.

Shi, C. and Soldatov, N.M. (2002) 'Molecular determinants of voltage-dependent slow inactivation of the ca²⁺ channel', *Journal of Biological Chemistry*, 277(9), pp. 6813–6821. doi:10.1074/jbc.m110524200.

Shim, K., Minowada, G., Coling, D. and Martin, G. (2005). Sprouty2, a Mouse Deafness Gene, Regulates Cell Fate Decisions in the Auditory Sensory Epithelium by Antagonizing FGF Signaling. *Developmental Cell*, 8(4), pp.553-564.

Shnerson, A. and Pujol, R. (1981) 'Age-related changes in the C57BL/6J mouse cochlea. I. Physiological findings', *Developmental Brain Research*, 2(1), pp.65-75.

Simmons, M.A. (2007) 'Tetraethylammonium', *xPharm: The Comprehensive Pharmacology Reference*, pp. 1–3. doi:10.1016/b978-008055232-3.62798-9.

Simonneau, L., *et al.* (2003) 'Comparative expression patterns of T-, N-, E-cadherins, betacatenin, and polysialic acid neural cell adhesion molecule in rat cochlea during development: Implications for the nature of Kolliker's organ', *The Journal of Comparative Neurology*, 459(2), pp.113-126.

Sirko, P., *et al.* (2018) 'Intercellular Ca²⁺ signalling in the adult mouse cochlea', *The Journal of Physiology*, 597(1), pp. 303–317. doi:10.1113/jp276400.

Skou, J.C. (1990). The energy coupled exchange of Na⁺ for K⁺ across the cell membrane. *FEBS Letters*, 268(2), pp.314–324. doi:[https://doi.org/10.1016/0014-5793\(90\)81278-v](https://doi.org/10.1016/0014-5793(90)81278-v).

Slepecky, N.B., *et al.* (1996) 'Post-translational modifications of tubulin suggest that dynamic microtubules are present in sensory cells and stable microtubules are present in supporting cells of the mammalian cochlea', *Hearing Research*, 91(1-2), pp. 136–147. doi:
[https://doi.org/10.1016/0378-5955\(95\)00184-0](https://doi.org/10.1016/0378-5955(95)00184-0).

Smith, C. and Dempsey, E. (1957) 'Electron microscopy of the organ of Corti', *American Journal of Anatomy*, 100(3), pp.337-367.

Souter, M., *et al.* (1997) 'Postnatal maturation of the organ of Corti in gerbils: Morphology and physiological responses', *The Journal of Comparative Neurology*, 386(4), pp.635-651.

Spicer, S. and Schulte, B. (1994) 'Differences along the place-frequency map in the structure of supporting cells in the gerbil cochlea', *Hearing Research*, 79(1-2), pp.161-177.

Steinert, J. (2023) *Patch clamp techniques for investigating neuronal electrophysiology, Scientifica*. Available at: <https://www.scientifica.uk.com/learning-zone/different-neuronalelectrophysiology-approaches> (Accessed: 26 September 2023).

Sten Hellström, *et al.* (1997) 'Interactions Between the Middle Ear and the Inner Ear: Bacterial Products', *Annals of the New York Academy of Sciences*, 830(1), pp.110–119.
doi:<https://doi.org/10.1111/j.1749-6632.1997.tb51883.x>.

Szűcs, A., *et al.* (2006) 'Differential expression of potassium currents in Deiters cells of the guinea pig cochlea', *Pflügers Archiv - European Journal of Physiology*, 452(3), pp.332-341.

Tanaka, Y., *et al.* (1979) Effect of EDTA in the Scala Media on Cochlear Potentials.

Proceedings of the Japan Academy, Series B, 55(1), pp.31-36.

Taylor, R., *et al.* (2012) 'Defining the Cellular Environment in the Organ of Corti following Extensive Hair Cell Loss: A Basis for Future Sensory Cell Replacement in the Cochlea', *PLoS ONE*, 7(1), p.e30577.

Taylor, R., *et al.* (2008). 'Rapid Hair Cell Loss: A Mouse Model for Cochlear Lesions. Journal of the Association for Research in Otolaryngology', 9(1), pp.44-64.

Teudt, I. and Richter, C. (2014) 'Basilar Membrane and Tectorial Membrane Stiffness in the CBA/Cal Mouse', *Journal of the Association for Research in Otolaryngology*, 15(5), pp.675694.

Trapani, J.G. and Korn, S.J. (2003) 'Effect of external pH on activation of the KV1.5 Potassium Channel', *Biophysical Journal*, 84(1), pp. 195–204. doi:10.1016/s0006-3495(03)74842-5.

Tritsch, N., *et al.* (2007) 'The origin of spontaneous activity in the developing auditory system', *Nature*, 450(7166), pp.50-55.

Valiquette, V., Guma, E., Cupo, L., Gallino, D., Anastassiadis, C., Snook, E., Devenyi, G.A. and Chakravarty, M.M. (2023). Examining Litter Specific Variability in Mice and its Impact on

Neurodevelopmental Studies. *NeuroImage*, 269, p.119888.

doi:<https://doi.org/10.1016/j.neuroimage.2023.119888>.

Valiunas, V., *et al.* (2005) 'Connexin-specific cell-to-cell transfer of short interfering RNA by gap junctions', *The Journal of Physiology*, 568(2), pp.459-468.

Vater, M., *et al.* (1997) 'Development of the organ of Corti in horseshoe bats: Scanning and transmission electron microscopy', *The Journal of Comparative Neurology*, 377(4), pp. 520–534. doi:10.1002/(sici)1096-9861(19970127)377:4<520::aid-cne4>3.0.co;2-4.

Vélez-Ortega, A., *et al.* (2017) 'Mechanotransduction current is essential for stability of the transducing stereocilia in mammalian auditory hair cells', *eLife*, 6.

Veenstra, R., (1996) 'Size and selectivity of gap junction channels formed from different connexins', *Journal of Bioenergetics and Biomembranes*, 28(4), pp.327-337.

Viana, L.M., *et al.* (2015) 'Cochlear neuropathy in human presbycusis: Confocal analysis of hidden hearing loss in post-mortem tissue', *Hearing Research*, 327, pp. 78–88.
doi:10.1016/j.heares.2015.04.014.

Vos, T., *et al.* (2015) 'Global, regional, and national incidence, prevalence, and years lived with disability for 301 acute and chronic diseases and injuries in 188 countries, 1990–2013: a

systematic analysis for the Global Burden of Disease Study 2013', *The Lancet*, 386(9995), pp.743-800.

Walters, B. and Zuo, J., (2013) 'Postnatal development, maturation and aging in the mouse cochlea and their effects on hair cell regeneration', *Hearing Research*, 297, pp.68-83.

Wan, G., *et al.* (2013) 'Inner ear supporting cells: Rethinking the silent majority', *Seminars in Cell & Developmental Biology*, 24(5), pp. 448–459. doi:
<https://doi.org/10.1016/j.semcdb.2013.03.009>.

Wang, Y., *et al.* (2009) 'Targeted connexin26 ablation arrests postnatal development of the organ of Corti', *Biochemical and Biophysical Research Communications*, 385(1), pp. 33–37. doi:10.1016/j.bbrc.2009.05.023.

Wangemann, P. (2002) 'K⁺ cycling and the endocochlear potential', *Hearing Research*, 165(12), pp.1-9.

Warren, R.L. *et al.* (2016) 'Minimal basilar membrane motion in low-frequency hearing', *Proceedings of the National Academy of Sciences*, 113(30). doi:10.1073/pnas.1606317113.

White, H.J. *et al.* (2023) *Anatomy, head and Neck, Ear Organ of Corti, National Center for*

Biotechnology Information. Available at: <https://pubmed.ncbi.nlm.nih.gov/30855919/>.

(Accessed: 26 September 2023).

Wiwatpanit, T., *et al.* (2018) 'Trans-differentiation of outer hair cells into inner hair cells in the absence of INSM1', *Nature*, 563(7733), pp.691-695.

World Health Organisation. (2022). *Deafness and hearing loss*, World Health Organization.

Available at: <https://www.who.int/news-room/fact-sheets/detail/deafness-and-hearing-loss>

(Accessed: 26 September 2023).

Wong, A., *et al.* (2014) 'Developmental refinement of hair cell synapses tightens the coupling of Ca²⁺influx to exocytosis', *The EMBO Journal*, 3(33), pp.247-264.

Wood, J.D. *et al.* (2004) 'Low endolymph calcium concentrations in deafwaddler2j mice suggest that PMCA2 contributes to endolymph calcium maintenance', *Journal of the Association for Research in Otolaryngology*, 5(2). doi:10.1007/s10162-003-4022-1.

Wu, Z. and Muller, U. (2016) 'Molecular Identity of the Mechanotransduction Channel in Hair Cells: Not Quiet There Yet. *Journal of Neuroscience*', 36(43), pp.10927-10934.

Xue, L. and Mei, Y. (2011) 'Synaptic vesicle recycling at the calyx of Held', *Acta pharmacologica Sinica*, 3(32). doi:<https://doi.org/10.1038/aps.2010.212>.

Yang, J., and Wang, J. B. (2000) 'Morphological observation and electrophysiological properties of isolated Deiters' cells from guinea pig cochlea', *Journal of clinical otorhinolaryngology*, 14(1), pp.29–31.

Yu, K., et al. (2019) 'Development of the Mouse and Human Cochlea at Single Cell Resolution', *bioRxiv*. doi:<https://doi.org/10.1101/739680>.

Zetes, D., et al. (2012) 'Structure and Mechanics of Supporting Cells in the Guinea Pig Organ of Corti', *PLoS ONE*, 7(11), p.e49338.

Zhang, X. and Gan, R.Z. (2013) 'Dynamic Properties of Human Round Window Membrane in Auditory Frequencies', *Medical engineering & physics*, 35(3), pp.310–318.
doi:<https://doi.org/10.1016/j.medengphy.2012.05.003>.

Zhao, L. et al. (2022) 'Design, synthesis, and biological evaluation of arylmethylpiperidines as KV1.5 Potassium Channel inhibitors', *Journal of Enzyme Inhibition and Medicinal Chemistry*, 37(1), pp. 462–471. doi:[10.1080/14756366.2021.2018683](https://doi.org/10.1080/14756366.2021.2018683).

Zhao HB. (2000) 'Directional rectification of gap junctional voltage gating between Deiters cells in the inner ear of guinea pig', *Neurosci Lett*, 296, pp.105–108.

Zhao, H. and Yu, N. (2006) 'Distinct and gradient distributions of connexin26 and connexin30 in the cochlear sensory epithelium of guinea pigs', *The Journal of Comparative Neurology*, 499(3), pp.506-518.

Zhou, Y. et al. (2019) 'Distribution and functional characteristics of voltage-gated sodium channels in immature cochlear hair cells', *Neuroscience Bulletin*, 36(1), pp.49–65. doi: <https://doi.org/10.1007/s12264-019-00415-3>.

Zhou, W. et al. (2022) 'Deiters cells act as mechanical equalizers for outer hair cells', *The Journal of Neuroscience*, 42(44), pp. 8361–8372. doi:10.1523/jneurosci.2417-21.2022.

Zhixian, W. and Yitong, Z. (1988) 'Atlas of the cochlea by light and electron microscopy', *Tianjin Science & Technology publishing House*, 1, pp.140-141.